

https://dspace.org/

Understanding kinetics and effect of process conditions during pretreatment of pine-sawdust (PSD) using torrefaction and solvolysis

Ikegwu, Ugochukwu Michael

2021

https://hdl.handle.net/10539/32944

Downloaded from a DSpace repository. https://dspace.org/



UNDERSTANDING KINETICS AND EFFECT OF PROCESS CONDITIONS DURING PRETREATMENT OF PINE-SAWDUST (PSD) USING TORREFACTION AND SOLVOLYSIS

Ikegwu Ugochukwu Michael

(2288926)

A thesis submitted to the School of Chemical and Metallurgical Engineering, Faculty of Engineering and the Built Environment, University of the Witwatersrand, Johannesburg, in fulfilment of the requirement for the Degree of Master of Science (MSc) in Engineering.

Supervisor: Prof. Michael O. Daramola

July 2021

ABSTRACT

The exploration and depletion of fossil fuels accompanied by the global warming and climate change challenge the world faces motivate the need for optimized pretreatment technique and efficient thermochemical conversion of biomass waste into energy at bench scale and industrial scale. This study focused on optimally using pine sawdust as a solid fuel. Particularly, this study aimed to understand the effect of process conditions on pine sawdust pretreatment (PSD). Two pretreatment techniques were considered: torrefaction process and solvolysis process. The process conditions studied between the two pretreatment techniques were based on literature and were benchmarked for easy comparison. Effects of process conditions on the pretreatment of PSD via the two techniques mentioned above and the kinetic analysis of the isothermal degradation of PSD during torrefaction were investigated.

Research efforts on using biomass as an alternative fuel source have continued to gain more focus with emphases on pretreatment, which could result in efficient thermochemical conversion processes. This is because of the significant improvement in the fuel properties of biomass (such as energy densification, increase in carbon content, and deoxygenation) offered by pretreatment processes. Therefore, understanding the process conditions during biomass pretreatment is essential in producing high-quality fuel for energy production and designing an efficient energy generation plant. The effect of process conditions such as temperature, time, Nitrogen-to-Solid ratio (NSR) and Liquid-to-Solid ratio (LSR) on the pretreatment of waste pine sawdust (PSD) via torrefaction and solvolysis was studied. Desirability function approach and genetic algorithm (GA) were employed in the investigation. Response surface methodology (RSM) based on Box-Behnken Design (BBD) was used to investigate the effect of the process conditions mentioned above on the higher heating value (HHV), mass yield (MY) and energy enhancement factor (EEF) of biochar/hydrochar obtained from the waste PSD. A total of 17 experiments were designed each for torrefaction and solvolysis process. The

benchmarked process conditions were temperature (200 – 300 °C), time (30 – 120 min) and NSR/LSR (4 – 5). In this study, the operating temperature was the most influential variable influencing the pre-treated PSD's fuel properties, with NSR and LSR having the least effect. The oxygen-to-carbon ratio and the HHV of the pre-treated fuel sample were compared for the two investigated pretreatment methods. Solvolysis showed a higher reduction in the oxygen-to-carbon ratio (47 %) of the PSD, while 44 % reduction was obtained for the torrefaction process. A higher mass loss and energy content was also recorded for solvolysis than that of the torrefaction process. From the optimization process results, the accuracy of the optimal process conditions was higher for GA (299 °C, 30.07 min & 4.12 NSR for torrefaction and 295.10 °C, 50.85 min & 4.55 LSR for solvolysis) than that of desirability function based on RSM. Each predictive model's significance was established using Fisher's test, Probability value, coefficient of determination (R^2) and Lack of Fitness test. The predictive model for the higher heating value during torrefaction recorded a predicted R^2 of 0.9805 while solvolysis recorded a predicted R^2 of 0.8593. The predictive model for the mass yield during torrefaction recorded a predicted R^2 of 0.8942 while solvolysis recorded a predicted R^2 of 0.9434. The developed models were reliable for evaluating the effect of the process conditions considered in this study by explaining at least 86 % (as seen in the predicted R^2) of the variation in the fuel (PSD) physicochemical properties during torrefaction and solvolysis.

The reaction kinetics of solid fuel is a critical aspect of energy production. This importance is because the fuel's energy component is determined during the process, and the overall fuel quality is evaluated to account for a defined energy need. In this study, a two-step first-order reaction mechanism was used to model the rate of mass loss of pine sawdust (PSD) during torrefaction using a thermogravimetric analyzer. The kinetic analysis was carried in a MATLAB environment using MATLAB R2020b software. Five temperature regimes including; 220 °C, 240 °C, 260 °C, 280 °C and 300 °C and retention time of 2 hours were used

to study the mechanism of the solid fuel reaction. Similarly, a combined demarcation time (i.e. estimating the time that demarcates the first stage and the second stage) and iteration techniques were used to determine the actual kinetic parameters that described the fuel's mass loss during torrefaction process. The fuel's kinetic parameters were estimated, while the kinetic model developed for the process was validated using the experimental data. The solid and gas distribution of the pseudo-components in the reaction mechanism were also reported. The first stage of the degradation process was characterized by the rapid mass loss evident at the start of the torrefaction process. In contrast, the second stage was characterized by a slower mass loss phase which followed the first stage. The activation energies for the first and second stage were 10.29 kJ mol^{-1} and 141.28 kJ mol^{-1} respectively, to form the solids. The developed model showed 98 – 99.9 % accuracy in predicting the mass loss of PSD during torrefaction at various temperatures. The biochar produced from the torrefaction process contained a high amount of the intermediate product (Pseudo-component B) that may benefit energy production. However, the final amount of biochar formed at the end of the process increased with increase in torrefaction severity (i.e. increase in temperature and time).

The outcome of this study has made available the technical set of data which can pave the way for further research in this field and offer relevant information for the implementation of these processes on a pilot scale. The knowledge derived from this study may also be extended to the pretreatment of other abundant and invasive biomass for efficient energy production.

Keywords: Pretreatment; Torrefaction; Solvolysis; Biomass; Genetic Algorithm; Desirability Function; Response Surface Methodology; Optimization; Isothermal Degradation; Kinetics; Thermogravimetric Analysis; Two-step Reaction Mechanism; Modelling.

DECLARATION

I, **Ikegwu Ugochukwu Michael**, hereby declare that this research was carried out solely by me and the content of this thesis represents my unique knowledge. At the same time, the consulted literature was cited correctly.



Signature

28 – 07 – 2021

Date

DEDICATION

I dedicate this thesis to my mom, Late Barr. Mrs Sophia Ikegwu and to God Almighty for the strength and wisdom to carry out this research. For through him, I have been strengthened to do all things (Philippians 4:13).

ACKNOWLEDGMENT

I wish to recognize the following people who have been of immerse support one way or the other towards successfully completing this research.

- To my supervisor Prof. Michael Daramola, for his support in securing funding for this study, continuous guidance, and constructive scrutiny during this study to produce quality research, I say a big thank you.

- My heartfelt gratitude goes to my daily supervisor Dr Maxwell Ozonoh, for his eternal advice and continuous guidance during this research.

- I sincerely appreciate my academic mentors and colleagues at the School of Chemical and Metallurgical Engineering, University of The Witwatersrand: Dr Nnanna Okoro-Jnr, Dr Thomas Aniokete, Dr Michael Bodunrin, Dr Ezinne Ibokwe, Dr Wunmi Shadare, Mr Uzo Enwerenuzo and Olayile Ejekwu, for their continuous support during this study.

- To the laboratory managers, and technicians: Mr Motlatsi Phali, Mr Bruce Mothibedi, Mrs Janeth, Mr Patho, and Miss Letta for the training I was given and the procurement of my equipment and materials, I say a big thank you.

- My sincere appreciation goes to the Department of Science and Technology: National Research Foundation (DST-NRF), grant number 123105, for the financial support accorded to me during the entire duration of my study.

- To the Sustainable Energy and Environmental Research Unit (SEERU), I say a heartfelt thank you for the continuous support, constructive criticism of my research proposal, and my thesis review.

- To the staff and students at the school of Chemical Engineering, University of Pretoria, I apricate all the efforts and assistance given to me while carrying out some analyses.

- To my dad Mr Ifeanyi Ikegwu and my siblings Chidinma Ikegwu and Ebuka Ikegwu, I say a big thank you for the continuous prayers and words of encouragement during my study.

- To my Uncle Mr Timothy Ikegwu and my aunt Mrs Philile Ikegwu who with warm hands accepted me, sheltered me, fed me, and encouraged me, God in his infinite mercies will reward you abundantly.

- To my aunt: Mrs Obioma and my cousins: Nnaemeka Obodoekwe, Chinonso Ikegwu, Oluchi Ikegwu, Uchenna Ikegwu, Chinaza Ikegwu and the most beautiful Gabriella Ikegwu, I say a big thank you for your continuous prayers, words of encouragements and disturbance during this study.

- My heartfelt gratitude also goes to my friends: Dare Badejo, Oreoluwa Jokodola, Ulo David, Ifunanya Obieli, and David Oyekunle, who through difficult times, reminded me how their expectations from me were high and helped out in any possible way they could.

- Finally, all would not have been possible if it was not for God. Thanks be to God.

List of Publications and Training

Publications

- **Ikegwu, U.M.,** Ozonoh, M., Daramola, M.O. Kinetic study of the isothermal degradation of pine sawdust (PSD) during torrefaction process. ACS Omega. 2021. https://doi.org/10.1021/acsomega.1c00327
- **Ikegwu, U.M.,** Ozonoh, M., Okoro, N.M., Daramola, M.O. Effect and optimization of process conditions during solvolysis and torrefaction of PSD using desirability function and generic algorithm. ACS Omega. 2021. https://doi.org/10.1021/acsomega.1c00857. (**In Press**)
- **Ikegwu, U.M.,** Okoro, N.M., Ozonoh, M., Daramola, M.O., Harding, K.G. Non-isothermal degradation kinetics and properties of PSD via TGA. SACEC. 2021. (**Abstract Accepted**).
- Okoro, N.M., **Ikegwu, U.M.,** Harding, K.G., Daramola, M.O. Evaluation of Fuel quality of Invasive Alien Plants and Tropical hardwoods as potential feedstock materials for pyro-gasification. Waste Biomass Valor. 2021. (**Under review**).

Training

- A day training on the thermogravimetric analyzer (TGA) at the Chemical and Metallurgy Engineering school, University of the Witwatersrand, Johannesburg, South Africa, 15th July 2020.

- A day-training on bomb calorimeter at the school of Chemical Engineering, University of Pretoria, South Africa, 25th September 2020.

TABLE OF CONTENT

Abstract ii

Declaration v

Dedication vi

Acknowledgment vii

List of Publications and Trainings ix

List of Figures xiv

List of Tables xvii

Glossary xix

1. INTRODUCTION 1

1.1. Background of Study 1

1.2. Problem Statement 4

1.3. Research Questions 6

1.4. Specific Objectives 7

1.5. Scope of the Study and Benefits of this Research 7

1.6. Thesis Layout 9

2. LITERATURE REVIEW 11

2.1. Introduction 11

2.2. Utilization of Coal and its Global Challenges 11

2.3. Biomass as a Sustainable Source of Renewal Energy and its Limitations 13

2.4. Overview of Torrefaction Pretreatment Process 18

2.4.1. Torrefaction pretreatment process: Effect of process conditions 21

2.4.2 Optimization of torrefaction process 29

2.5. Overview of Solvolysis Pretreatment Process 35

2.5.1. Solvolysis reaction mechanism 36

2.5.2. Solvolysis pretreatment process: Effect of process conditions 39

2.5.3. Optimization of solvolysis process 45

2.6. Comparison Between Fuel Properties of Biochar and Hydrochar 49

2.7. Kinetic Analysis of Biomass Degradation 55

2.8. Biomass Selection 57

2.9. Challenges and Outlook 58

2.10. Summary 61

3. EXPERIMENTAL PROCEDURE AND ANALYSIS 64

3.1. Torrefaction and Solvolysis Study 64

3.1.1. Materials and methods 64

3.1.1.1. Sample preparation 64

3.1.1.2. Characterization of feedstock 65

3.1.2. Torrefaction experiment 66

3.1.3. Solvolysis experiment 67

3.1.4. Experimental design: Box-Behnken Design (BBD) 68

3.1.4.1. Statistical test and analysis 69

3.1.5. Desirability function optimization 69

3.1.6. Genetic algorithm optimization 70

3.2. Kinetic Study 71

3.2.1. Material and Methods 71

3.2.1.1. Sample preparation 71

3.2.2. Thermogravimetric analysis 72

4. OPTIMIZATION OF PROCESS CONDITIONS DURING SOLVOLYSIS AND TORREFACTION OF PSD USING DESIRABILITY FUNCTION AND GENETIC ALGORITHM 73

4.1. Introduction 73

4.2. Experimental Procedure and Analysis 77

4.3. Results and Discussion 77

4.3.1. Physicochemical properties of raw and pre-treated PSD 77

4.3.2. Predictive model development and statistical analysis 83

4.3.3. Comparative analysis of the effect of process conditions on torrefaction and solvolysis process 96

4.3.3.1. Effect of process conditions on HHV and EEF 96

4.3.3.2. Effect of process conditions of mass yield 98

4.3.4. Optimization of process conditions 102

4.3.4.1. Optimization using desirability function 103

4.3.4.2. Optimization using genetic algorithm (GA) 104

4.3.4.3. Comparison of optimization technique: (RSM and GA) 105

4.3.4.4. Results compared with literature 108

4.4 Conclusion 118

5. KINETIC STUDY OF ISOTHERMAL DEGRADATION OF PINE SAWDUST (PSD) DURING TORREFACTION PROCESS 120

5.1. Introduction 120

5.2. Experimental and Modelling Procedure 125

5.2.1. Kinetic model formulation 125

5.2.2. Kinetic model solution 127

5.3. Results and Discussion 130

5.3.1. Isothermal degradation of PSD during torrefaction in a TGA 130

5.3.2. Estimation of kinetic parameters 132

5.3.3. Kinetic model validation 135

5.3.4. Predicted solid and gas distribution 137

5.3.5. Results compared with literature 140

5.4. Conclusion 143

6. GENERAL CONCLUSION AND RECOMMENDATION 144

6.1. General Conclusions 144

6.2. Recommendations 147

REFERENCES xxii

LIST OF FIGURES

Figure 1.1. Overall Thesis layout and road map 10

Figure 2.1. (a) Woody biomass (b) Crop biomass (c) Municipal waste (d) Animal waste 15

Figure 2.2. Distribution of various sources of renewable energy. (Antonio et al., 2016) 16

Figure 2.3. Schematic representation of the pretreatment of biomass. Adapted from Paulien et al. (2010)**.** 18

Figure 2.4. Stages of hydrothermal conversion of biomass**.** (Adapted from Kruse & Karlsruhe (2008)). 37

Figure 2.5. Relationship between HHV and the mass yield of char produced 53

Figure 2.6. Van Krevelen diagram of various biomass in torrefaction and solvolysis 54

Figure 3.1. Experimental flowchart for torrefaction and solvolysis study 65

Figure 3.2. Flow chart showing the development of the function file for GA optimization 71

Figure 3.3. Experimental flowchart for kinetic study 72

Figure 4.1. Van Krevelen diagram of PSD in (a) torrefaction and (b) solvolysis 82

Figure 4.2. Predicted responses against actual responses of (a) EEF (b) HHV and (c) MY for torrefaction process 93

Figure 4.3. Predicted responses against actual responses of (a) EEF (b) HHV and (c) MY for solvolysis process 94

Figure 4.4. Normal plot of residual for (a) HHV (b) EEF and (c) MY for torrefaction process 95

Figure 4.5. Normal plot of residual for (a) HHV (b) EEF and (c) MY for solvolysis process 95

Figure 4.6. 3D response surface plots of HHV, MY and EEF for torrefaction process 99

Figure 4.7. 3D response surface plots of HHV, MY and EEF for solvolysis process 101

Figure 4.8. Optimal conditions for (a) torrefaction and (b) solvolysis pretreatment process 103

Figure 4.9. Genealogy of the optimization: (a) Torrefaction and (b) Solvolysis process 104

Figure 4.10. Pareto plots showing the optimal responses for torrefaction and solvolysis 105

Figure 5.1. Two-step kinetic model 125

Figure 5.2. Flowchart algorithm used in MATLAB for estimating the kinetic parameters and the solid distribution during the torrefaction of PSD 129

Figure 5.3. Mass loss curves during the torrefaction of PSD using a TGA 131

Figure 5.4. Logarithmic plots of the mass loss for the (a) first stage and (b) second stage 133

Figure 5.5. Arrhenius plots for the determination of activation energies and pre-exponential factors for each pseudo-component (kb, kc, kv1, kv2) 135

Figure 5.6. Experimental and modelled mass loss of PSD torrefaction at different temperatures 136

Figure 5.7. Solid and gas distribution during torrefaction of PSD at (a) 220 °C, (b) 260 °C and (c) 300 °C 138

Figure 5.8. Formation of final char at different temperatures 139

Figure A.1. Log of pine wood xlv

Figure A.2. Pine wood chips xlv

Figure A.3. Muffle furnace xlvi

Figure A.4. Kinetic modelling script file xlvi

Figure A.5. Kinetic modelling function file xlvii

Figure A.6. Ordinary differential equation function file xlvii

Figure A.7. Solid distribution plot script file xlviii

Figure A.8. Genetic algorithm function file for torrefaction xlviii

Figure A.9. Genetic algorithm function file for solvolysis xlix

Figure A.10. Solid and gas distribution during torrefaction of PSD at 240 °C xlix

Figure A.11. Solid and gas distribution during torrefaction of PSD at 280 °C l

LIST OF TABLES

Table 2.1. Proximate and ultimate analysis of the ranks of coal**.** Radovic (1997). 12

Table 2.2. Proximate and Ultimate analysis of coal. Sanwal et al. (2018). 13

Table 2.3. Process conditions employed for the torrefaction of different biomass and their corresponding improved fuel properties. 27

Table 2.4. Summary of developed predictive models explaining the interactional effect of process conditions during torrefaction. 32

Table 2.5. Process conditions employed during the solvolysis pretreatment of different biomass and their corresponding improved fuel properties. 43

Table 2.6. Summary of developed predictive models explaining the interactional effect of process conditions during solvolysis. 47

Table 2.7. Summary of process conditions and obtained fuel properties from the literature reviewed. 52

Table 3.1. Experimental Process conditions and coded levels in BBD. 68

Table 4.1. Physicochemical properties of raw PSD. 78

Table 4.2. Ultimate analysis of some pre-treated PSD. 81

Table 4.3. Experimental design and responses for the torrefaction process. 85

Table 4.4. Experimental design and responses for the solvolysis process. 86

Table 4.5. Analysis of Variance (ANOVA) of the torrefaction models. 89

Table 4.6. Analysis of Variance (ANOVA) of the solvolysis models. 91

Table 4.7. Comparison between the predicted and calculated values of the responses at optimum process conditions. 107

Table 4.8. Percentage changes in ultimate analysis of torrefied fuel (Pine wood). 109

Table 4.9. Comparison of mass yield and energy yield from this study with literature. 111

Table 4.10. Optimum conditions for torrefaction and solvolysis pretreatment from this study and literature. 115

Table 5.1. Lignocellulosic and proximate analysis of air-dried pine sawdust (PSD). 128

Table 5.2. Estimated kinetic parameters for the torrefaction of pine sawdust. 134

Table 5.3. Statistical test of kinetic model for prediction of mass loss. 137

Table 5.4. Kinetic parameters for different types of biomass reported in the literature 141

Glossary

Abbreviation	Definition (units)
PSD	Pine sawdust
MY	Mass yield (%)
EY	Energy yield (%)
HHV	Higher Heating Value (MJ kg^{-1})
EEF	Energy Enhancement factor (-)
LSR	Liquid-to-Solid ratio (-)
NSR	Nitrogen-to-Solid ratio (-)
GA	Genetic Algorithm
TGA/TA	Thermogravimetric Analyzer
DTG	Differential Thermogravimetric Analysis
RSM	Response Surface Methodology
VM	Volatile Matter (%)
FC	Fixed Carbon (%)
MC	Moisture Content (%)
C	Carbon content (%)
H	Hydrogen content (%)
N	Nitrogen content (%)
O	Oxygen content (%)
S	Sulphur content (%)
EPA	Energy Policy Act
SAIREC	South Africa International Renewable Energy Conference
GHG	Green House Gas
CHL	Cellulose Hemicellulose Lignin

HTZ	Total temp. width at half the vertical length of max. mass loss rate
FCCD/CCD	Face Central Composite Design
BBD	Box-Behnken Design
SFED	Single Factor Experimental Design
KAS	Kissinger-Akahira-Sunose
FWO	Flynn-Wall-Ozawa
CCSU/CCS	Carbon Capture Storage and Utilization
SANEDI	South Africa National Energy Development Institute
GDP	Gross Domestic Profit
SF	Severity Factor
T	Temperature (°C)
t	Time (min)
OH	Hydroxyl group
LIA	Loss of Iodine Adsorption
GCY	Gain in Activated Carbon Yield
ASTM	American Standard Testing Method
P-Value	Probability value
F-Test	Fisher test
LOF	Lack of Fitness test
R^2	Coefficient of determination
r	Pearson correlation coefficient
Adj.R^2	Adjusted coefficient of determination
Pred.R^2	Predicted coefficient of determination
D	Desirability function
MATLAB	Matrix Laboratory software

ANOVA	Analysis of Variance
DF	Degree of Freedom
OFAT	One Factor at a Time
A,B,C,V_1,V_2	Pseudo Components
W	Mass of solid char (mg)
m_o	Initial mass of solid (mg)
M_B^*	Mass at demarcation time (mg)
t^*	Demarcation time (min)
$E_{a,i}$	Activation energy of component *i* (kJ mol^{-1})
m_i	Mass of component *i* (mg)
$K_{1,2}$	Rate constant of stage one and two (s^{-1})
$K_{b,c,v1,v2}$	Rate constant of pseudo-components (s^{-1})
R	Rate gas constant (0.008314 kJ K^{-1} mol^{-1})
RSS	Residual Sum of Squares

CHAPTER ONE

1. INTRODUCTION

1.1. Background of Study

In recent years, Africa's population has increased dramatically, culminating in different challenges such as the rise in agricultural practices to provide basic human needs (e.g. food, housing, and clothes, to name a few). These practices have contributed to the rise in biomass production. Another consequence of this population boom is the rise in electricity and fuel demand to run our homes, businesses, cars. It has been projected that Africa's population will reach around 1.7 billion in 2025 (United Nations (UN), 2015), thereby compounding the challenges mentioned above.

Biomass can be described simply as a renewable organic material. According to the U.S. Department of Energy (DOE) and U.S. Department of Agriculture (USDA) (2009), biomass is simply an organic matter with stored energy. From literature, after the several descriptions attributed to biomass, one can say that biomass can be described as any organic matter made from wood (woody biomass) or crops (agro biomass) or animal waste, that can be a renewable source of energy. There has been a misunderstanding between biomass and fossil fuel, though they are closely related and interwoven. The difference between biomass and fossil fuel is the "age" (U.S. Department of Energy (DOE); U.S. Department of Agriculture (USDA), 2009).

Trees and crops collapse to the earth's surface. They usually are deposited beneath the earth's crust (the uppermost layer of the earth's atmosphere) for millions of years after multiple human operations on the planet. This extracted biomass is referred to as fossil fuels, after going through natural processes underneath the earth's atmosphere. Such fossil fuels act as an essential natural resource, but they are unrenewable and are the fundamental causes of global warming. On the other hand, agro-waste, which can sometimes be referred to as biomass, has been described as the valueless residue of agricultural products (Abou *et al.,* 2010). In a more

comprehensive literature description, agricultural practices yield two outcomes: the product also known as the yield, and the waste also known as the residue. This residue is called agro waste, as the name implies "agro – agriculture" and "waste – valueless". Among other biomass uses, biomass for electricity generation has been given much attention in recent years. This attention has been due to the energy content present in biomass—this energy content in biomass results from the sunlight stored by plants during photosynthesis.

In 2010, a study was carried out to quantify the utilization of agro-waste in Egypt. It was revealed that about 30 – 35 million tons of agro-waste are generated yearly and only about one-third is being used as organic manure to grow more crops and animal feed (Abou *et al.*, 2010). The need to utilize the recent significant increase in biomass generated due to the increase in farming activities cannot be overemphasized. Biomass is sometimes discarded by open-burning which brings about the emission of greenhouse gases. These gases are harmful to the environment and the ozone layer, thereby causing global warming. Biomass is also allowed to rot, which causes environmental and air pollution at the initial stage and after some years, rot underground, thereby forming coal. Ways of reducing global warming have been the main discussion internationally. For the global temperature to reduce to about 2 ^{o}C, the Intergovernmental Panel on Climate change and the International Energy Agency have recommended that sustainable use of biomass against open burning disposal, should be employed (Mahawar *et al.*, 2015).

Without ignoring the existing useful products gotten from biomass, research efforts have been, in recent years, concentrated on converting biomass into useful resources. Some of such are; the use of onion matrix for treatment of wastewater from textile industry using an ion-exchange technique (Bello *et al.*, 2016); the use of orange seed as a corrosion inhibitor; the use of coconut bark to produce activated Carbon, to mention a few. A recent idea is the production of electricity using citrus fruits through the process of electrolysis. Energy, which is also a basic

need of man, can be generated from biomass through a process known as gasification. Fossil fuel is the most prevalent energy source, but its depreciable nature has created the need to source alternative energy sources. To find solutions to the prevalent non-renewable fossil fuels and global warming, research efforts on biomass as a clean and renewable energy source have been embraced and given priority (Piotrowska *et al*., 2010). Research evidence from the production of energy (bioenergy) from biomass indicates that bioenergy will become the most common energy source in the coming years (Kaushal & Tyagi, 2017). However, to effectively migrate from the thermochemical conversion (i.e. gasification) of fossil fuel (coal) to biomass, gasification process needs to be understood and why coal has been used. Understanding the importance of coal during the gasification process will also highlight the important fuel properties of coal and how biomass can provide similar quality to achieve equal or greater efficiency when gasifying biomass in place of coal.

Therefore, gasification could be described as a process whereby coal or a coal-like material is subjected to heat in the presence of steam or oxygen to produce mainly hydrogen gas and carbon mono-oxide (Anukam *et al.,* 2017). Gasification is usually done between 600 ^{o}C and 1000 ^{o}C depending on the type of gasification (either at high temperature or with a catalyst) and the gasifier (Umeda *et al.,* 2019). Gasification has been proposed as one of the most efficient thermochemical conversion processes of biomass to bioenergy.

Some of the fuel properties which has favoured the use of coal over the years as a feed material for the gasification process are its; higher heating value, carbon-to-oxygen ratio, hydrogen-to-oxygen ratio, to mention a few. Over time, from past research, it has been proposed that coal is classified into four, namely; lignite, sub-bituminous, bituminous, and anthracite in increasing age, higher heating value and fuel quality.

However, the proximate analysis of biomass has shown promising results posing that it is a suitable supplement/replacement for coal and exhibits similar characteristics of lignite coal

having a heating value between 29.92 – 30.54 MJ/Kg (Bogale, 2010). Still, these physical and chemical characteristics can be improved through thermal pretreatment, chemical pretreatment and biochemical pretreatment (Yu *et al*., 2014). Therefore, biomass pretreatment could be described simply as a process through which biomass's physical and chemical properties are improved.

1.2. Problem Statement

Currently, the energy industry worldwide is under pressure to generate electricity without threats to the environment. Non-renewable energy systems and sources (e.g. coal & petroleum) are considered responsible for pollution that endangers the planet. Renewable sources (e.g. biomass, solar, wind, hydro.) are environmentally sustainable, but some appear intermittent and costly relative to fossils (non-renewable). Today, researchers are focused on various technologies and process conditions that will improve energy security and efficiency to satisfy the rising worldwide energy demands. Coal reserves are substantial in Africa (e.g. South Africa and Nigeria). Nigeria also has large oil reserves for energy generation, while South Africa depends on coal to produce about 95 % of its electricity (Falcon, 2013). Both countries' coal and petroleum are fast depleting, and their conversions into energy pose a huge environmental threat due to emissions. The new 10-year innovation plan proposed by the Minister of Science and Technology, South Africa, has also shown a need to address energy shortages in South Africa (South Africa, 2016).

Furthermore, South Africa and Nigeria have abundant agricultural waste materials resulting from different agricultural activities in the countries. For example, the two countries are the largest corn and sugarcane producers in Africa (Mohlala *et al*., 2016). The implication is that both countries generate a lot of wastes, such as corn cobs, stover, and bagasse. Furthermore, both countries have enormous forestry and timber industries through which wood waste such as pine sawdust (PSD) are produced (Lopez *et al.*, 2018). Such waste materials are disposed

indiscriminately and are therefore environmentally harmful. The use of non-waste biomass materials for energy production is not cost-effective (Zafar, 2018). However, the conversion of coal and biomass blends through gasification will significantly reduce emissions and energy generation costs. Secondly, recycling waste materials into useful products such as biofuels will be instrumental in waste management in South Africa and Nigeria.

The limitations to the effective use of biomass as a replacement for coal are; its high moisture content, oxygen content, low bulk and energy densities, and poor grindability (Hernández *et al.*, 2018; Serowik *et al*., 2017; Tumuluru, 2015). For an effective process, the fuel materials should be pre-treated. Significantly, the fuel (coal and biomass) quality can be upgraded through biomass pretreatment (e.g. by torrefaction & solvolysis pretreatment). Some of the benefits of these pretreatments are the energy densification and deoxygenation of biomass (Louwes *et al*., 2017). The pretreatment of biomass will also limit the difficulties associated with operating the gasifier efficiently, save the cost of energy production and gas cleaning, and enhance the gasifier's performance. Although this process improves the biomass's fuel quality, it degrades the biomass, further affecting the energy yield. Furthermore, while going green and considering the drop in the fuel properties of biomass compared to coal, the co-combustion/co-gasification of pre-treated biomass with coal can effectively foster the implementation of these pretreatment methods and subsequently the valorization of biomass. Hence, studies on improving the fuel properties of biomass need to be done to promote the co-combustion of pretreated biomass with coal as this will reduce the use of coal gradually while augmenting for the drop in the fuel properties of biomass.

Therefore, it is vital to understand and develop a model that will predict the rate of degradation of biomass with respect to torrefaction temperature and residence time. Almeida *et al.* (2010) established that the degree of torrefaction could efficiently be measured quantitatively using biomass degradation. The design of an efficient reactor for torrefaction depends on the

residence time required to achieve a complete biomass feed conversion. This time is dependent on mass transfer, heat transfer, and the solid degradation rate during the process. Many researchers have used an empirical approach to model the degradation of biomass due to the lack of a mechanistic model based on a physical law (Lee & Lee, 2014). However, recent studies have shown that kinetics gives an efficient description of the process. Therefore, the thermal degradation of biomass can be accurately predicted by the pretreatment process's reaction kinetic model. Unlike torrefaction, the introduction of water in solvolysis pretreatment process limits the degradation of biomass modelling to an empirical approach because of the absence of a physical law describing the process.

Understanding the process conditions to achieve the objectives mentioned above was essential to ensure the gasification process's energy efficiency and the sustainability of the biomass resource in South Africa and Nigeria. In this context, this study aimed at establishing kinetic and empirical models for predicting improved fuel characteristics (such as; the yield, the higher heating value and the energy enhancement factor) of pre-treated pine sawdust biomass. Two pretreatment methods were employed, namely; solvolysis and torrefaction pretreatments. Validation of the models was also carried out. Therefore, the following fundamental research questions and goals were intended to ensure that the research objectives were fulfilled.

1.3. Research Questions

1. Can a predictive empirical model, based on regression analysis technique, be developed to predict fuel characteristics (mass yield (MY), higher heating value (HHV), and energy enhancement factor (EEF)) of PSD and explain the effect of operating temperature, residence time and Liquid-to-Solid Ratio/Nitrogen-to-Solid Ratio, during torrefaction and solvolysis pretreatment method?
2. Can Genetic Algorithm (GA) be used to optimize the pretreatment process in (1)?

3. Is there a difference in the quantity and quality of biochar produced from these two pretreatment methods?
4. Can a suitable kinetic model be developed to explain the isothermal degradation of Pine sawdust (PSD) of South African origin during torrefaction process using the experimental dataset from a thermo-gravimetric analyzer (TGA)?

1.4. Specific Objectives

1. To develop an empirical model that can predict the fuel characteristics (MY, HHV, and EEF) of PSD and explain the effect of operating temperature, residence time and Liquid-to-Solid Ratio/Nitrogen-to-Solid Ratio during torrefaction and solvolysis pretreatment methods, and compare the quality of biochar produced from both pretreatment methods.
2. To optimize the pretreatment processes in (1) using a Genetic Algorithm (GA).
3. To develop a 2-step kinetic model to explain the isothermal degradation of PSD of South African origin during torrefaction process using the experimental dataset from a thermo-gravimetric analyzer (TGA).

1.5. Scope of the Study and Benefits of this Research

This study investigated the effect of process conditions on the pretreatment of pine sawdust (PSD). The pretreatment methods were limited to torrefaction and solvolysis, and the process conditions studied were restricted to temperature, time, liquid-to-solid ratio, and nitrogen-to solid ratio. This study did not cover the lignocellulosic composition and proximate analysis changes after pretreatment but was limited to the mass yield, ultimate analysis and the energy content changes. The fuel (PSD) used in this study was obtained in South Africa, and all analyses were done on an air-dried basis. This study did not cover the fuel's non-isothermal degradation but developed a kinetic model explaining the isothermal degradation of PSD during only the torrefaction process. The data used for developing the kinetic model was

restricted to the data obtained from the thermogravimetric analyzer. The study did not include an economic and feasibility study of the pretreatment processes investigated. Notwithstanding, the following are highlighted as the benefits that can be derived from this study.

1. This study provides insight for implementing torrefaction and solvolysis pretreatment processes on a large scale by providing optimal operating conditions that will ensure increased efficiency.
2. Knowledge on the comparison between torrefaction and solvolysis process regarding the physicochemical properties of the char produced was established. This knowledge will give informed decision to further research on the process to adopt based on different factors.
3. Relevant kinetic data that explains the thermal degradation of PSD was provided to the research body of knowledge which will assist in designing an optimized and efficient reactor for carrying out the pretreatment of PSD and can be extended to similar biomass.
4. This study also provides relevant data to evaluate the torrefaction process's efficiency, considering the minimum energy needed, which will play a vital role in simulating pretreatment processes in a static and dynamic environment.
5. Lastly, this research's execution significantly contributes to further advancement in the quest to provide green energy and green economy. These advancements will add to the efforts made by other researchers in offering solutions to climate change and global energy insecurity, resulting from the indiscriminate burning of biomass waste, and the non-renewable nature of fossil fuels, respectively.

As a result of these benefits, this research can pave the way for further research in this field. More relevant data can be made available to stakeholders to make informed decisions on implementing these technologies on an industrial scale in a coal-biomass co-firing power plant.

1.6. Thesis Layout

Contained in this thesis are six (6) chapters. Chapter one serves as the introductory chapter to this thesis. It contains the identified problems relevant to this field of study and motivates for the research's execution. It also contains the objectives, scope and contributions of this study. Chapter two contains a review of relevant and recent literature concerning the objectives and scope of this research. Chapter three contains the experimental procedure and analysis carried out in this study. Chapter four focuses on the effect and optimization of process conditions during solvolysis and torrefaction of PSD using desirability function based on RSM and genetic algorithm (GA). Chapter five focuses on the kinetic study of the isothermal degradation of PSD during torrefaction process. Chapter six contains the conclusions drawn from the execution of this research and possible recommendations that can help improve the experiment's efficiency and the results obtained from this study. Figure 1.1 shows the overall thesis layout and road map taken in the execution of this study.

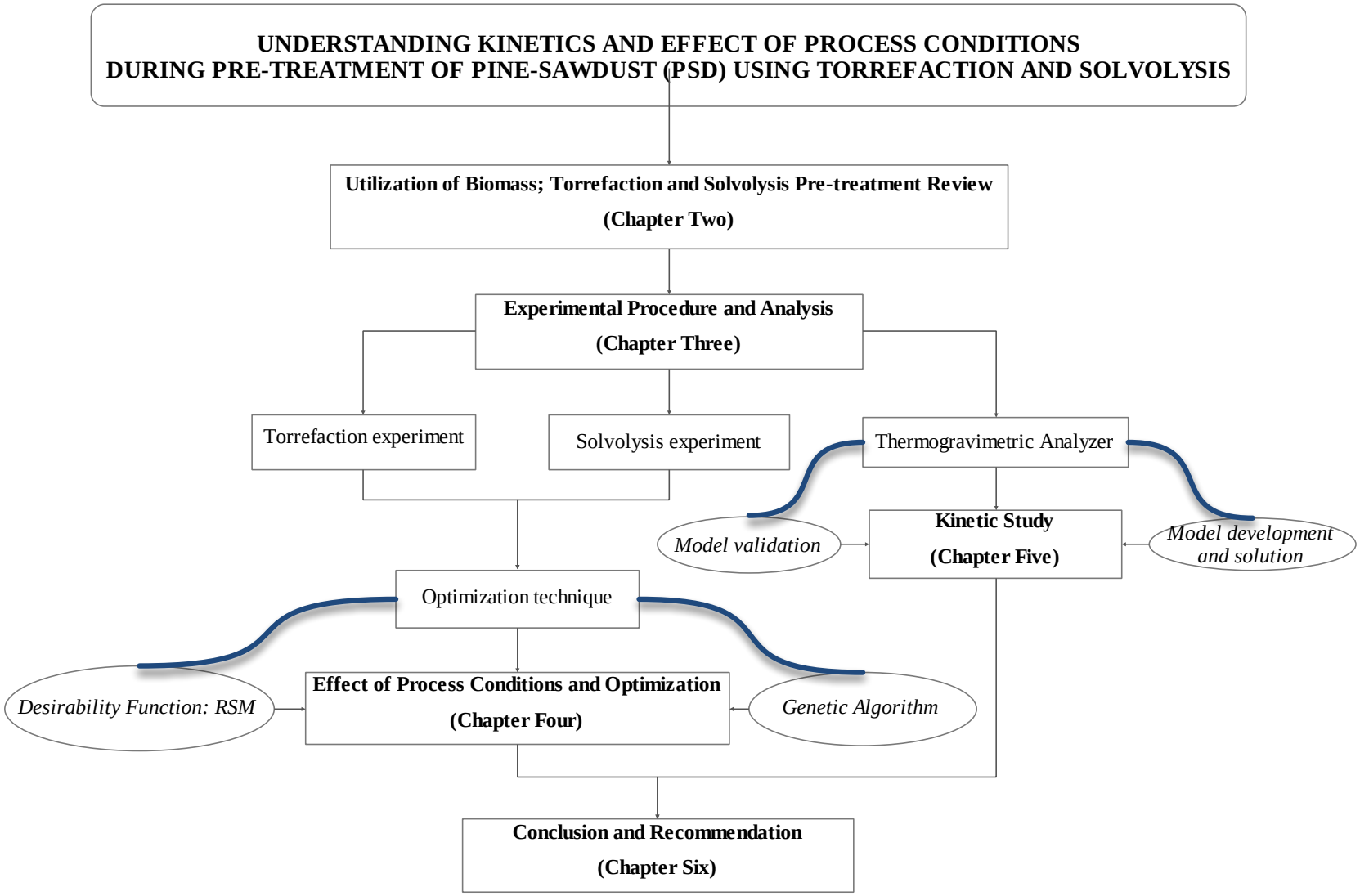


Figure 1.1. Overall Thesis layout and road map

CHAPTER TWO

2. LITERATURE REVIEW

2.1. Introduction

This chapter presents a thorough and comprehensive review of the two pretreatment processes, namely; torrefaction and solvolysis process, for the effective thermochemical conversion process of biomass. It begins with presenting a brief introduction of the pre-existing fossil fuel (coal) used for energy conversion via thermochemical conversion and its challenges, paving the way to explore biomass as an alternative. Furthermore, previous studies on the torrefaction and solvolysis processes were thoroughly reviewed and reported. The effects and optimization of various process conditions employed in the pretreatment processes were also critically reviewed. These reviewed process conditions stood as a basis for the experimental procedures employed in this study (Chapter three). Penultimately, previous studies centred on modelling the iso-thermal degradation of biomass via thermogravimetric analysis were reviewed, and pilot studies were reported in detail in Chapter six. Finally, other literature highlighting pilot studies where torrefaction and solvolysis have been employed, coupled with the results obtained and the knowledge gap identified in this research field are also reported in this chapter.

2.2. Utilization of Coal and its Global Challenges

Coal has generally been defined as a sedimentary rock, usually brown or black, with high Carbon and energy contents (Energy Information Administration, 2008). It is regarded as a non-renewable source of energy because it takes millions of years to get formed. Coal forms through physical, chemical and biological processes of accumulated plants residues (Kharagpur and Web, 2019). It is one of the most essential and common solid fuel known to man for energy generation and is a typical example of fossil fuel.

Coal is classified based on its characteristics such as; age, higher heating value, colour, proximate and ultimate analysis. Ranks of coal are classified according to the metamorphism

of the coal. Table 2.1 shows the proximate and ultimate analysis of the different ranks of coal. The ranks of coal in increasing order are; lignite coal, sub-bituminous coal, bituminous coal and anthracite coal and their approximate ages are 60 million years, 100 million years, 300 million years and 350 million years, respectively.

There have been similarities in the analysis of coal carried out by different researchers. As shown in Table 2.2, the lignite coal studied by Sanwal *et al.* (2018) has shown that most of the characteristics fell within the range of values reported by the other researchers. Coal as a fuel has different characteristics which play vital roles when it is used for energy generation. For instance, the calorific value, volatile matter, and ash content are considered before its use for energy production. Typically, the attraction towards coal as a source of energy is due to its high calorific value, also known as the higher heating value (HHV). Grootegeluk, common coal in South Africa, has been studied to have a calorific value of 19.8 MJ/kg and a relatively high ash content of 34.9 %. The high energy content of coal can be seen through its high calorific value.

Table 2.1. Proximate and ultimate analysis of the ranks of coal**.** Radovic (1997).

Proximate analysis (%)				Ultimate analysis (%)					
	VM	FC	MC	C	H	N	O	S	HHV(MJ) kg^{-1}
Lignite			70-30	65-72	5	<1	30	0	<16.28
Sub-bituminous			30-10	72-76	5-2	1	29-1	0-4	~23.26
Bituminous	15-31	69-86	10-5	76-90	5-2	2	29-1	4	27.91-34.88
Anthracite	2-14	87-98	5	90-95	2	>2	1	4-0	>34.88

Table 2.2. Proximate and Ultimate analysis of coal. Sanwal *et al.* (2018).

	Proximate analysis (%)				Ultimate analysis (%)				
	M	V	FC	A	C	H	N	S	O
Lignite coal	32.24	28.66	26.54	9.4	52.658	3.982	0.22	4.789	38.351

It was estimated that as of 2010, the estimated amount of coal in the South African's coal reserve was about 15 billion tonnes (Hartnady, 2010). Given South Africa's large dependency on coal for the generation of electricity, measuring up to about 88 % of coal consumed by Africa (Ma *et al.*, 2018), there has been a predicted production peak in 2020 which could cause an adverse effect on the economy and climate of South Africa. South Africa's dependency on coal for power generation is a big concern. South Africa stands as the 6^{th} largest coal miners and exporters globally and in possession of 6 % of the world's coal reserve. The coal industry contributes the largest quota of foreign exchange earnings and has the highest income from mining activities. It has been reported that coal contributes positively to South Africa's economy, and it serves as the mainstay of industrialization, contributing many employments to the people and an appreciable income (Falcon, 2013).

However, due to the extended numbers of years required for coal to form naturally beneath the earth surface, it has generally been classified as a non-renewable form of energy. As a fossil fuel, coal causes a large volume of green-house gas emission during its thermochemical conversion process. These emissions make it a non-eco-friendly source of energy. As a result of its carbon emission, coal exploration contributes to the world's global warming challenges. Furthermore, coal's high ash content may reduce the energy conversion system's efficiency, hence; increasing operational difficulties.

2.3. Biomass as a Sustainable Source of Renewal Energy and its Limitations

In recent years, the world has given increasing attention to the utilization of waste biomass feedstocks for energy generation via thermochemical conversion processes due to its

abundance, renewability, and considerable low carbon emission (Duan *et al*., 2020). This interest by the global energy industry is fostered by the constant fluctuation of petroleum products over the years; the concerns of climate change which results from global warming; and a need for energy security which cannot be offered by a non-renewable source.

In this study, Biomass can be described as any organic matter that includes; crops, woods, animal waste, that has high energy content. The energy content of agro-based (wood and crop) biomass are gotten from the process termed photosynthesis. Photosynthesis is the process whereby the plant absorbs carbon dioxide and water in the presence of sunlight, to produce carbohydrates (energy in the form of chemical, consisting of starch, sugar, cellulose, and lignin) and oxygen. The sunlight being absorbed is responsible for the high energy content. One of the challenges, peculiar to the efficient utilization of solar energy, is storage. Biomass through photosynthesis offers some form of a solution by storing some energy from the sun. This energy can in-turn be converted into other forms via thermochemical conversion processes.

The fuel and energy gotten from biomass are called biofuel and bioenergy, respectively. According to the Renewable Energy (Electricity) Act 2000 (Ness & Moghtaderi, 2003), the following are the primary biomass; agricultural crop residues, woody wastes, forestry wastes, and waste from food production industry, animal husbandry waste, municipal wastes, and black liquor. According to Dowaki & Mori (2005), biomass is regarded as one of the most sustainable sources of energy, and as a result, should be explored.

Biomass produces cleaner fuel than coal or other fossil fuels (e.g. petroleum) that produces many greenhouse gases. Biomass exhibits carbon-neutral characteristic and contains insignificant sulphur content, thereby eliminating the threat of emitting sulphur oxides (Mohan *et al.,* 2006). An estimated figure of about 14 % of the world's energy has been attributed to biomass. This figure has to rise as it has a significant role in carrying out global energy planning

and ensuring energy security (Şensöz, 2003). In accordance to the Renewable Fuel Standard, established by the Energy Policy Act of the United States in 2005, 4 billion gallons of renewable fuel was produced in 2006, and an expected increase to 36 billion gallons is expected by 2022 (United States EPA, 2020). Figure 2.1 shows the potential and more eco-friendly sources of biomass fuels for energy generation.



(a) (b)

(c) (d)

Figure 2.1. (a) Woody biomass (b) Crop biomass (c) Municipal waste (d) Animal waste

Source: www.biomassmagazine.com

First accessed: 01-Oct-2019

Figure 2.2 shows the distribution of the various renewable energy sources currently being explored (Antonio *et al.,* 2016). Amongst the key findings of Antonio and colleagues, wood fuel was reported as the most (68 %) supplier of energy amongst the biomass resources, with hydrogenated vegetable oil being the lowest (0.3 %) since 2013. This shows the feasibility of utilizing woody biomass for effective thermochemical conversion process. During the South Africa International Renewable Energy Conference (SAIREC) in 2015, it was estimated that 7.7 million jobs were created globally in 2014. In 4 decades for the first time, 2014 was the

first year a significant growth in the economy was not associated with the growth of CO_2 from the use of fossil fuels, which stood as a record for renewable energy (Adib *et al*., 2015).

The recent research focus on biomass has significantly shown the several benefits of biomass and bioenergy. Some of these merits are; it is a renewable and sustainable source of energy; the fuel produced from biomass is CO_2 neutral (i.e. it leaves a zero-carbon footprint, which tends to proffer solutions to global warming). The valorization of biomass also enables the use of nonedible matters, which creates a ripple effect on solving environmental pollution by reducing biomass waste. Also, biomass contains relatively low ash, high fixed carbon and little or no trace elements. It creates new jobs and income for the ever-growing population. The exploration of biomass tends to create diversification in energy sources to guarantee energy security and conserve fossil fuels. As waste biomass has zero value, it is a cheap raw material source for all the biomass-derived useful products such as fertilizers, building materials, biofuels, to mention a few.

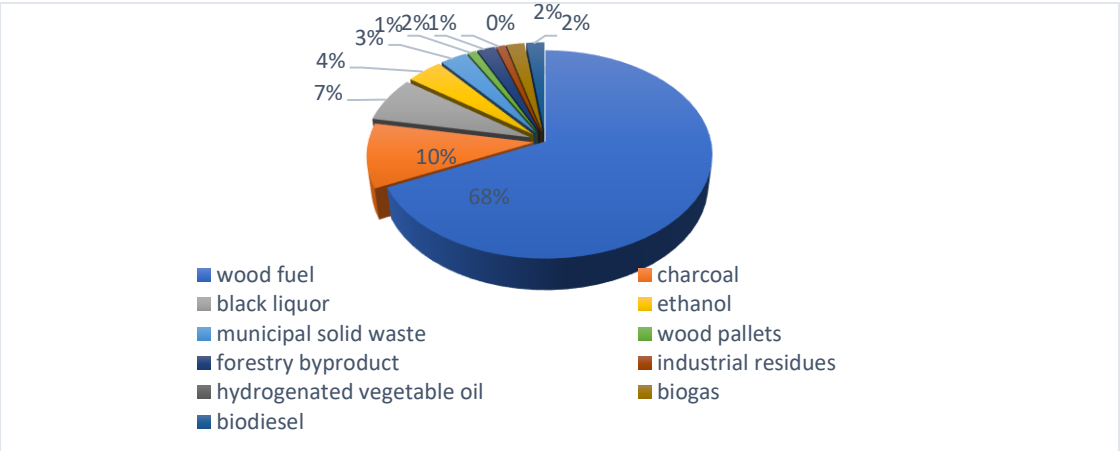


Figure 2.2. Distribution of various sources of renewable energy. (Antonio *et al*., 2016)

However, biomass has its limitations in terms of its application for energy generation. For example, raw biomass's moisture content makes the transportation of raw biomass from the waste sites (e.g. farm) to the plant site energy and cost-inefficient. This inefficiency is because

a significant amount of the cost of transportation and energy will be used to transport water encompassed in the moisture content of raw biomass. Likewise, raw biomass has auto-decaying properties, which poses a challenge for storage over a long time. The lignocellulosic nature of biomass reduces the biomass's grindability, thereby increasing transportation costs due to its size. Another limitation of using biomass for energy generation is inadequate knowledge to consider various biomass qualities and properties. This knowledge will be critical in carefully reviewing different biomass, and subsequently authenticating them for biofuel production. Other limitations attributed the use of biomass is; the high investment cost associated with it; the insufficient knowledge on the proper pretreatment technologies employed on biomass; and optimization of biofuel product for usage. Therefore, it is crucial to improve the raw biomass qualities to increase the efficiency of the thermochemical conversion process. Importantly, solving the energy in-security and emission of GHG issues in Africa and the world at large through the utilization of unconsolidated biomass waste should be considered as a priority (Pathak *et al.*, 2010).

The process of improving the fuel qualities of biomass material is called biomass pretreatment. There are different methods by which this can be achieved. They include; mechanical (physical), biological, chemical, and thermal pretreatments. Each of these methods is utilized depending on the quality of fuel required and its subsequent use. Generally, biomass exhibits some characteristics that require them to be pre-treated before conversion into biofuels and biogas.

Woody biomass is considered lignocellulosic biomass because of its CHL (Cellulose, Hemicellulose and Lignin) properties (Vassilev *et al.*, 2010). The cellulose is responsible for the firmness and stiffness of plants. It is an organic compound with the formula $(C_6 H_{12} O_5)_n$ with an unbranched polymer of glucose. Hemicellulose belongs to a group of different polysaccharides which contains both 5-carbon and 6-carbon sugars. Lignin is a more complex

molecule other than cellulose and hemicellulose, with a 3-D structure having phenyl-propane units linked to its chain.

In the processing of lignocellulosic biomass, the first step is the pretreatment step, i.e., removing the lignocellulosic biomass's refractory behaviour. Pretreatment of biomass leads to a change in the biomass's chemical structure orientation, as shown in Figure 2.3. According to Ashok *et al.* (2015), pretreatment of biomass is simply a process whereby the natural resistive behaviour of the carbohydrate lignin shield inhibits the interaction between the enzymes, heat or chemical hemicellulose is removed. Pretreatment is an essential step to take to upgrade the fuel quality of biomass. In this case, pretreatment is therefore defined as a process whereby the inhibiting characteristics of biomass are reduced through different methods, to improve the quality of fuel produced from it under a given optimal condition. For this study, torrefaction and solvolysis pretreatment methods will only be covered in this review.

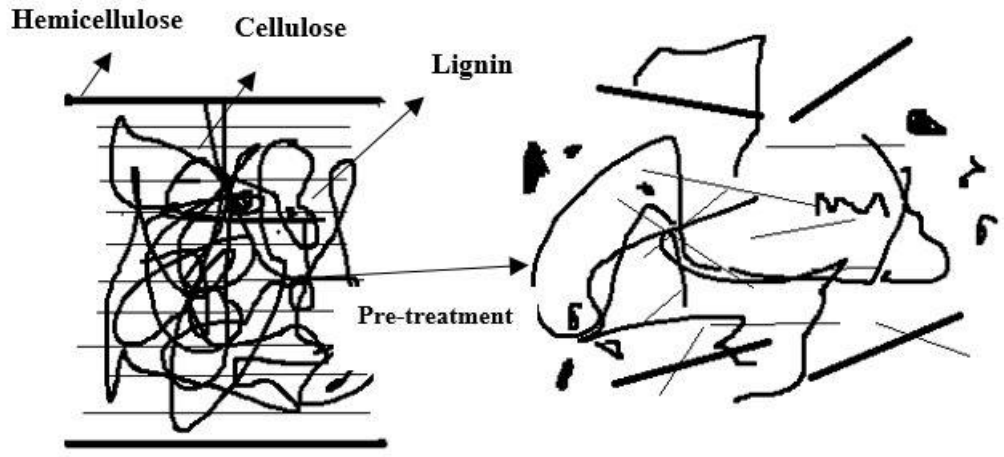


Figure 2.3. Schematic representation of the pretreatment of biomass. Adapted from Paulien *et al. (*2010)**.**

2.4. Overview of Torrefaction Pretreatment Process

Torrefaction is a thermal pretreatment process that involves processing a biomass feedstock (either grown or waste) in a torrefaction reactor often referred to as a torrefier. This process produces a charred product termed "biochar", that can be used as fuel for thermochemical

conversion in a coal-fired power plant (Anukam *et al*., 2017; Barskov *et al*., 2019). Torrefaction involves the heating of a known mass of biomass in an inert atmosphere (absence of oxygen) for a particular time and producing a torrefied product. This product generally poses improved fuel properties compared to raw biomass. For this study's purpose, the benefits of biochar as regards bioenergy generation will only be considered.

Torrefaction is often referred to as a mild pyrolysis process because of the low range operating temperatures between 200 and 300 °C in an inert atmosphere (usually nitrogen) as the carrier gas to prevent full combustion within a residence time of 15 mins – 2 hrs (Li *et al*., 2018; van der Stelt *et al*., 2011; Yu *et al*., 2019). During the torrefaction process, different reactions occur, namely: loss of free moisture content, devolatilization of light compounds, decomposition of a fraction of the lignocellulosic composition, and biochar formation (Cha *et al*., 2016). The biochar produced after these processes has a similar physical appearance as conventional coal with similar chemical and fuel properties. Hence, torrefied biomass can considerably measure up to coal by producing good quality energy via thermochemical conversion (Sikarwar *et al*., 2017).

Three main products are gotten from a typical torrefaction process, namely; the solid product which is called the biochar, the liquid product which is called the condensable volatile organic compounds (majorly consisting of water, some organics and aromatic compounds), and the gas which is known as the un-condensable inorganic compounds (majorly consisting of CO, CO_2, traces of H_2 and CH_4) (Felfli *et al.*, 2005; Stelte, 2012). The main essence of carrying out torrefaction is to improve the fuel properties of biomass. These fuel properties are; the Higher Heating Value (HHV), the grindability, the hydrophobicity, the oxygen-to-carbon ratio and hydrogen-to-carbon ratio. Torrefaction pretreatment process has been reported to improve the fuel properties mentioned above (Brachi *et al*., 2019; Grycova *et al.*, 2020; Rago *et al*., 2020).

Numerous efforts have been made to give insights and critically review the techno-economic assessment of replacing coal with torrefied biomass in a coal-fired power plant for hydrogen-rich syn-gas production (Akbari *et al*., 2020; Ozonoh *et al*., 2019). A wide range of biomass (both cultured and waste) has been used as feedstocks for the torrefaction process. Some of these biomasses are; spruce, straw, grass, rice husk (Grycova *et al*., 2020), oil palm fibre, eucalyptus (Lu *et al*., 2012), beechwood (Ohliger *et al*., 2013), pinewood (Chen *et al.*, 2016), pine sawdust (Gong *et al*., 2016), sap and heartwood (Phanphanich and Mani, 2011), corncob (Li *et al*., 2018), birch wood (van der Stelt *et al*., 2011), timothy hay (Nhuchhen *et al.*, 2018). Some other biomass that has been used are sugarcane bagasse, bamboo, banyan, willow, reed canary grass, walnut shell, tomato peels and bug weed, to mention a few.

Recent review papers have been published to highlight the progress and new areas of interest in the torrefaction process. With increased understanding of this process over the years, breakthroughs and promising observations have been reported in recent review articles. For instance, Barskov *et al*. (2019) reviewed experimental procedures for the torrefaction of lignocellulosic, food waste and non-lignocellulosic biomass and enumerated that average torrefaction process conditions yielded enhanced biofuels. Nunes *et al*. (2014), reviewed the viability of using torrefied biomass and coal in a co-firing plant for generating power. Ribeiro *et al*. (2018) reviewed the already existing techniques employed in carrying out torrefaction. The importance of process parameters employed during torrefaction pretreatment process on the product biochar was also highly emphasized. Emphases of the effect of the torrefier design on the product were also made. Olugbade & Ojo (2020) reviewed pre-existing torrefaction technologies including; wet, dry and ionic-liquid torrefaction and their different operating mechanism. Great attention was focused on both the torrefier design and the techno-economical aspect of implementing the thermochemical conversion of torrefied biomass. Cahyanti *et al*. (2020a&b) reviewed impact of torrefaction process on the environment. The economic

challenges such as the high competitiveness faced by torrefied biomass were also evaluated. The review concluded that the integration of torrefaction with other processes would significantly increase its economic viability.

Although numerous review journals have been published on the various aspects of torrefaction process in the last decade, very few of these researchers have given attention to the review of detailed effects of process conditions employed during torrefaction process on the produced biochar, modelling the process as well as optimizing the operating parameters for optimal biochar yield. Hence, the following subsections give a short review of the recent studies centred around the interactional effect of operating temperature, residence time and mass of biomass feed employed during torrefaction process and optimizing the process.

2.4.1. Torrefaction pretreatment process: Effect of process conditions

The decomposition of the lignocellulosic composition of biomass during torrefaction process plays a significant role in producing quality biochar. The operating temperatures employed during torrefaction is greatly responsible for this decomposition (Kumar *et al*., 2020). Some other process conditions contributing to this decomposition reaction are the biomass's residence time in the torrefier, the flow rate of carrier gas, and the biomass feed mass.

The effect of mass feed on torrefaction of biomass has been investigated using a thermogravimetric analyzer. This effect is being highlighted by the HTZ (i.e. the total temperature width at half the maximum mass loss rate) recorded using a TA instrument. A large mass of biomass feed translates to a large quantity of biomass particles between the surfaces inside the torrefier. Due to the low conductivity property of biomass, studies have reported a limitation in the transference of heat from the heating source of the torrefier to the biomass sample. This limitation results in an increase in the temperature gradient around the biomass sample's cross-sectional area as the heating rate increases (Ceylan, 2015; Gai *et al*.,

2013; Gajera *et al*., 2020). As a result of this heating limitation, this suggests that higher temperatures will be required to ensure uniform decomposition of the lignocellulosic components throughout the biomass sample.

Several researchers have studied the effect of the operating conditions employed during the torrefaction pretreatment process to compare the biochar's fuel properties to the raw biomass feed. Grycova *et al*. (2020) carried out a study to determine the operating temperature and residence time at which quality biochar can be produced from the torrefaction of sorghum biomass, straw and rice husk. The experiments were carried out within a temperature range of 200 and 300 °C and residence time of 10 and 45 min. It was reported that at torrefaction temperatures between 275 and 300 °C, it was significant enough to decompose the hemicellulose. The further degradation of cellulose and a fraction of the lignin suggested that the heating time should preferably be increased than the temperature. It was also reported that although the fuel properties of biochar kept increasing with increasing temperature, the increase in the carbon-to-oxygen ratio content and the higher heating value at the start temperature of 200 °C was insignificant for all the biomass samples. This observation suggested that torrefaction temperature had a more significant effect on the biochar. However, the increase in temperature resulted in a massive decrease in the mass yield, which affected the biochar's energy yield. It was concluded that the minimum residence time for torrefaction should be 45 min to see a significant change in biochar qualities. The torrefaction process should also be kept at an average temperature (225 – 250 °C) to minimize the mass loss to be economically viable.

Jagodzińska *et al*. (2020) studied the effect of torrefaction temperature and residence time on the biochar properties. This investigation was carried out on wheat-barley straws and wheat-rye chaff. Temperature range of 280 – 320 °C and residence time of 30 – 75 min were studied.

It was reported that the influence temperature has on the product yield of biochar is higher than that of time. It was concluded that the biochar produced at 320 °C while holding the biomass for 75 mins in the batch reactor was considered a quality fuel. Employing these operating conditions reduced the mass of biomass by 40 %.

The torrefaction of four different biomasses of Columbia origin, namely; *Pinus Maximinoi; Pinus Patula; Eucalyptus Grandis; Gmelina Arborea,* were studied by Pérez *et al.* (2019). While holding the torrefaction time constant at 30 min, the effect of torrefaction temperature between 200 and 300 °C were reported. As traditionally observed, the mass yield of the biochar significantly dropped with the increase in temperatures. It was observed that early temperatures such as 200 °C recorded an insignificant reduction in mass. Furthermore, a reduction in energy yield was recorded with increasing temperature. Although there was only a slight increase in the fuel ratio (fixed carbon-to-volatile matter ratio) for one of the biomass sample at 200 °C (this is as a result of the proximate analysis of the specie), there was a highly significant reduction in the VM-to-FC ratio for all samples for temperatures beyond 200 °C. It was concluded that torrefaction provides a promising future for the thermochemical conversion of biomass. Similarly, Nhuchhen *et al.* (2018) reported that the variation of the heating rate of the torrefaction process below 50 °C/min relatively has a lower impact on the fuel properties of biomass.

Yılgın *et al*. (2019) reported the biochar properties produced from beechwood sawdust. The investigated torrefaction temperature was between 220 and 300 °C. The residence time was left at 10 min while the heating rate was set such that it took 40 min to reach the operating temperature. No moisture was recorded for the biochar produced. This observation was because the minimum temperature was well enough to remove all free moisture present in the biomass sample. A 35 % increase in the higher heating value of the biochar (being the highest) was

recorded at 300 °C, and it recorded a massive 50 % reduction in mass yield of biochar. It was concluded that mild torrefaction (260 °C) would be most suitable to avoid a massive mass reduction in biomass and produce coal-like biochar that measures up to its higher heating value.

Wang *et al*. (2018) reported the physicochemical properties of biochar produced from stem wood, stump and bark. Operating temperatures and residence time of 225 – 300 °C and 30 – 60 min were employed. The severity of torrefaction is proportional to the temperature and time employed during the process. It was reported that both the hemicellulose and cellulose compositions reduced with increase in severity. The study also suggested that the impact of temperature on the mass yield of biochar was significantly higher than the influence of time. The same observation was reported for the higher heating value of biochar. Higher torrefaction severity (i.e. higher temperature and time) resulted in a decrease in the hydrogen-to-carbon ratio and the oxygen-to-carbon ratio. The significant reduction in particle size and the energy required for the grinding of biochar with increasing torrefaction severity was also reported. It was concluded that the mild torrefaction of biomass (275 °C) was efficient to significantly improve the fuel properties and grindability of biochar while obtaining a relatively high mass yield.

The effect of temperature, time and flow rate of carrier gas on torrefied ground coffee residue was studied by Pathomrotsakun *et al*. (2020). While varying the temperature, time and flow rate of gas between 200 – 300 °C, 30 – 60 min and 50 – 250 mL/min respectively, it was reported that temperature had the most significant effect on the fuel properties. In contrast, the flow rate effect was marginal. Hence, the least gas flow rate studied (50 ml/min) was suggested as the best condition to employ, with a severe temperature of 300 °C and residence time of 30 min. It was concluded that torrefaction of biomass while employing these conditions, can efficiently produce biochar with comparable properties as sub-bituminous coal.

Li *et al*. (2018) carried out a comparative analysis of corncob biomass's torrefaction in a carbon dioxide and nitrogen atmosphere. Although CO_2 was recommended for the torrefaction process based on the results obtained, both atmospheres significantly improved corncob's fuel properties. At the most severe torrefaction temperature (300 °C), under the nitrogen and carbon dioxide atmosphere, the biochar's heating values improved by a factor of 1.5 and 1.46 respectively.

Martín-Lara *et al*. (2017) studied process parameters' effect on torrefied olive tree pruning's fuel properties. This study reported a significant improvement in the fuel properties of raw olive tree biomass. The effect of torrefaction temperature was reported to have higher significance than operating time on the biomass sample's proximate and ultimate analyses. However, operating time was reported to significantly improve the higher heating value of biomass than the torrefaction temperature. It was also reported that the decomposition of hemicellulose during torrefaction was predominant while a mild decomposition of cellulose took place at severe torrefaction temperatures. The promising future of the torrefaction process was established as it could convert lignocellulosic biomass into coal-like materials. This conclusion was made based on the improvement in carbon-to-oxygen and carbon-to-hydrogen ratios and the decomposition of the lignocellulosic composition of raw biomass at severe temperature (300 °C).

A study on enhancing fuel properties of torrefied energy and sweet sorghum biomass was carried out by Yue *et al*. (2017). While employing torrefaction temperatures between 250 and 300 °C and residence time of 30 min, it was reported that the mass yield significantly reduced with increase in torrefaction temperature. The higher heating value of energy and sweet sorghum was significantly improved compared to raw biomass. However, as the torrefaction

temperature increased from 275 to 300 °C, the higher heating value reduced for only energy sorghum.

Table 2.3 provides detailed process conditions employed by different authors and their corresponding fuel properties of biochar produced from torrefaction pretreatment process. The difference in the various biochar's fuel properties can be attributed to the difference in the different biomass's chemical structure and composition. Also, the use of different operating conditions can result in different fuel properties of biochar. The difference in the fuel properties of biochar produced from pinewoods between different authors, as seen in Table 2.3 suggests that the same type of biomass can exhibits different properties when subjected to different process conditions.

In conclusion, the process condition such as; operating temperature, residence time, the flow rate of inert gas, and the mass of biomass feed substantially impact the mass and energy yield of torrefied biomass, with temperature having the most influence on the fuel properties of biochar. Though severe torrefaction temperature produces a coal-like product with enhanced fuel properties, employing a mild temperature with a long residence time, relatively produce biochar comparable to coal while conserving a large mass of the biomass feed. The enhanced biochar produced via torrefaction pretreatment process can efficiently be co-gasified with coal in a coal firing plant.

Table 2.3. Process conditions employed for the torrefaction of different biomass and their corresponding improved fuel properties.

Biomass	T (°C)	t (min)	flowrate (mL/min)	MY (%)	EY (%)	HHV (MJ/kg)	Ref.
Sugarcane bagasse	300	5	500	80	90	20.19	Anukam *et al*. (2017)
Corncob	220 – 300	30	100	69 – 95	85 – 95	17 – 25	Li *et al*. (2018)
Wood pellets	210 – 310	15 – 60	10000	86 – 39	61 – 99	20 – 27	Yu *et al*. (2019)
Wood residues	220 – 270	30 – 75	NR	43 – 94	50 – 97	21 – 23	Felfli *et al*. (2005)
Empty fruit bunch	220 – 300	30	500	27 – 46	NR	17 – 20	Uemura *et al*. (2011)
Mesocarp fibre				48 – 67		19 – 22	
Kernel shell				70 – 80		19 – 22	
Woody fir pellets	200 – 250	15	3300	52 – 90	65 – 94	21 – 24	Brachi *et al*. (2019)
Olive pomace				56 – 80	75 – 95	24 – 27	
Sorghum	200 – 300	10 – 45	10000	25 – 82	55 – 95	17 – 23	Grycova *et al*. (2020)
Straw				20 – 84	50 – 95	17 – 23	
Rice husk				45 – 90	57 – 97	17 – 19	
Spruce				30 – 90	52 – 98	20 – 24	
Mango branches	300	30	500	70	NR	21	Rago *et al*. (2020)
Waste newspaper				73		19.56	
Polyethylene				99		47.54	
Beechwood	270 – 300	15 – 60	500 –1000	NR	NR	NR	Ohliger *et al*. (2013)
Pine wood	220 – 280	30	400	NR	NR	NR	Chen *et al*. (2016)
Pine saw dust	230 – 290	30 – 60	400	50 – 95	70 – 97	20 – 26	Gong *et al*. (2016)
Pine chips	225 – 300	30	200	52 – 89	71 – 94	18 – 25	Phanphanich *et al*. (2011)
Sap and heart wood				52 – 88	72 – 92	19 – 28	

Wheat-barley straw	280 – 320	30 – 75	NR	NR	NR	NR	Jagodzińska *et al*. (2020)
Wheat-rye chaff							
Pinus maximinoi	200 – 300	30	150	70 – 98	75 – 98	NR	Pérez *et al*. (2019)
Pinus patula				68 – 98	77 – 97		
eucalyptus grandis				70 – 98	80 – 97		
Gmelina arborea				55 – 98	65 – 96		
Beech wood	220 – 300	10	100	50 – 90	68 – 94	NR	Yılgın *et al*. (2019)
Spruce stem	225 – 300	30 – 60	1000	58 – 92	68 – 93	20 – 24	Wang *et al*. (2018)
Spruce stump				46 – 93	56 – 94	20 – 23	
Spruce bark				61 – 90	72 – 97	21 – 24	
Coffee residue	200 – 300	30 – 60	50 – 250	NR	NR	25 – 32	Pathomrotsakun *et al*. (2020)
Olive tree	200 – 300	10 – 60	4000	57 – 87	64 – 102	19 – 20	Martín-Lara *et al*. (2017)
Sweet sorghum	250 – 300	30	2000	43 – 65	NR	20 – 27	Yue *et al*. (2017)
Energy sorghum				51 – 70		21 – 24	
Timothy hay	220 – 300	15 – 45	4000	50 – 90	38 - 82	19 - 23	Nhuchhen *et al*. (2018)

T – Temperature; t – Time; LSR – Liquid-to-Solid Ratio; NSR – Nitrogen-to-Solid Ratio; MY – Mass Yield; EY – Energy Yield; HHV – Higher Heating Value; NR – Not Reported.

2.4.2 Optimization of torrefaction process

Several researchers have indicated the need to optimize the process conditions employed during the torrefaction process. From literature, it can be observed that the higher heating value of torrefied biochar increases as the mass yield reduces. Hence, there is a need to achieve an optimized process to ensure an optimal energy yield (i.e. both the higher heating value and the mass yield). Also, the quantity and quality of biochar produced as a feedstock for coal firing plants can be improved by optimizing the process. Therefore, it can be said that the optimization of the torrefaction process is simply the maximizing of the higher heating value of biochar and the minimizing of the mass loss of feed biomass.

Lee & Lee (2014) carried out the optimization of the torrefaction of some biomass samples via regression analysis. Seven biomass samples, namely; Eucalyptus, Larch, Acacia, Mixed softwood, Yellow poplar, Albasia and Oil palm residues, were used as feed biomass for the process. The technique used for the optimization was known as the mass loss and energy gain method. Regression analysis technique was used to model the higher heating value and the mass loss of the process with respect to the severity (i.e. torrefaction temperature and residence time) of the process. It was reported that the optimization technique used was efficient in optimizing the process. The authors concluded that the optimal conditions for the seven types of biomass's torrefaction were averagely 248.55 °C and 60 min.

Singh *et al*. (2019) optimized the process conditions for the torrefaction of *Acacia Nilotica* biomass using the Response Surface Methodology (RSM) based on Face central Composite Design (FCCD). This design was chosen because it requires a relatively small number of experiments and provides adequate means of studying the process conditions' interactional effect. The developed models were significant and accurate enough to predict the higher heating value and energy yield as a function of the torrefaction temperature, residence time and heating rate. It was concluded that the optimal operating conditions for the torrefaction process

were 252 °C, 60 min and 5 °C/min. Also, the authors indicated torrefaction as a promising technology for enhancing the fuel properties of biomass. In conclusion, the authors reported that the importance of optimizing torrefaction process is; it helps to reduce operational cost when upscaling to an industrial level. These improved fuel properties also increase the efficiency during the thermochemical conversion of the biochar in a coal firing plant.

The same experimental design was employed by Kumar *et al*. (2020) to optimize the torrefaction of Eucalyptus biomass. Similar observations that temperature and time had negative and positive effects on the mass yield and higher heating value of biochar, respectively, were reported by the authors with temperature having a more significant effect. It was concluded that the optimal torrefaction operating conditions were near 280 °C and 60 min.

RSM based on Central Composite Design was also used by Keivani *et al*. (2018) to optimize the process conditions during red pine wood biomass torrefaction. Significant effect of torrefaction temperature and residence time on fuel properties of biochar was reported, and the optimal conditions were recorded to be approximately 300 °C and 30 min. As previous authors have concluded, it was also reported by Keivani and colleagues that torrefied biomass could efficiently act as a supplement fuel in a coal-fired plant.

Buratti *et al*. (2018) used RSM based on Box-Behnken Design (BBD) to optimize the process conditions during coffee residues' torrefaction. A three-level, 3-factor approach was used to determine the interactional effect of the process conditions. The models developed based on BBD were reported to give high statistical accuracy. The optimal torrefaction temperature and time were reported to be 271.7 °C and 20 min, respectively.

As observed from the above literature, different optimal conditions have been suggested for the torrefaction of different biomass types. It can therefore be inferred that the optimal conditions for the torrefaction of any biomass sample depend on the type of biomass; the

experimental procedures employed; the operating conditions studied; and the fuel properties that are of interest. Although various optimization techniques have been used to optimize this pretreatment process, Response Surface Methodology has been widely reported to give high statistical accuracy for modelling this process. The developed models, techniques employed, and their optimized process conditions reviewed in this chapter are summarised in Table 2.4 for torrefaction pretreatment method.

The standard technique behind the different methods employed to optimize the torrefaction process is to maximize the energy content while achieving a sizeable mass yield of biochar. Lee & Lee (2014) used the severity factor to combine the operating temperature and time effect, as shown in Equation (2.1).

The severity factor (SF) equation illustrates that while SF increases linearly with time, the SF increases exponentially with temperature. This equation shows the strong influence of operating temperature on the final fuel properties of char produced.

$$SF = \log\left\{t \times exp\left[\frac{T_r - T_o}{14.75}\right]\right\} \quad (2.1)$$

Where SF is Severity Factor; t is time (min); T_r is torrefaction temperature (°C); T_o is reference temperature (100 °C).

Table 2.4. Summary of developed predictive models explaining the interactional effect of process conditions during torrefaction.

Biomass	Model Technique	Model	Optimal Condition	Ref.
Eucalyptus	Energy gain and Mass loss	$HHV = 0.0289SF + 0.7670$ $ML = -0.1351SF + 1.7603$	245.3 °C 60 min	Lee & Lee (2014)
Larch		$HHV = 0.0699SF + 0.5168$ $ML = -0.0802SF^2 + 0.8591SF - 1.29$	250.5 °C 60 min	
Yellow poplar		$HHV = 0.0685SF + 0.526$ $ML = -0.1652SF + 1.941$	245.3 °C 60 min	
Mesocarp		$HHV = 0.04SF^2 - 0.427SF + 2.048$ $ML = -0.198SF + 2.137$	246.8 °C 60 min	
Acacia		$HHV = 0.039SF + 0.707$ $ML = -0.037SF^2 + 0.317SF + 0.375$	247.8 °C 60 min	
Albasia		$HHV = 0.041SF + 0.694$ $ML = -0.037SF^2 + 0.319SF + 0.373$	248.2 °C 60 min	

Mixed softwood		$HHV = 0.065SF^3 - 1.15SF^2 + 6.81SF - 12.57$ $ML = -0.12SF^3 + 2.09SF^2 - 12.26SF + 25.05$	256.0 °C 60 min	
Acacia nilotica	RSM (FCCD)	$HHV = 21.26 - 0.73T - 0.028t - 0.028\beta$ $+0.0001Tt + 0.0001T\beta - 0.00008t\beta + 0.00002T^2$ $-0.0003t^2 - 0.0002\beta^2$ $MY = -287.37 + 3.307T - 0.337t + 0.470\beta$ $+0.0003Tt - 0.0018T\beta + 0.0046t\beta - 0.0074T^2 + 0.0027t^2$ $- 0.0184\beta^2$	252.0 °C 60 min 5 °C/min	Singh *et al.* (2019)
Eucalyptus	RSM (FCCD)	$HHV = 21.39 + 2T + 0.46t - 0.05Tt + 0.72T^2$ $-0.17t^2$ $MY = 59.49 - 17.93T - 2.17t + 1.10Tt + 1.22T^2$ $+0.524T^2$	280.0 °C[a] 60 min	Kumar *et al.* (2020)
Pinewood	RSM (FCCD)	$HHV = 155.95 + 9.93T + 10.5t + 4.73Tt$ $-3.15T^2 - 3.06t^2$ $MY = 61.42 - 19.74T - 14.29t - 0.7874Tt$ $+5.15T^2 + 12.39t^2$	299.7 °C 28 min	Keivani *et al.* (2018)
Coffee chaff	RSM (BBD)	$HHV = 22215.6 + 1923.9T + 305.7t - 41.7\beta$ $+408.4T^2 + 403.6t^2 + 285.7\beta^2 - 271.6Tt$	271.1 °C 20 min 5 °C/min	Buratti *et al.* (2018)

		$-370.4T\beta + 354.5t\beta$ $ML = 28.81 + 14.75T + 4.27t + 0.87\beta - 1.14T^2$ $-0.62t^2 + 0.91\beta^2 - 0.30Tt - 0.76T\beta + 0.25t\beta$		
Spent coffee grounds	RSM (BBD)	$HHV = 27409.4 + 3859.5T + 403.3\ t + 412.6\beta$ $-246.8T^2 + 551.2t^2 + 279.5\beta^2 - 477.4Tt$ $-227.3T\beta - 346.5t\beta$ $ML = 24.694 + 15.73T + 4.11t + 1.12\beta - 2.16T^2$ $+0.36t^2 + 0.213\beta^2 + 0.42Tt - 0.123T\beta - 0.852t\beta$	256.0 °C 20 min 25 °C/min	Buratti *et al.* (2018)

HHV (MJ/kg) – Higher Heating Value; ML (%) – Mass Loss; MY (%) – Mass Yield; SF (-) – Severity Factor; T (°C) -Temperature; t (min) – Time; β (°C/min) – Heating rate; RSM – Response Surface Methodology; FCCD – Face Central Composite Design; BBD – Box-Behnken Design; [a] – Determined based on maximum HHV.

2.5. Overview of Solvolysis Pretreatment Process

In recent years, solvolysis pretreatment has begun to gain research attention due to its promising results in enhancing biomass fuel properties. Solvolysis pretreatment, often referred to as a liquid hot water pretreatment process has been described as an eco-friendly biomass pretreatment process because of its non-usage of chemicals and deionized water (Jin *et al*., 2016; Lei *et al.,* 2013). Other terminologies used to describe this process are hydrothermal, hydro thermolysis, aqueous fractionating and subcritical water pretreatment (Paulien *et al*., 2010).

Solvolysis pretreatment is a process whereby biomass is immersed into water at high temperatures between 150 – 260 °C (Hassan *et al*., 2018; He *et al*., 2018; Rackemann *et al*., 2019; Yang *et al*., 2015). Generally, this process, at a mild temperature of 150 °C, initially lead to partial solubilization of the hemicellulose present in the biomass. As the temperature approaches 180 °C and above, the lignin begins to dissolve. The common nomenclature for solvolysis product is termed “hydrochar”. This hydrochar can be furtherly used as a fuel for energy production and sometimes for soil amendment. For this study's purpose, only hydrochar as a coal supplement in a coal-firing plan will be discussed.

Like the torrefaction process, higher temperatures and residence time have been reported to decrease the solid yield and increase the higher heating value of biomass (Wang *et al.*, 2018). The typical operating conditions employed during solvolysis pretreatment process entails the use an inert gas (i.e. Nitrogen gas) to purge out the oxygen from the reactor, with the operating temperature between 150 – 260 °C and residence time of 5 – 240 min (Kambo & Dutta, 2014; Rafein *et al*., 2015).

Several reactions take place during the solvolysis pretreatment process. Three main products are derived from solvolysis pretreatment of biomass namely; the liquid product (which contains

some useful ions extracted from biomass such as phosphorus and bio-oil), the gaseous product (which comprises of H_2O, CO_2, H_2, CO and CH_4), and the solid product (hydrochar, i.e. a carbon-rich material). For this study, attention is given to only the solid product. This product known as hydrochar has been indicated to measure up to the quality of coal and be efficiently used as fuel in a coal firing plant for thermochemical conversion (Wu *et al*., 2018).

2.5.1. Solvolysis reaction mechanism

The reaction that explains the mechanism behind the conversion of biomass into a coal-like fuel during the solvolysis pretreatment process and the kinetics has been reported to be currently unknown. This knowledge gap is due to the limited research studies carried out in this area (Ahmed *et al*., 2019; Funke *et al.*, 2010). As shown in Figure 2.4, solvolysis (i.e. hydrothermal carbonisation) reaction occurs at the subcritical water region (Kruse & Karlsruhe, 2008). This subcritical water region is characterised by water being held by pressure between a temperature higher than the boiling point of water (100 °C) and the critical temperature (374 °C) of water. Andrea & Karlsruhe considered three different reactions that could take place at different temperatures and pressures, with the three reactions being able to convert biomass into various valuable products. The three possible reactions are namely; Hydrothermal Carbonisation (HC) (i.e. solvolysis), Hydrothermal Liquefaction (HL), and Hydrothermal Gasification (HG).

As a general knowledge from physical science, the properties of water under a subcritical condition change spontaneously. As the subcritical temperature is reached, the dielectric constant of water decreases. Hence, reducing hydrogen bonds' strength in water produces a high ionization constant, leading to water transformation into an acidic hydronium ion and basic hydroxide ions (Gordillo & Mart, 2001; Savage, 1999).

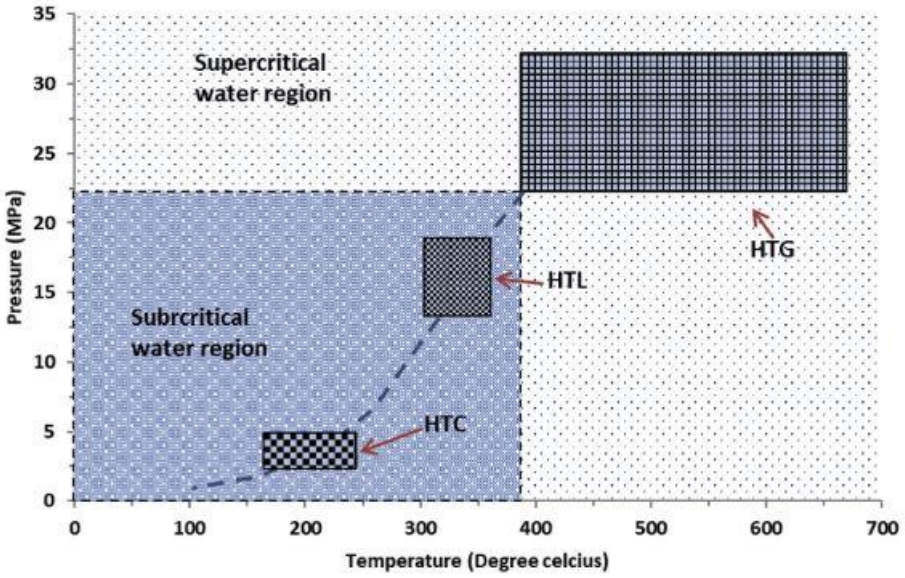


Figure 2.4. Stages of hydrothermal conversion of biomass**.** (Adapted from Kruse & Karlsruhe (2008)).

The acidic mutation of water at the subcritical temperature region provides a suitable medium for acid catalysed reaction of the organic compounds during solvolysis without any additional acid solvent. During solvolysis pretreatment of biomass, the biomass sample's moisture content also provides a suitable medium for this reaction.

Decomposition reaction of the lignocellulosic component of biomass is quite different from the decomposition under an inert atmosphere. The hemicellulose reactivity, cellulose, and lignin in a hydrothermal medium are relatively more complicated than in a torrefaction process. As a result of the weak hydrothermal stability of hemicellulose, Bach & Skreiberg (2016) reported that the decomposition of hemicellulose efficiently occurs at low solvolysis temperatures between 150 – 200 °C. Since cellulose possesses a more crystalline structure than hemicellulose, it makes it more hydrothermally stable, pushing its decomposition temperature range to 200 – 250 °C. The hydrothermal operating temperature has been inferred as insufficient to decompose the lignin component of biomass due to lignin's high thermal stability (Kruse *et al*., 2011).

Several studies have been carried out on the pretreatment of some biomass via solvolysis method. Some of these biomasses are oil palm (Nakason *et al.*, 2017), corn stalk (Lei & Tian, 2016), prairie cordgrass (Lei *et al*., 2013), *miscanthus* (Kambo and Dutta, 2014), food waste (Ul *et al*., 2018), cedarwood (Li *et al*., 2018). Some other biomass types previously studied are corn stover, rice husk, Tahoe mix, loblolly pine, stem spruce, stem birch, to mention a few.

Various researchers have identified solvolysis pretreatment method as a promising technology for enhancing the fuel properties of biomass such as the higher heating value, the oxygen-to-carbon ratio, the hydrogen-to-carbon ratio, the grindability. Over the last decade, some researchers have compiled and reviewed the various aspects of solvolysis process. For instance, Ahmed *et al*. (2019) reviewed the various effect of process conditions employed in the production of hydrochar from lignocellulosic biomass. They gave insights to the promising prospects of this technology for the energy industry. Bach & Skreiberg (2016) and He *et al*. (2018) reviewed the significant difference in the chemical composition and fuel properties of both biochars (i.e. from torrefaction) and hydrochar (i.e. from solvolysis) with the results showing similar qualities. The process conditions employed, as well as their respective advantages and challenges, were also reviewed.

He *et al*. (2015) reviewed the various roles of each process parameters during the production of hydrochar for biogas production. The reaction undergone by the lignocellulosic components of biomass during hydrothermal treatment were also reviewed. Wang *et al*. (2018) reviewed the process conditions of forming a carbon-rich hydrochar from biomass waste via hydrothermal pretreatment. Recommendations on future studies, to exploit this technology's potential in the bioenergy industry were also reviewed.

Acharya *et al.* (2015) reviewed the similarities and difference between dry torrefaction and wet torrefaction (i.e. solvolysis) of biomass. Although similar enhanced fuel properties of charred

products were reported, the authors identified differences in the individual processes' cost. It was concluded that biomass having high moisture content should be pre-treated using wet torrefaction. An article by Shen (2020) also reviewed the process behind the conversion of waste biomass and plastics to high energy hydrochar and the various uses of hydrothermal carbonisation products.

Although several articles have been published over the last decade on the pretreatment of biomass via solvolysis as well as studying the effect of process conditions on the fuel and physicochemical property of biomass, none of the above authors above has specifically reviewed the interactional effect of process conditions such as; temperature, time and liquid-to-solid ratio, on the fuel properties and yield of hydrochar. A review on optimising process conditions for producing carbon-rich hydrochar from biomass waste via solvolysis process lacks literature. Hence, the following subsection will provide a short review of these interactional effects and the optimization of the process conditions.

2.5.2. Solvolysis pretreatment process: Effect of process conditions

As discussed in the preceding subsection, different reactions occur during the pretreatment of biomass via the solvolysis process. One of these reactions is the depolymerisation of the lignocellulosic components. This reaction dramatically influences the quality of hydrochar produced. Some of these qualities that need to be improved are the; oxygen-to-carbon ratio, hydrogen-to-carbon ratio, higher heating value. These qualities depend on the process conditions employed during the process, such as the operating temperature, residence time, liquid-to-solid ratio, heating rate, reactor design.

Lynam *et al*. (2015) investigated the effect of process conditions on five different types of biomass. The effects of three process conditions were studied, namely; the temperature (200 – 280 °C), time (5 and 20 min) and liquid-to-solid ratio (LSR) (5 and 10). It was reported that

severe temperatures significantly reduced the hydrochar yield. However, increasing the residence time reduced the mass yield marginally. It was also reported that as the LSR increased, there was a reduction in the mass yield of biochar and energy densification. A significant reduction in the hemicellulose component of the biomass was also recorded. It was concluded that the solvolysis process could efficiently enhance the fuel properties of biomass. However, there is a need to optimize the process conditions as it is seen that as the mass yield reduces, the energy densification increases.

Sermyagina *et al*. (2015) also reported the effect of temperature, time and LSR on the qualities of hydrochar. Similar observations of the reduction of hydrochar yield with increasing temperature, time and LSR were also reported. On the contrary, increasing process conditions were accompanied by the increase in higher heating value. The authors concluded that biomass becomes structurally unstable with the increased presence of water under the subcritical region, which gives rise to more rapid decomposition of biomass.

Mäkelä *et al*. (2015) carried out a study on the interactional effect of process condition on the fuel properties of hydrochar from paper mill sludge. It was reported that the influence of the process conditions was in the ordering temperature>time>LSR. It was also reported that the increment of the carbon content was responsible for the energy densification of hydrochar. It was concluded that the hydrochar produced was comparable to sub-bituminous coal and could serve as a supplement for the production of energy in a coal firing plant.

Bach *et al*. (2016) reported the effect of process conditions and compared the usage of wet and dried biomass feedstock on the fuel properties of hydrochar produced via solvolysis pretreatment. The hydrogen-to-carbon and oxygen-to-carbon ratios were reported to improve with increasing temperatures. It was reported that the mass and energy yield for the dried feedstock were both lower than that of the fresh (wet) feedstock. It was concluded that fresh

biomass feedstock should be used in solvolysis pretreatment, although feedstock's biological decomposition could occur during transportation and storage.

Dai *et al*. (2018) carried out the solvolysis pretreatment of milled bamboo while studying the effect of the process conditions on the fuel properties of the hydrochar produced. While using an LSR of 10 throughout the experiment, it was reported that the higher heating value of hydrochar significantly improved with the highest value attributed to the highest temperature. The pyrolytic behaviour of hydrochar was also reported. The DTG graphs concluded that the absence of the hemicellulose decomposition peak indicated that it had been wholly solubilised.

Hashemi *et al*. (2019) enhanced the production of biogas from safflower straw by hydrothermally pre-treating it. The authors concluded that biogas' yield could be significantly increased by pre-treating biomass at less severe conditions. Other researchers like Aguado *et al*. (2020); Gong *et al*. (2019); Park *et al*. (2020); Zhang *et al*. (2017) have also recently enhanced the fuel properties of biomass via wet torrefaction. All the authors mentioned reported the promising future regarding this technology as it significantly upgrades biomass to a coal-like sample for energy production. These authors also concluded that temperature, time and LSR all play significant roles in to achieve an efficient thermochemical conversion process.

Table 2.5 shows the detailed process conditions employed by the different authors reviewed in this study and their corresponding fuel properties of hydrochar produced from solvolysis pretreatment process. The reported data in Table 2.5 shows that quality fuel can be achieved while employing mild process conditions during the solvolysis pretreatment process.

Conclusively, the process conditions employed during the solvolysis pretreatment process include operating temperature, residence time, liquid-to-solid ratio, type of biomass, moisture content of biomass, and type of reactor, have a significant impact on the mass and energy yield of hydrochar produced via solvolysis process. Although temperature accounts for the most

influence on the improved properties, time and LSR when studied together, also affect these properties. The use of deionised water has also proved to eliminate the risk of using acids and toxic chemical to carry out this process. Solvolysis/wet-torrefaction/hydrothermal carbonisation have shown to adequately produce a coal-like hydrochar suitable for thermochemical conversion in a coal firing plant. However, the operational cost associated with this process needs to be evaluated and other challenges.

Table 2.5. Process conditions employed during the solvolysis pretreatment of different biomass and their corresponding improved fuel properties.

Biomass	T (°C)	t (min)	LSR	MY (%)	EY (%)	HHV (MJ/kg)	Ref.
Prairie cord grass	170 – 220	40	NR	NR	NR	NR	Lei *et al*. (2013)
Bamboo sawdust	150 – 230	5 – 35	10	70 – 95	85 – 98	18 – 21	Dai *et al*. (2018)
Sugarcane bagasse	170	75	12	NR	NR	NR	Rackemann *et al.* (2019)
Humulus lupulus	180 – 260	10	40	30 – 50	40 – 50	18 – 25	Yang *et al.* (2015)
Plumeria alba				40 – 50	50 – 60	21 – 26	
Calophyllum				60 – 70	60 – 80	20 – 24	
inophyllum L.							
Miscanthus	190 – 260	5 – 30	6 – 12	48 – 84	NR	19 – 26	Kambo & Dutta (2014)
Oil palm	150 – 190	10 – 240	NR	72 – 85	NR	NR	Rafein *et al.* (2015)
Norway spruce	175 – 225	10 – 60	5	60 – 72	70 – 75	22 – 25	Bach *et al.* (2016)
Birch branches				53 – 74	59 – 76	20 – 22	
Oil palm	140 - 200	60 – 240	5 – 15	62 – 78		21 – 25	Nakason *et al.* (2017)
Cotton stalk	200	180 - 2640	32.5	53 – 38	NR	NR	Lei & Tian (2016)
Food waste	200 – 300	60	3	5 – 7	11 – 13	20 – 31	Ul *et al*., (2018)
Cedarwood	200 – 260	10	10	48 – 77	NR	24 – 28	Li *et al.* (2018)
Corn stover	200 – 280	5 – 20	5 – 10	45 – 95	55 – 90	NR	Lynam *et al*. (2015)
Rice hulls				65 – 85	77 – 87		
Tahoe mix				63 – 87	70 – 88		

Switch grass				30 – 85	40 – 85		
Loblolly pine				60 – 87	62 – 98		
Wood chips	180 – 250	180 – 360	6 – 8	50 – 73	73 – 80	22 – 28	Sermyagina *et al*. (2015)
Paper mill sludge	180 – 260	60 – 375	1 – 2	59 – 98	54 – 98	20 – 31	Mäkelä *et al*. (2015)
Safflower straw	120 – 18	60 – 300	11	NR	NR	NR	Hashemi *et al*. (2019)
Almond-tree	175 – 300	10 – 60	NR	NR	NR	19 – 29	Aguado *et al*. (2020)
Empty fruit bunch	200	5	8	69 – 98	73 – 99	18 – 19	Gong *et al*. (2019)
Rice straw				74 – 99	77 – 102	16 – 17	
Sugarcane bagasse				74 – 99	76 – 101	18 – 19	
Miscanthus	160 – 200	NR	10	NR	NR	18 – 19	Park *et al*. 2020)
Rice husk	150 – 240	60	20	48 – 87	50 – 90	16 – 18	Zhang *et al*. (2017)

T – Temperature; t – Time; LSR – Liquid-to-Solid Ratio; NSR – Nitrogen-to-Solid Ratio; MY – Mass Yield; EY – Energy Yield; HHV – Higher Heating Value; NR – Not Reported.

2.5.3. Optimization of solvolysis process

Similar to the torrefaction process, several researchers have indicated the importance to optimize the solvolysis process. Optimizing the mass and energy yield of the solvolysis process translates to producing an economically profitable mass of hydrochar and a quality hydrochar comparable to conventional coal. Some researchers have modelled and optimised this process.

For instance, Mäkelä *et al*. (2015) used RSM based on Box-Behnken design to optimize the process conditions such as; temperature, residence time, and LSR during solvolysis pretreatment process. Five responses were employed: char yield, energy yield, carbon content, oxygen-to-carbon ratio and the energy densification. The authors reported that although temperature and time were statistically significant for all responses, LSR was statistically insignificant. It was concluded that temperature had the most significant effect on all responses. Similar observations were reported for the solvolysis pretreatment of palm kernel shell by Gan *et al*. (2019).

Nizamuddin *et al*. (2019) optimised the temperature, residence time, particle size and LSR of rice husk during solvolysis using RSM based on Central Composite Design (CCD). This design was reported to show a high level of efficiency in developing a significant model. However, the number of experimental runs was large, translating to increased laboratory labour, cost and time. The authors also reported a non-significance of the LSR, while the temperature was reported as the most significant variable.

Zhang *et al*. (2020) carried out the optimization of process conditions during the solvolysis pretreatment of wheat straws to produce coal-like pellets from hydrochar, using RSM based on a Single Factor Experimental Design (SFED). A couple of process conditions were considered including temperature, time, moulding pressure and moisture content and the estimated optimal

conditions were reported to be 231 °C, 25 min, 130 MPa and 13 %, respectively. It was concluded that temperature significantly increased the fuel properties of the pellets.

Yu *et al*. (2020) determined the optimal temperature to produce quality fuel and activated carbon from hydrochar. Loss of iodine adsorption value of activated carbon and gain of activation carbon yield technique was used to determine the optimal temperature. The reported optimal temperature was estimated to be at 230 °C. It was also reported that temperature exhibits a substantial effect on the fuel's properties and activated carbon.

For the first time, the optimization of the process temperature and time for the solvolysis pretreatment of a non-lignocellulosic waste was carried out by Kannan *et al*. (2017). RSM based on CCD was used to design the process. Similar observations of temperature being the most significant were also reported with optimal conditions estimated at 184 °C and 112 min. Comparable properties of hydrochar from non-lignocellulosic waste to that produced from lignocellulosic waste were reported.

Kang *et al*. (2019) studied the interactional effect and optimized the process conditions during the solvolysis treatment of corn stalk biomass. RSM based on CCD was used to design and optimise the conditions. The authors reported that temperature and the LSR were quite significant in estimating the energy yield of hydrochar. It was concluded that the optimal operating conditions based on the experimental procedure used were 182 °C, 40 min and 13 LSR.

As observed from the above-referenced studies, the optimal conditions for achieving an enhanced hydrochar highly depend on the parent biomass, the experimental procedure, and the optimization technique. Table 2.6 shows the various optimization techniques, developed models, and the optimisation process conditions of the literature reviewed in this study.

Table 2.6. Summary of developed predictive models explaining the interactional effect of process conditions during solvolysis.

Biomass	Model Technique	Model	Optimal Conditions	Ref.
Papermill sludge residue	RSM (BBD)	NR (Check supplementary data)	NR	Mäkelä *et al*. (2015)
Palm kernel shell	RSM (CCD)	$HHV = 14.378 + 0.044T + 0.019t - 6.446SLR$ $MY = 60.76 - 5.77T - 0.789t + 1.27SLR$	220 °C 30 min 1:10	Gan *et al*. (2019)
Rice straw	RSM (CCD)	$MY = 44.77 - 8.37T - 1.27t + 0.101PS + 0.124SLR$ $+0.175Tt + 0.128TPS - 0.165TSLR - 0.221tPS$ $-0.129tSLR + 0.011PSSLR + 2.56T^2 + 0.13t^2$ $-0.264PS^2 + 0.458SLR^2$	180 °C 20 min 3 1:15	Nizamuddin *et al*. (2019)
Wheat straw	RSM (SFED)	HHV and MY were not used as responses	-	Zhang *et al*. (2020)

Pinus Sylvestris var	LIA/GCY [a]	NR	230 °C	Yu *et al*. (2020)
Shrimp waste	RSM (CCD)	$MY = 3.99T + 0.88t - 0.0031Tt - 0.001T^2 - 0.0013t^2 - 371.42$	180 °C [b] 112 min	Kannan *et al.* (2017)
Cornstalk	RSM (CCD)	$MY = 23.883 + 0.163T + 0.486t + 20.522SLR - 0.0023Tt - 0.016TSLR - 0.040tSLR - 0.00086T^2 + 0.001748t^2 - 1.911SLR^2$ $HHV = 1.73 + 0.141T + 0.078t + 2.12SLR + 0.00062Tt - 0.00099TSLR + 0.00062tSLR - 0.00035T^2 - 0.00263t^2 - 0.319SLR^2$	182 °C 40 min 3.8:50 LSR	Kang *et al*. (2019)

HHV (MJ/kg) – Higher Heating value; MY (%) – Mass Yield; SLR (-) – Solid Liquid Ratio; T (°C) – Temperature; t (min) -Time; SLR (-) – Solid Liquid Ratio; PS (mm) – Particle Size; RSM – Response Surface Methodology; CCD – Central Composite Design; BBD – Box-Behnken Design; SFED – Single Factor Experimental Design; NR – Not Reported; [a] – Loss of Iodine Adsorption and Gain in Activated Carbon Yield; [b] Determined based on maximum mass yield.

The liquid-to-solid ratio employed during solvolysis was reported to have a marginal effect on the final fuel properties of hydrochar. Conclusively, Response Surface Methodology has shown to efficiently model and optimize the process parameters. However, the type of design still needs to be considered based on statistical accuracy, laboratory labour, cost, and time.

2.6. Comparison Between Fuel Properties of Biochar and Hydrochar

As earlier stated, biochar is the solid product formed after torrefaction, while hydrochar is the solid formed after the solvolysis process. Having highlighted the effect of process conditions on the independent pretreatment methods, disparities have been identified between the fuel properties of biochar and hydrochar, with respect to the process conditions employed. This review indicates that many studies have been done to review the influence of process conditions on biomass fuel properties via torrefaction and solvolysis independently. However, limited attention has been given in carrying out a comparative analysis of both methods (i.e. torrefaction and solvolysis) while benchmarking the process conditions.

Both torrefaction and solvolysis pretreatment of various biomass waste (lignocellulosic and non-lignocellulosic) using different operating conditions were investigated by numerous researchers. The overall operating conditions and results of the broad literature reviewed in this chapter are presented in Table 2.7 for torrefaction and solvolysis pretreatment process. According to the literature reviewed in this chapter, the operating temperature and residence time employed during the torrefaction pretreatment process is generally ranged between 200 – 320 °C and 5 – 75 min while for solvolysis pretreatment is generally ranged between 150 – 300 °C and 5 – 2640 min, respectively. These process conditions on the properties of the biochar and hydrochar produced such as; mass yield, energy yield, fixed carbon, volatile matter, ash content, ultimate analysis, moisture content and the higher heating values, are summarized in Table 2.7.

The solid yield of biochar/hydrochar refers to the percentage fraction of mass remaining after the pretreatment process to the initial mass of biomass feed to the process. The energy yield refers to the percentage mass fraction of energy remaining after the process. The energy yield is a function of the mass yield and the higher heating value. During torrefaction and solvolysis process, the mass and energy yields have decreased with an increase in the process's severity, i.e., increased operating temperature and residence time.

Among the various process conditions employed during the two pretreatment processes, the temperature has been recorded to significantly affect the mass yield and energy yield of the char produced than other process parameters. Also, the flow rate of the gas employed during torrefaction and the liquid-to-solid ratio has also been found to have a marginal effect on the mass loss and the fuel properties of the biochar and hydrochar, respectively.

Other inherent biomass properties such as; moisture content, lignocellulosic composition, ash content, and volatile matter have also contributed to char's final fuel properties. From Table 2.7, the average recorded mass yield from the literature reviewed in this chapter were 55 % for torrefaction and 70 % for solvolysis. Although solvolysis pretreatments were done at milder temperature range, the percentage mass loss was similar to that of torrefaction in a more severe temperature region. Hence, a more severe solvolysis process will see a further mass loss compared to torrefaction pretreatment.

Furthermore, as seen in Table 2.7, the average energy yields reported were 65.2 % for torrefaction and 70.4 % for solvolysis. These energy yield values show that solvolysis pretreatment provides a higher means of increasing the biomass energy’s content than torrefaction pretreatment method. This advantage is because water at its subcritical region is highly efficient in dissolving most of the hemicellulose, cellulose and a fraction of the lignin component in biomass.

For all the biomass studied in the reported literature, average fixed carbon content was reported to between 30.3 % and 28.4 %, after passing through torrefaction and solvolysis processes, respectively. These values are in close range with lignite coal, as shown in Table 2.2, having a value of 26.54 %. On the contrary, biomass contains more volatile matter than lignite coal, having average values of 58 % and 74.8 % after torrefaction and solvolysis process respectively, compared to 28.66 % for lignite coal (as can be seen in Table 2.2).

Increasing the severity of the two pretreatment processes has increased the fixed carbon and reduced biomass's volatile matter. This observation agrees with the inferred pathway during the pretreatment process, whereby biomass loses its moisture content and its light compounds (i.e. aromatic compounds, hydrocarbons), increasing the percentage fraction of fixed carbon in the char. The combustion characteristics (i.e. ignition temperature, mass transfer, heat and energy transfer, flammability test, combustion rate and time) of any solid fuel are highly dependent on the fixed carbon and volatile matter content of the fuel.

The high ash content in biomass makes it an inefficient solid fuel compared to coal. As shown in Table 2.7, after pretreatment of biomass, the ash content (9.8 % and 0.54 %) of the produced char via torrefaction and solvolysis respectively, has shown to be in the same range with lignite coal (9.4 %) (as can be seen in Table 2.2). Ash content has been reported to hinder the efficient heating of biomass during thermochemical conversion. Ash also represents the little fraction of biomass with no value and no energy content utilised in agriculture as fertilizers. The variation of fixed carbon and volatile matter in different biomass sources after pretreatment as reported in Table 2.7 can be attributed to the variation of ash content and lignocellulosic composition of the different biomass.

Table 2.7. Summary of process conditions and obtained fuel properties from the literature reviewed.

Process conditions and its fuel properties	Torrefaction	Solvolysis
Temperature [°C]	200 – 320 (260)	150 – 300 (200)
Residence time [min]	5 – 75 (30)	5 – 2640 (60)
Solid mass yield [%]	20 – 98 (55)	30 – 99 (70)
Energy yield [%]	50 – 102.4 (65.2)	40 – 98 (70.4)
FC [%]	17.3 – 49.8 (30.3)	8 – 34.3 (28.4)
VM [%]	30 – 80.3 (58)	60.5 – 91.6 (74.8)
Ash [%]	3 – 17.2 (9.8)	0.06 – 0.8 (0.54)
Hydrogen/Carbon ratio [-]	0.08 – 0.84 (0.12)	0.09 – 0.13 (0.11)
Oxygen/Carbon ratio [-]	0.2 – 0.86 (0.46)	0.5 – 0.9 (0.54)
Moisture [%]	0.87 – 20	3 – 15 (14.7)
HHV [MJ/kg]	17 – 28 (22.3)	18 – 28 (25)

FC – Fixed Carbon; VM – Volatile Matter; HHV – Higher Heating Value. Numbers in brackets represent average values derived from the data reported in the literature.

Figure 2.5 illustrates the relationship between the solid mass yield and the higher heating value (HHV) of biochar and hydrochar. Figure 2.5 was derived by plotting all the higher heating values and the corresponding mass yields of different biochar and hydrochar reported in the literature reviewed in this study. As summarized in Table 2.7, as mass yield reduced from 98 % to 20 % during torrefaction, and 99 % to 30 % during solvolysis, the HHV increased from 17 MJ/kg to 28 MJ/kg after torrefaction and 18 MJ/kg to 31 MJ/kg after solvolysis. This observation reiterates that although both torrefaction and solvolysis favour the higher heating value of biomass, solvolysis offers a higher HHV than torrefaction method. Similarly, although both pretreatments significantly reduce the char's mass yield, solvolysis results in a higher mass loss than torrefaction while employing similar process conditions.

One of the challenges of biomass as a solid fuel is its hydrophilic nature. The pretreatment of biomass helps remove the inherent moisture content of biomass and convert it into a hydrophobic material. Similar to the HHV of char, as the pretreatment severity increases, the hydrophobicity of char increases. Table 2.7 indicates that both torrefaction and solvolysis processes can reduce the biomass moisture content comparable to anthracite coal (~10 %) (as shown in Table 2.1).

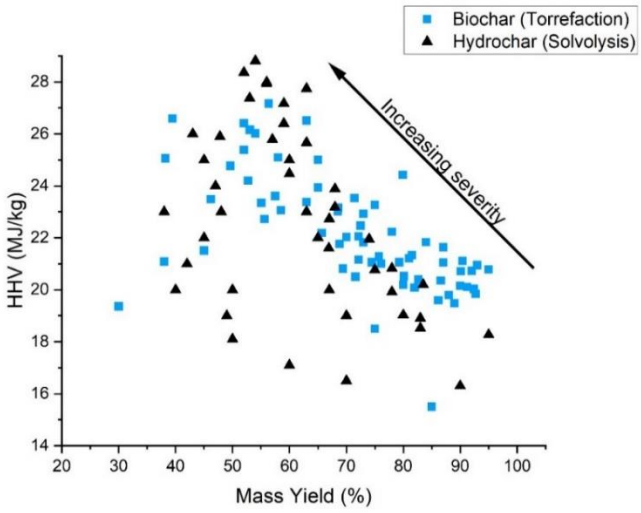


Figure 2.5. Relationship between HHV and the mass yield of char produced

Figure 2.6 represents the Van Krevelen diagram for the various biomass reviewed in this chapter. This figure shows the relationship between the atomic hydrogen-to-carbon (H:C) ratio and the atomic oxygen-to-carbon (O:C) ratio as the pretreatment severity increases. This figure was derived by plotting the H:C ratios of various biochar and hydrochar against their corresponding O:C ratios obtained from the literature reviewed in this study. Coal generally has lower O:C and H:C ratios than biomass. The ultimate analysis (i.e. carbon, hydrogen, nitrogen, oxygen and sulphur content) of solid fuel significantly affects the HHV of the fuel. Higher O:C ratio results to lower HHV of solid fuel. The low HHV of biomass is one of the short-comings of its utilization for energy production. However, torrefaction and solvolysis pretreatment methods have been proved to address this high O:C ratio deficiency. Although the torrefaction and solvolysis tend to reduce the O:C and H:C ratios as the severity of the process increases (i.e. increase in temperature and time), solvolysis offers a higher reduction in these ratios that torrefaction. Increasing the carbon content and reducing the oxygen content is known as carbonization and deoxygenation, respectively. This process eventually raises the HHV of the solid fuel.

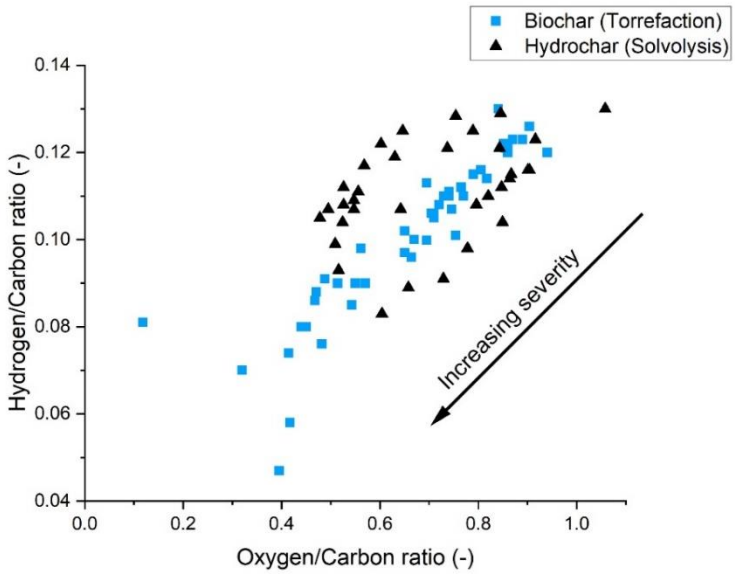


Figure 2.6. Van Krevelen diagram of various biomass in torrefaction and solvolysis

The enhancement of this fuel property is primarily attributed to the decomposition of the hemicellulose and a fraction of the lignin. Due to hemicellulose's thermal instability, its decomposition occurs at a mild temperature (150 – 275 °C) while that of cellulose occurs afterwards (270 – 350 °C). The decomposition of the lignocellulosic component of biomass involves several complex reactions of which some of them involve; decarboxylation, dehydration, to mention a few. These reactions lead to the removal of the oxygen molecule and the hydrogen molecule while conserving the carbon content hence decreasing the H:C and O:C atomic ratios. Table 2.7 shows that for the various biomass reviewed in this study, the overall range of the H:C ratios were between 0.08 – 0.84 and 0.09 – 0.13 for torrefaction and solvolysis, respectively. Furthermore, as reported in Table 2.7, the broad range of the O:C ratios were between 0.2 – 0.86 and 0.5 – 0.9 for torrefaction and solvolysis, respectively. The data reported show comparable ratios with coal.

2.7. Kinetic Analysis of Biomass Degradation

Having reviewed the reactions (i.e. mass loss) during the thermal pretreatment of biomass and showing the reliability of empirical models to predict the thermal degradation of biomass, kinetics based on physical laws have shown to be efficient when describing the thermal degradation process.

Two approaches have been generally employed to study the kinetics of the thermal degradation of biomass namely; the non-isothermal approach (Ali *et al.*, 2018; Barzegar *et al.*, 2020; Ceylan, 2015; Raza *et al*., 2019; Sharma *et al.*, 2019; Yu *et al.*,2016) and the isothermal approach (Anca-Couce *et al.*, 2014; Bach *et al.*, 2016; Duan *et al*., 2020; Edgar, 2019; Peduzzi *et al.*, 2014; Ranzi *et al.*, 2008).

The thermogravimetric analyzer (TGA) has been used to carry out these analyses. The data obtained from the TGA is highly reliable for carrying out these analyses. This reliability is

because a thermogravimetric analyzer can control the conditions (i.e. type of gas, the flow rate of gas, temperature, and time) of the thermal process and record the rate of mass loss of biomass while eliminating the effect of cooling time on the final mass loss of biomass.

Carrying out the kinetic analysis of the non-isothermal degradation of biomass by the authors referenced above suggested that multiple reactions occur during the thermal degradation process. This phenomenon can be observed through the variation of activation energies across various conversion while employing different model-free and model-fitting techniques to model the process such as; Friedman method, Coats and Redfern methods, Kissinger-Akahira-Sunose (KAS) method, Flynn-Wall-Ozawa (FWO) method, to mention a few.

The introduction of the isothermal kinetic method, first adopted by Di Blasi & Lanzetta (1997), was initially used to study the thermal degradation of pure xylan in an inert atmosphere. The Arrhenius pre-exponential factors and the activation energies were the characteristic parameters used to describe the process. Later on, Peduzzi *et al*. (2014) modified the technique by introducing the pseudo-components in the model and assuming several reaction steps in series. This modification made it possible to implement this kinetic model technique on various species of biomass.

The established kinetic model gives a relationship between the anhydrous weight loss of biomass and severity (i.e. temperature and time) of the thermal process. The formulated kinetic reaction equations from pilot studies are detailed in Chapter 5. Also, estimated kinetic parameters developed for various biomass types reported in the literature, reviewed in this study, are detailed in Chapter five.

Carrying out the kinetic modelling of the thermal degradation of biomass is vital because the biomass weight loss rate during the process gives essential data required to design an efficient

reactor for the process and the kinetic analysis gives vital information on the energy needed to carry out the thermal pretreatment of fuel (PSD).

2.8. Biomass Selection

As enumerated earlier in this chapter, there are different type of biomass that can be used for energy production (Figure 2.1). However, for an effective thermochemical conversion of biomass into syngas, woody biomass (Lignocellulosic biomass) has been identified as most suitable. This is because of its high energy content, low moisture content, and its fixed carbon content compared to other types of biomasses. As stated earlier, several researchers have studied the pretreatment and thermochemical conversion of different woody biomass. These studies have highlighted the different fuel properties of each biomass. The information from these studies informed the choice of pine sawdust of South African Origin for this study. Other factors that were considered were the availability, ease of planting, cultivation requirements (such as water requirement, sunlight, land size, etc.). Furthermore, it is important to state that biomass is one of the most inconsistent natural and renewable sources of energy. This is because its fuel properties are dependent on the degree of its exposure to sunlight, the amount of water it has absorbed, the geographical area, etc. Although pine wood is not home to South Africa, it was introduced into the country years ago. Pine wood is regarded as a hard wood which is easily grown in South Africa and is mostly used by the wood industry for furniture. This translates into the generation of large waste, hence the choice of biomass for this study. Ozonoh *et al.* (2019) carried out a study on the co-gasification of three lignocellulosic biomass: sugar cane bagasse, corn cob, and pine sawdust, with coal. Amongst the lignocellulosic biomass of South African origin, pine sawdust produced the best lower heating value when co-gasified with coal. The modelled profit obtained from running a co-gasification plant of raw pine sawdust and coal was estimated to be the highest. Hence, for this study, pine sawdust of

South African origin was selected while exploring two pretreatment methods to improve its fuel properties and further lead to a more profitable co-gasification of pine sawdust with coal.

2.9. Challenges and Outlook

Several researchers and stakeholders in different parts of the world published articles in this field of study and have given several oral presentations and seminars on the need to go green for sustainability. Some of the critical areas currently exploited to solve global warming and energy insecurity are; carbon capture storage and utilization (CCSU), thermochemical conversion of biomass, photovoltaic cells, to mention a few.

A recent seminar hosted by the South African National Energy Development Institute (SANEDI) in 2020 was conducted to discuss the progress on the Carbon Capture Storage (CCS) project in South Africa. It was suggested that although this flagship program to tackle the issues of climate change is highly effective and beneficial, there are some underlying challenges currently facing the implementation of this technology. Some of these drawbacks are; funding, loss of jobs, culture, government policies relating to the carbon tax, public perception and land use.

Currently, Norway is one of the few countries currently pioneering biomass for energy generation and implementing carbon capture technology. In Africa, countries like South Africa, Nigeria, and Mozambique have been identified as the largest contributors to carbon emissions through fossil fuel exploration. However, only South Africa has shown efforts in cutting down on her carbon emission. South Africa's stakeholders in this field have identified some of the challenges currently facing implementing these technologies. For example, 85 % of South Africa's energy is gotten from fossil fuels, and many jobs are created in the coal mining sector. The migration from coal to biomass will see a drastic reduction in jobs and a reduction in the

energy available for the population except proper contingencies are put in place to see the easy transformation to green energy.

Another drawback faced by this field is the availability of biomass feedstock and competition with food crops. Researchers have indicated that the use of only biomass for energy will not be economically viable. Whereas the co-gasification of blends of biomass and coal will show more sustainability and reduce the carbon emission. Also, lignin in lignocellulosic biomass has been a challenge for its utilization for energy production. The industry has identified the difficulty in breaking this component during the thermochemical conversion, which increases the cost of energy production from biomass. This draw-back has led to the search of non-terrestrial biomass which does not contain lignin. Breakthroughs have been made through research by coming up with some thermophilic bacterium that can break down the lignin component without pretreatment. The cost of pre-treating biomass has also been identified to be costly. This challenge has been one reason why lots of research is currently being carried out in this field, and lots of financial grants are provided for the continuous funding of these projects.

New technologies and research areas are currently coming up in this research area. Some of them are ways to increases photosynthesis efficiency (i.e. increasing the amount of energy that plants can absorb and store from the sun); the use of plasma as a source of heating during the thermochemical conversion of biomass; and more efficient ways of pre-treating biomass for an efficient thermochemical conversion process. Several pretreatment methods have been developed to increase efficiency and to produce different final products. Amongst other methods are leaching, biological pretreatment, torrefaction and solvolysis as discussed in this study.

Studies have indicated that as the Gross Domestic Profit (GDP) of a country rises, energy consumption rises. As such, industrialization and development of a country are indicated by its

increase in GDP. Hence, as countries try to develop, more energy is required for consumption. This observation can be seen in counties like China and India. The electrification of these countries has resulted in massive economic growth. The current oil market has seen a drastic fall in oil price, and this has had and will continue to harm the economy of countries who rely on oil for most of its GDP. Fracking has remained in use because of the cost of oil, which makes it economically viable. The fall in the oil price will see fracking phase off, leading to a shortage of oil for energy production.

Over the last decade, the high cost of energy has seen the price of food increase, leading to an increase in the poverty rate across the globe. The current energy consumed by the world yearly currently stands at 16 terawatts; meanwhile, the sun provides 86,000 terawatts of energy yearly. This discovery has led to researchers focus on ways of harnessing this energy from the sun for utilization. Although the sun alone can solve every energy insecurity issue faced by the world, this energy storage has been its primary challenge. Hence, it has been suggested that all renewable forms of energy have to be explored and harnessed to make up for the world's energy demand.

An online course on Our Energy Future hosted by the University of California San Diego was put together to discuss the current energy challenges and possible plans to meet the global energy demand. Prof. George Tynan from Mechanical and Aerospace Engineering, UC San Diego, enumerated possible solutions to be put in place to meet this global energy demand. The suggestions were as follows; improved efficiency in recording energy usage by 2 % yearly; 5 million acres of photovoltaic cells; 1 million 2 Megawatt turbines over a 2 million kilometres land area; 800 clean coal power plants; 700 new nuclear power plants; replacement of fossil fuels with biofuels and solar; an increased vehicle fuel efficiency; and implementation of a carbon tax. These, therefore, calls for more research in areas like bioenergy from biomass, artificial photosynthesis, superconductivity, nanoscience, and fusion energy research.

Conclusively, having highlighted the challenges in this field and the current stage and progress made in achieving cleaner energy technology and green economy, these researches need to be carried out to provide relevant data and information for stakeholders to implement on an industrial scale.

2.10. Summary

In this section, conclusive remarks are made concerning the influence of process conditions during torrefaction and solvolysis and the role of these pretreatments in achieving an efficient thermochemical conversion process. Also, the research gaps in the field and how this study contributes to closing the gaps are discussed.

Based on the literature reviewed in this chapter, it can be said that torrefaction and solvolysis pretreatment methods can adequately enhance the fuel properties of waste biomass to comparable characteristics of coal. Thus, highlighting the great potential of these methods for effective thermochemical conversion of biomass into useful biofuels.

The fuel properties of interest during pretreatment are; the higher heating value, the fixed carbon content, and the oxygen-to-carbon and hydrogen-to-carbon atomic ratio. Also, due to the structural decomposition of the lignocellulosic structure of woody biomass, the hydrophobicity of biomass increases due to the dehydration reaction taking place during the process involving eliminating the OH group in the structure thereby reducing the affinity for hydrogen bond formation. The hydrophobicity nature of enhanced biochar/hydrochar increases the shelf life of biomass and can eliminate a significant fraction of raw biomass transportation cost.

Concurrently, due to water's subcritical property during solvolysis, the hemicellulose component drastically dissolves, accompanied by a large fraction of the cellulose and little of

the lignin at lower temperature regions than torrefaction. The structural decomposition of biomass leads to improved grindability. This improved grindability will encourage biomass for thermochemical conversion in a power plant as most plants only allow pulverized feed materials.

Although these pretreatment methods reviewed in this chapter have shown a positive effect on biomass's fuel properties, the fuel properties of various biomass differ and their behaviour during the pretreatment processes. The same type of biomass can also differ in its fuel properties and behaviour during pretreatment processes. Some of these factors that are responsible for this variation in fuel properties of the same type of biomass are; specie of plant, part of the plant (stem, branch, root), geographical factors (i.e. exposure to sunlight, the intensity of sunlight, proximity to a water source, the climate of an area, exposure to pollution), age of plant before harvesting, contamination during transportation and storage, to mention a few.

Having consulted the relevant literature extensively, few studied have extensively studied the effect of process conditions during solvolysis pretreatment. Till date, a bench-marked comparison between torrefaction and solvolysis is yet to be reported in the literature. Although several efforts have been made in optimizing the process conditions during torrefaction and solvolysis processes, using a genetic algorithm to increase the accuracy of optimization is lacking in the literature. Also, having established the unique behaviours of different types of biomass and the need to study various types, till date, solvolysis pretreatment method has not been applied to the pretreatment of pine sawdust (PSD) which is considered to contain a high energy content and constitutes a high fraction of wood waste produced in South Africa. Furthermore, a reliable kinetic study describing PSD degradation during thermal pretreatment (i.e. torrefaction) lacks literature.

However, this study offers some solutions and helps to bridge these knowledge gaps by studying kinetics and the effect of process conditions during the pretreatment of PSD via solvolysis and torrefaction process, while comparing the char produced from both processes using bench-marked process conditions. The subsequent chapters present the methods followed in this study's execution and the results obtained based on the research.

CHAPTER THREE

3. EXPERIMENTAL PROCEDURE AND ANALYSIS

This chapter presents the detailed sample preparation method and the analytical techniques followed for PSD characterization. The experimental procedures followed for the actualization of this study's aim are also presented in this chapter. The experimental procedures are divided into two studies, namely; torrefaction and solvolysis study and kinetic study. Figure 3.1 gives the detailed steps taken during the torrefaction and solvolysis study. The procedure taken in carrying out the kinetic study is as shown in Figure 3.3. Detailed in the subsections of this chapter is the description of each step highlighted in the figures.

3.1. Torrefaction and Solvolysis Study

3.1.1. Materials and methods

3.1.1.1. Sample preparation

The Pinewoods used in this study were wastes obtained from the precinct of the University of The Witwatersrand, Johannesburg, South Africa, as shown in Figure A.1 of the Appendix. The wood samples were air-dried for 48 hours to prepare it for size reduction. The wood samples' particle size was reduced to an average dimension of 10 x 15 x 20 (l x b x w) mm (as seen in Figure A.2) and finally to 0.6 mm using a Mössner Rekord SSF 520 vertical band saw and a pulveriser respectively. A mesh sieve was used to ensure particle size less than 600 μm of pulverised sawdust. The dried Pine Saw Dust (PSD) was then stored in an air-tight plastic bag for further experiments.

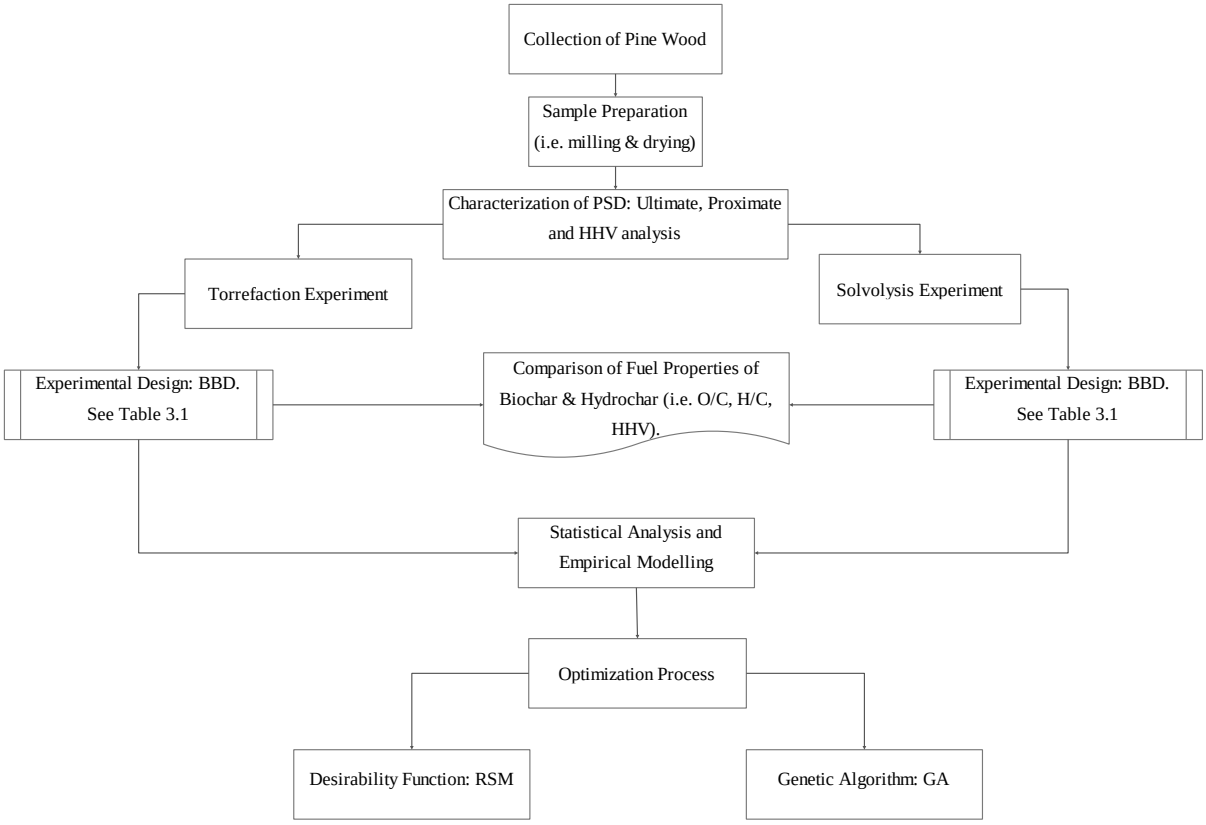


Figure 3.1. Experimental flowchart for torrefaction and solvolysis study

3.1.1.2. Characterization of feedstock

PSD properties were characterised before and after torrefaction and solvolysis experiments. Specifically, the proximate and ultimate analyses were carried out, and the HHV for PSD were determined. The proximate analyses were done in compliance with the ASTM E1756-08, E872-82, E1755-01, (2015a, 2015b, 2013). The free moisture content present in PSD was reported as the mass loss after oven drying the sample at 105 °C for 24 hours. While using a Thermogravimetric Analyzer (TGA), PSD was further heated at 950 °C in a Nitrogen atmosphere. The mass loss after this heating was reported as the volatile matter. The remainder of the biomass sample was combusted at 550 °C for 3 hours, with the remaining non-combusted sample reported as the ash content. The fixed carbon was calculated as the unaccounted mass during this process and is illustrated in Equation (3.1). The ultimate analyses were carried out in compliance with the ASTM D3176-89, (2002). Particularly, a Flash 2000 analyzer (Thermo-

fisher Scientific, USA) was used for these analyses. The oxygen content of the fuel was estimated by difference, as expressed in Equation (3.2).

$$\%FC = 100 - \%(MC + VM + Ash) \quad (3.1)$$

Where *FC* is the Fixed Carbon; *MC* is the Moisture Content, and *VM* is the Volatile Matter.

$$\%O = 100 - \%(C + H + S + N) \quad (3.2)$$

The HHV of all samples were determined using a Parr Oxygen Bomb Calorimeter. All analyses were carried in triplicate, and the average values were reported to ensure repeatability of results.

3.1.2. Torrefaction experiment

A 500 ml steel reactor was used to carry out the torrefaction experiment with a muffle furnace as the heating source, as shown in Figure A.3 of the Appendix. For each run, Nitrogen-to-Solid Ratio (NSR) of 4, 5 and 6, equivalent to mass feeds of 15 g, 12 g, and 10 g respectively were placed in the reactor and inserted into the furnace having an inlet and outlet opening for gas. Nitrogen was used as the carrier gas and was kept constant at a flow rate of 60 ml/min throughout the experiment. Torrefaction experiment was allowed to start from room temperature, and 8 min was the allowable time, set for each final temperature to be reached. PSD was held at each final temperature for a designated time as determined by the experimental design shown in Table 4.3 of Chapter four. Stainless steel exhibits some level of heat resistance, so there is bound to be a temperature drop inside the reactor. However, this was considerably compensated during the combustion of the solid fuel inside the reactor. During the pretreatment process, with the use of a type-K thermocouple, the temperature inside the reactor was discovered to be slightly higher than the furnace temperature. This was because the combustion process of the fuel material inside the reactor tends to increase the temperature inside the reactor when compared to the external temperature. This temperature difference was also

dependent on the amount of fuel undergoing the combustion process. After each run, the furnace was allowed to cool to room temperature before removing the biochar from the reactor to avoid oxidation.

The HHV for each biochar produced was also analysed using a Parr Oxygen Bomb Calorimeter. The mass yield and energy enhancement factors were calculated using Equations (3.3) and (3.4). The Ultimate analyses of some selected biochar were performed as described in Section 3.1.1.2.

$$MY\% = \frac{M_C}{M_f} \times 100 \tag{3.3}$$

$$EEF\ (-) = \frac{HHV_C}{HHV_f} \tag{3.4}$$

Where *MY* is the Mass Yield; M_c is the mass of Char; M_f is the Mass Feed; *EEF* is the Energy Enhancement Factor; HHV_c is the HHV of Char, and HHV_f is the HHV of Feed.

3.1.3. Solvolysis experiment

Solvolysis experiment was performed using a 500 ml high-pressure cylindrical stainless-steel reactor (High-Pressure Equipment Company, PA USA). A constant mass feed of 10 g was used while varying the volume of de-ionized water between 40 ml, 50 ml, and 60 ml, to account for the Liquid/Solid Ratio of 4, 5, and 6, respectively. Before each run, Nitrogen gas was used to purge the reactor for 5 mins then sealed to ensure an inert atmosphere. Similar to torrefaction experiment, each run was allowed to begin from room temperature and eventually raised to different final temperatures and kept for a residence time based on the experimental designs shown in Table 4.4 of Chapter four. After each run, the moisture hydrochar was rinsed using de-ionized water and eventually filtered. The residue (hydrochar) was then oven-dried at 105 °C for 24 hours to remove any free moisture. The dried hydrochar was further analysed. The mass yield and EEF were also calculated using Equations (3.3) and (3.4), respectively.

3.1.4. Experimental design: Box-Behnken Design (BBD)

Response surface methodology (RSM) based on Box-Behnken Design (BBD) model is one of the most conventional methods of developing and optimizing the process conditions involved in any process. It is also efficient for studying the effects on the process involved, with a relatively small number of experimental runs which saves time, labour and cost. A 3-factor Box-Behnken statistical design approach (BBD) was used to study the interactional and main effects of process conditions as well as the quadratic effect on three responses namely; Mass Yield (MY), Higher Heating Value (HHV), and Energy Enhancement Factor (EEF) of the biochar/hydrochar. BBD is usually sufficient to fit a quadratic model of the form illustrated in Equation (3.5) and explain how the factors affect the responses (Cotana *et al*., 2015).

$$\gamma = \alpha_0 + \sum_{j=1}^{i} \alpha_j x_j + \sum_{j=1}^{i} \alpha_{jj} x_j^2 + \sum_{k<j} \alpha_{kj} x_k x_j \quad (3.5)$$

Where γ is the experimental responses as indicated in Table 3.1; α_0 is the intercept; α_j , α_{jj} and α_{kj} are partial regression coefficient; *i* represents the number of process conditions and x_j represents the three independent variables.

Table 3.1. Experimental Process conditions and coded levels in BBD.

Independent Variable Input	Un-coded factors	Coded level factors			Responses
		-1	0	+1	
Temperature (^{o}C)	P_1	200	250	300	HHV
Time (min)	P_2	30	75	120	(MJ/kg); EF;
NSR/LSR (-)	P_3	4	5	6	% MY

HHV: Higher heating value; EF: Efficiency; MY: Mass yield; NSR: Nitrogen-to-solid ratio; LSR: Liquid-to-solid ratio.

Two experimental designs comprising of 17 experiments each, with 5 centre points each to estimate the pure error and lack of fit, were developed to model and optimize the process conditions. The process conditions employed during torrefaction in this study were premised on other studies published in the literature for other biomass types. Similar process conditions were employed for solvolysis experiment to create a basis for comparison between biochar and hydrochar. The process conditions and the coded levels implemented in this design is shown in Table 3.1.

3.1.4.1. Statistical test and analysis

Design-Expert version 12 software was used to carry out the statistical tests and analysis to make inferences about the developed models in this study. A 95% confidence level (i.e. P = 0.05) was employed to check the significance of each model developed in this study, and each variable and interactional effects present in the model equations. Several statistical tests such as; *P* test, *F* test, lack of fitness (LOF) test, coefficient of determination (R^2), adjusted coefficient of determination (adj. R^2), and predicted coefficient of determination (pred. R^2), were employed to make accurate inferences about the developed models. The model was further used to develop 3-dimensional response surface plots to study process conditions' interactional effect.

3.1.5. Desirability function optimization

The desired function approach deals with simultaneously optimizing a design's responses by carrying out a multi-response analysis while concentrating within a range of process conditions, targeting, minimizing or maximizing a process condition (Derringer and Suich, 1980). The methodology explained by Derringer & Suich was adopted in this study. This approach requires that each response be transformed into a dimensionless desirability function (d_i) in order of importance between 1 and 0 (i.e. 1 being given to the response with most importance and 0 to

the least important). Eventually, the total desirability function (D) is deduced by determining the geometric average of each response's desirability values as expressed in Equation (3.6).

$$D = \left(d_1^{v_i} \times d_2^{v_2} \times d_3^{v_3}\right)^{1/n} \quad (3.6)$$

v_i signifies the importance each response from the model is allocated and it ranges between 0 and 1 (i.e. $0 \leq v_i \leq 1$). The sum of v_i is always 1 (i.e. $\sum_{i=1}^{n} v_i$) where n is the number of responses (3 in this study). d_i is the desirability of each response. In essence, the target is to achieve a D value close or equal to 1, which will indicate that all response achieved their aim. Same importance and desirability were given to all three responses to achieve maximum energy content and a maximum mass yield. The same Design Expert 12 software was used in conducting this analysis.

3.1.6. Genetic algorithm optimization

Genetic algorithm (GA) is a common technique used to develop high-quality solutions to optimization problems by applying biological mutation techniques on models which explains experimental data. GA operates based on the principle of probability and evolution. This technique has been widely suggested to be an efficient method of optimising models, giving a high accuracy level (Whitley, 1994). MATLAB R2020b software was used in carrying out this analysis. The model equations developed using the Design-Expert software were used in writing the function code. Figure 3.2 represents the flow chart used in developing the script for this analysis.

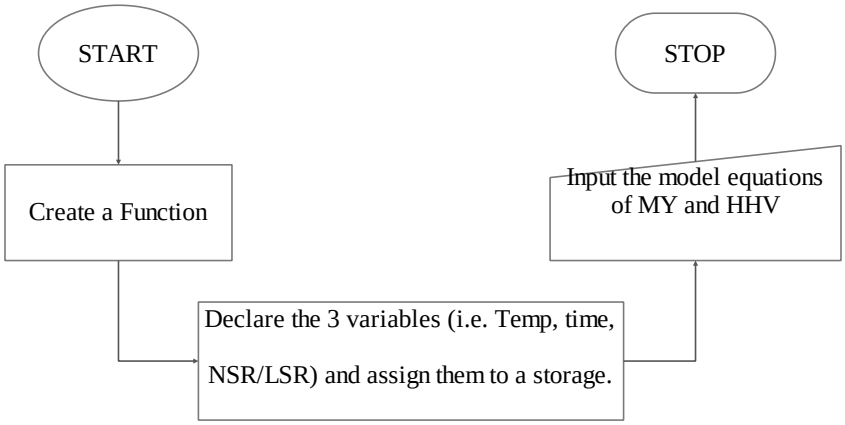


Figure 3.2. Flow chart showing the development of the function file for GA optimization

After creating the function file according to the flow chart, the '*optimtool*' function is used to call the optimization interface. The multi-objective optimization was chosen as the solver because there was more than one response. A double vector population type was used. The feasible population was used as the creation and the mutation function because it provides the most accurate values. The generated function files for carrying out the optimization of torrefaction and solvolysis via genetic algorithm are shown in Figure A.8 and A.9 of the Appendix.

3.2. Kinetic Study

3.2.1. Material and Methods

3.2.1.1. Sample preparation

The similar procedure described in section 3.1.1.1 was followed to prepare the PSD sample to carry out the kinetic analysis.

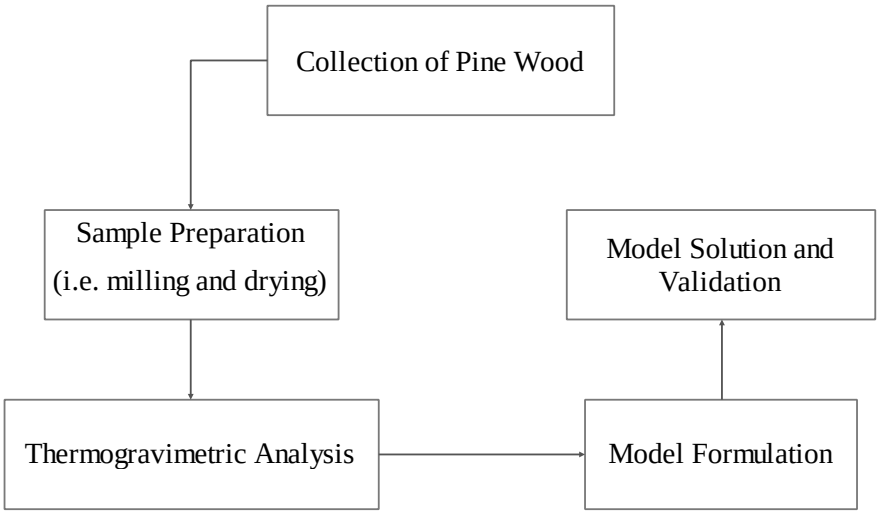


Figure 3.3. Experimental flowchart for kinetic study

3.2.2. Thermogravimetric analysis

A thermogravimetric analyzer was used to carry out the torrefaction of the biomass samples. For each run, an initial mass of 10 mg of each sample was loaded in the TGA and a nitrogen gas of flow rate; 100 ml/min, was supplied for the experiment. The experiment was allowed to start at room temperature till it got to 105 ^{o}C, and it was then allowed to stay for 3 mins for further drying. It was then heated to pre-set torrefaction temperatures (220, 240, 260, 280 and 300 ^{o}C) and held isothermally for 2 hours. Different but slow heating rates were used for the different pre-set temperature to achieve the same non-isothermal period, which 5 min was the allowable time for the temperatures to rise from 105 ^{o}C to the various pre-set temperatures. This method was employed to reduce the effect of the non-isothermal period due to its difficulty in modelling. When the TGA reached the pre-set temperatures, the mass recorded was taken as the initial mass to eliminate the complexity of modelling the non-isothermal period. The initial time was set at the time the pre-set temperature was reached.

CHAPTER FOUR

4. OPTIMIZATION OF PROCESS CONDITIONS DURING SOLVOLYSIS AND TORREFACTION OF PSD USING DESIRABILITY FUNCTION AND GENETIC ALGORITHM

4.1. Introduction

Due to the depletion of fossil fuels as well as its adverse environmental effects, research efforts on the use of biomass as an alternative source of energy have in recent times, increased. The over-dependency on fossil fuel can be reduced through biomass utilization (Lynam *et al*., 2015).

Studies on the valorisation of biomass have shown that biomass is a salient renewable fuel that could be converted into different energy forms. However, some of the biomass's physicochemical properties (e.g. moisture content and others) may affect the energy conversion system's efficiency if the fuel is not pre-treated. Therefore, it will be necessary that the fuel is pre-treated to enhance its quality and hence; meet the global energy demand (Gong *et al*., 2016).

Several thermochemical conversion methods have been employed to improve the fuel properties of biomass (Aguado *et al.*, 2020; Cahyanti *et al.*, 2020; Kumar *et al*., 2020; Lu *et al*., 2020; Raymundo *et al.*, 2020; Vasudev *et al.*, 2020; Wallace *et al.*, 2019). Torrefaction and solvolysis are the most common pretreatment methods. Thus, they require a low-temperature operation, enabling a cost-effective process (Acharya *et al*., 2015). Biomass materials are pre-treated to improve fuel qualities such as; the higher heating value (HHV), carbon content, hydrogen-to-oxygen ratio, and reduce moisture content. Other methods through which the fuel quality can be enhanced include acid and alkaline hydrolysis, leaching, fast and slow pyrolysis. These pretreatment methods help to remove the high moisture content present in biomass. It

also helps to solubilize the hemicellulose, reduce the crystalline nature of the cellulose, increase the surface area by improving the grindability and breaking the resistive lignin structure. In this case, the biomass's shelf life is increased, and the fuel is maximised as a solid fuel for energy production.

Generally, when raw biomass is compared to pre-treated biomass materials in terms of the biochar/hydrochar produced from torrefaction and solvolysis processes, the fuel properties such; good grindability, unyielding characteristics to biodegradation, and effective thermochemical conversion to mention a few (Dai *et al.*, 2018; Gucho *et al.*, 2015; Pérez *et al.*, 2019), are more improved for pre-treated biomass than raw biomass.

Torrefaction is a process whereby biomass is subjected to temperatures between 200 – 300 ^{o}C in an inert atmosphere (Prins *et al.*, 2006; Tran *et al.*, 2013). This process is termed a thermal pretreatment process. In this process, nitrogen is used as the inert gas and researchers have used it for pinewood (Chen *et al.*, 2016; Winjobi *et al.*, 2017), beechwood (Yılgın *et al.*, 2019), coffee residue (Pathomrotsakun *et al.*, 2020) torrefaction, respectively.

Cha *et al*. (2016) reviewed the torrefaction of lignocellulosic biomass and highlighted the different reactions taking place namely; loss of free moisture content, devolatilization of light compounds, decomposition of a fraction of the lignocellulosic composition and the production of biochar. Yu *et al.* (2019) study showed that torrefaction offers a remarkable improvement to wood pallets as a solid fuel by improving the energy densities and grindability. Wang *et al.* (2011), studied the effect of torrefaction on a cotton stalk and wheat straw. Improved HHV, grindability and a hydrophobic nature were reported.

It was also reported by Chen *et al.* (2018) that biomass torrefaction could reduce the tar production during pyrolysis of biochar and as well, increase the biochar yield. Chen and his co-workers also carried out rice husk's torrefaction to evaluate the solid, liquid and gaseous

product from the process, and an apparent de-oxygenation effect was observed. The chemical composition analysis also showed that torrefaction is mainly associated with the decomposition of the hemicellulose. The association between increased torrefaction temperatures and increased higher heating values was also reported. Yue *et al*. (2017) carried out the torrefaction of biomass (sorghum), and the results indicated that torrefaction is attractive for fuel quality improvement. Similarly, the results from the pretreatment of corn cob carried out by Li *et al*. (2018) affirm the results of this study, which suggests torrefaction as a promising method of enhancing the properties of biomass.

Solvolysis, also referred to as hydrothermal pretreatment, is a pretreatment process which produces a solid product termed hydrochar. This solid hydrochar also exhibits improved fuel properties such as; reduced oxygen-to-carbon ratio, increased higher heating values (HHV), and improved hydrophobicity compared to raw and torrefied biomass (Yan *et al.,* 2017). Solvolysis process has also been described as an eco-friendly process because deionized water is used instead of chemicals (Jin *et al*., 2016; Lei *et al.,* 2013). Therefore, solvolysis is defined as a pretreatment process whereby biomass is submerged in water at high temperatures between 150 – 300 °C for some time in an inert atmosphere (Hassan *et al*., 2018; Rackemann *et al*., 2019).

Solvolysis pretreatment has been very efficient in pre-treating biomass with high moisture content and biomass with low moisture content. Due to the subcritical nature of water at a mild temperature range of 150 – 180 °C, the solvolysis process facilitates the solubilization of the hemicellulose, cellulose, and lignin component at low temperatures compared to torrefaction. This phenomenon is responsible for the low mass yield attributed to solvolysis process and eventually an enhanced HHV compared to torrefied biomass.

Several researchers have investigated the effect of solvolysis on the properties of biomass. Lynam *et al*. (2015) reported the influence of solvolysis on five different biomasses with loblolly pine inclusive. It was reported that there was a drastic mass loss of 40 % for pine with a 1.3 enhancement factor of the HHV. Zhang *et al*. (2017) carried out solvolysis treatment on rice husk between 150 – 240 °C for 60 minutes. Results showed the high dependence of the HHV on the reaction temperature. Similar observations were reported for Miscanthus biomass by Park *et al*. (2020). Nakason (2017) investigated the effect of the liquid-to-solid ratio (LSR) and reported that an increased LSR tends to reduce the mass yield of hydrochar and increase the higher heating value. Hashemi *et al*. (2019) enhanced the production of biogas from safflower straw by hydrothermally pre-treating it. The authors concluded that biogas' yield could significantly be increased by pre-treating biomass at less severe conditions.

The operating temperature and the residence time have been considered to be critical process conditions that affect the physicochemical properties of both biochar and hydrochar. Other operating conditions are the mass of biomass feed (embedded in the Nitrogen-to-Solid ratio for torrefaction), the Liquid-to-Solid ratio for solvolysis, the particle size, the type of reactor, and the milling technique. The enhancement of biomass (fuel) properties depends on the operating conditions used during the pretreatment process. Therefore, the effect of these conditions on the final fuel properties should be well understood. Furthermore, understanding the modelling and optimisation process conditions will play a crucial role in designing an efficient industrial application process. Based on these focuses, it will be feasible to produce bio-char and hydrochar briquettes with higher bulk energy density. Therefore, these briquettes can serve as an efficient feedstock for the thermochemical conversion process (Atienza-Martínez *et al.*, 2017; Wu *et al*., 2018). According to the authors mentioned above, the reduction in the mass yield of the biochar/hydrochar at increased temperature is a massive setback in biomass

pretreatment. Hence, it is necessary to optimize the process conditions to produce quality biochar and hydrochar for effective gasification.

Only a few published works have investigated the effect and optimization of process conditions on the solvolysis pretreatment of Pine Saw Dust (PSD). More so, fewer studies have reported the comparative analysis of solid fuel produced from solvolysis and torrefaction at the same operating conditions. Notably, assessing the desirability function and genetic algorithm for optimising the process conditions for torrefaction and solvolysis of biomass (PSD) has not been reported in the literature. As a result of these knowledge gaps stated above, this research aimed to study the effect of process conditions during the torrefaction and solvolysis pretreatment of Pine Saw Dust (PSD) and determine the optimal process conditions using the desirability function and the genetic algorithm approach. The RSM based on the BBD method was used for the experimental design, and the data obtained were employed in the modelling and optimization processes.

4.2. Experimental Procedure and Analysis

Effect of process conditions on torrefaction and solvolysis pretreatment were studied using the Box-Behnken Design, and the optimization was carried out using the desirability function and genetic algorithm (GA). The detailed experimental procedures, analyses and optimization techniques are presented in Section 3.1 of Chapter 3.

4.3. Results and Discussion

4.3.1. Physicochemical properties of raw and pre-treated PSD

The physicochemical properties that bring about the need to explore PSD as a good biofuel source are shown in Table 4.1. The lignocellulosic analysis of PSD as carried out by Shi and Wang (2014) gives a reasonable reason why PSD contains a high percentage of volatile matter, as seen in Table 4.1. The high volatile matter can be attributed to the high fraction of both the

hemicellulose and cellulose in PSD. The low ash content (0.59 %) suggests that PSD can be efficient in producing biogas. This suggestion is because ash hinders the thermochemical conversion process of biomass (Nhuchhen and Abdul Salam, 2012) and reduces the higher heating value of biomass (Nhuchhen and Afzal, 2017). The low inherent moisture content also makes PSD suitable for the torrefaction process, although solvolysis is highly suitable for biomass with high moisture content. The absolute and relative errors derived from the analyses carried out in triplicates are also reported in Table 4.1. The absolute errors of the measured values also represent the standard deviations while the absolute errors for values which were calculated by different (i.e. Fixed Carbon and Oxygen contents) were calculated using the propagation of error analysis. The relative errors showed that, compared to the actual measured values, the errors associated with its measurements were relatively low, indicating good repeatability.

Table 4.1. Physicochemical properties of raw PSD.

Error	Proximate analysis (wt.%, ad)				Ultimate analysis (wt.%, ad)					HHV (MJ/kg)
	M	A	V	FC[b]	C	H	O[b]	N	S	
	8.55	0.59	71.80	19.06	50.54	7.08	41.66	0.15	0.57	19.89
Absolute error	0.19	0.02	0.42	0.63	0.39	0.02	0.42	0.01	0.01	0.52
Relative error	0.02	0.03	0.01	0.03	0.01	0.003	0.01	0.06	0.01	0.03

ad – air-dry basis; M – moisture; A – ash; V – volatile; FC – fixed carbon; He – Hemicellulose; Ce – cellulose; Li – lignin. [b] by difference.

The Oxygen-to-Carbon (O:C) ratio of 0.82 and Hydrogen-to-Carbon (H:C) ratio of 0.14 obtained for the raw PSD was comparable to studies reported by Sanwal *et al.* (2018) on lignite

coal O:C ratio of 0.73 and H:C ratio of 0.08. However, the mean O:C and H:C ratios were significantly reduced by torrefaction and solvolysis, as shown in Table 4.2.

It can be observed from Table 4.2 that the fraction of carbon significantly increased as the severity (i.e. the operating temperature and residence time) of the experiments increased for both pretreatment processes. Comparing Torr2 and Torr3 (as seen in Table 4.2), it can be seen that the carbon contents increased with NSR. This observation may be attributed to the fact that there is more uniform heating for a lesser mass feed of biomass, thereby breaking the oxygen bonds present in the sample. An increase in the LSR during solvolysis pretreatment increased the carbon content. This observation could be due to the influence of the subcritical nature of water during solvolysis, and its tendency to destroy the hydrogen and oxygen bonds presents in the biomass, thereby increasing the fraction of the carbon content. The oxygen and hydrogen content of pre-treated PSD considerably reduced, which resulted from the removal of the volatile compounds having these atoms during torrefaction and solvolysis. In particular, the reduction in the oxygen content of torrefied PSD can be attributed to the decarboxylation and deoxygenation reactions that occur during the pretreatment process. Similarly, the removal of the excess moisture content, CO_2, CO and other acidic compounds resulted in the significant reduction in the oxygen content of PSD during torrefaction. The removal of the carboxylic group, which has a hydrogen atom, also reduces the hydrogen content of PSD during torrefaction.

The Van Krevelen plots (Figure 4.1) also show the elemental changes during the PSD pretreatment. These significant changes were as a result of the different depolymerization reaction taking place during pretreatment processes. It was observed that there was a linear relationship between the H:C and the O:C ratio for both pretreatment processes. The colour

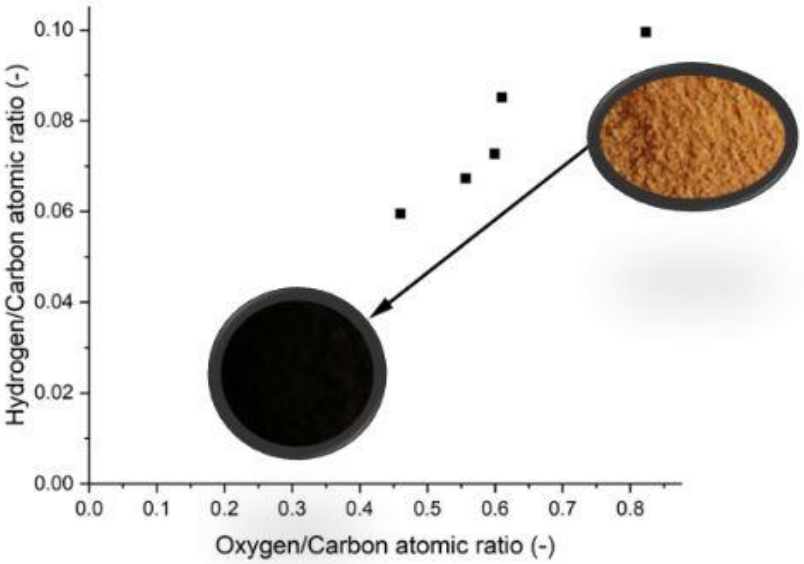
changes were also evident as it changed from a light brown colour to a black colour as the severity of the pretreatment process increased.

Conclusively, the increment in the carbon content of PSD after pretreatment can considerably increase the combustion characteristics (i.e. ignition temperature, mass transfer, heat and energy transfer, flammability test, combustion rate and time.) of PSD accompanied by an increase in the higher heating value (Park *et al*., 2020). The changes in the ultimate analysis of pretreated biomass were in agreement with the findings made by Gong *et al*. (2016) and Dai *et al*. (2018) for the torrefaction of PSD and solvolysis pretreatment of bamboo, respectively. These observations suggest that torrefaction and solvolysis pretreatments can improve gasification process.

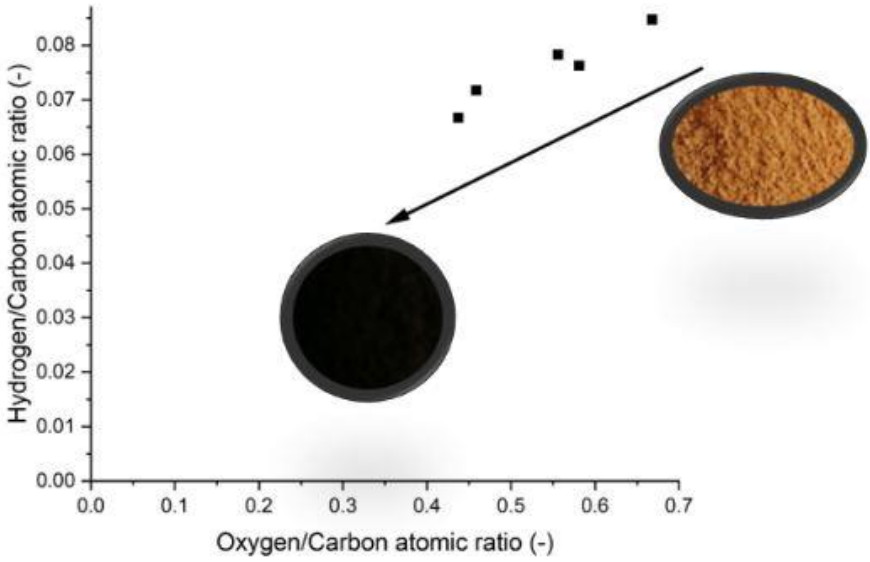
Table 4.2. Ultimate analysis of some pre-treated PSD.

Sample ID	Temp (°C)	Time (min)	NSR/LSR (-)	Ultimate analysis (%)				
				C	O[b]	H	N	S
Torr1	200	30	5	51.76	42.6	5.15	0.14	0.35
Torr2	250	120	4	59.56	35.69	4.33	0.15	0.27
Torr3	250	120	6	61.34	34.15	4.13	0.13	0.25
Torr4	300	30	5	58.75	35.84	5.00	0.13	0.28
Torr5	300	120	5	65.56	30.18	3.90	0.13	0.23
Solv1	200	30	5	56.67	37.86	4.80	0.15	0.52
Solv2	250	120	4	59.94	34.84	4.57	0.14	0.51
Solv3	250	120	6	64.96	29.81	4.66	0.14	0.43
Solv4	300	30	5	60.81	33.81	4.76	0.14	0.48
Solv5	300	120	5	66.13	28.93	4.41	0.15	0.38

Torr – Torrefaction; Solv – Solvolysis; NSR – Nitrogen/Solid Ratio; LSR – Liquid/Solid Ratio; C – Carbon; O – Oxygen; H – Hydrogen; N – Nitrogen; S – Sulphur; [b] calculated by difference.



(a)



(b)

Figure 4.1. Van Krevelen diagram of PSD in (a) torrefaction and (b) solvolysis

4.3.2. Predictive model development and statistical analysis

The detailed experimental runs, including the responses, are presented in Tables 4.3 and 4.4 for torrefaction and solvolysis, respectively. Randomized order was observed to reduce the effect of a sequential variation in the results.

The relationship between the process conditions and the responses used in this study were developed using the actual equations and the coded equation in the form of the quadratic regression depicted in Equation (3.5) of Chapter 3. The coded equations shown in Equation (4.1) – Equation (4.6) were used to study the relative impact of the process conditions on the responses by comparing the factor coefficients and its signs. The actual equations, as shown in Equation (4.7) – Equation (4.12) were used to make predictions about the responses given any set of process conditions. The actual equations were developed based on the units and value scale of each process condition.

$$\mathrm{HHV(Torr)}(MJ/kg) = 22.25 + 1.69X_1 + 0.496X_2 + 0.113X_3 + 0.088X_1X_2 - 0.100X_1X_3 + 0.085X_2X_3 + 0.229X_1^2 + 0.269X_2^2 + 0.242X_3^2 \quad (4.1)$$

$$MY(Torr)(\%) = 72.76 - 12.19X_1 - 2.82X_2 - 1.11X_3 - 3.32X_1X_2 - 0.685X_1X_3 - 0.108X_2X_3 + 3.20X_1^2 - 2.32X_2^2 - 1.07X_3^2 \quad (4.2)$$

$$EEF\ (Torr)(-) = 1.12 + 0.085X_1 + 0.025X_2 + 0.006X_3 + 0.0047X_1X_2 - 0.005X_1X_3 + 0.004X_2X_3 + 0.012X_1^2 + 0.014X_2^2 + 0.012X_3^2 \quad (4.3)$$

$$HHV(Solv)(MJ/kg) = 23.74 + 1.62X_1 + 0.459X_2 - 0.354X_3 \quad (4.4)$$

$$MY(Solv)(M\%) = 70.18 - 7.86X_1 - 5.89X_2 - 2.43X_3 - 2.41X_1X_2 - 1.47X_1X_3 + 0.195X_2X_3 - 2.91X_1^2 - 2.96X_2^2 - 3.92X_3^2 \quad (4.5)$$

$$EEF(Solv)(-) = 1.20 + 0.082X_1 + 0.023X_2 - 0.018X_3 \quad (4.6)$$

$$\text{HHV(Torr)}(MJ/kg) = 23.88 - 0.005X_1 - 0.028X_2 - 1.947X_3 + 0.00004X_1X_2 - 0.002X_1X_3 + 0.0019X_2X_3 + 0.00009X_1^2 + 0.00013X_2^2 + 0.242X_3^2 \quad (4.7)$$

$$MY(Torr)(\%) = 220.02 - 1.30X_1 + 0.491X_2 + 13.20X_3 - 0.0015X_1X_2 - 0.014X_1X_3 - 0.0024X_2X_3 + 0.0025X_1^2 - 0.00115X_2^2 - 1.07X_3^2 \quad (4.8)$$

$$EEF\ (Torr)(-) = 1.20 - 0.00025X_1 - 0.0014X_2 - 0.098X_3 + 1.96E-06X_1X_2 - 0.0001X_1X_3 + 0.000095X_2X_3 + 4.61E-06X_1^2 + 6.68E-06X_2^2 + 0.012X_3^2 \quad (4.9)$$

$$HHV(Solv)(MJ/kg) = 16.67 + 0.032X_1 + 0.010X_2 - 0.354X_3 \quad (4.10)$$

$$MY(Solv)(\%) = -95.36 + 0.592X_1 + 0.334X_2 + 43.83X_3 - 0.0011X_1X_2 - 0.029X_1X_3 + 0.004X_2X_3 - 0.001X_1^2 - 0.0015X_2^2 - 3.92X_3^2 \quad (4.11)$$

$$EEF(Solv)(-) = 0.842 + 0.0016X_1 + 0.0005X_2 - 0.018X_3 \quad (4.12)$$

Table 4.3. Experimental design and responses for the torrefaction process.

				Experimental values			Model values		
Run	Temp: X_1 (°C)	Time: X_2 (min)	NSR: X_3 (-)	HHV (MJ/kg)	Mass Yield (%)	EEF (-)	HHV (MJ/kg)	Mass Yield (%)	EEF (-)
1	300	30	5	23.92	70.78	1.20	23.72	73.11	1.20
2	200	75	6	21.33	88.72	1.07	21.20	90.68	1.06
3	250	120	4	23.11	68.33	1.16	22.96	69.16	1.16
4	200	120	5	21.41	89.14	1.08	21.41	90.19	1.08
5	250	75	5	22.28	73.88	1.12	22.16	74.35	1.12
6	300	120	5	25.06	56.81	1.26	24.89	60.19	1.26
7	250	75	5	22.31	72.13	1.12	22.16	74.35	1.12
8	200	75	4	20.84	90.14	1.05	20.77	91.64	1.04
9	250	75	5	22.11	72.96	1.11	22.16	74.35	1.12
10	300	75	6	24.41	64.27	1.23	24.30	66.03	1.22
11	250	120	6	23.44	66.45	1.18	23.37	66.58	1.18
12	250	30	6	22.25	70.62	1.12	22.20	72.96	1.12
13	250	75	5	22.28	72.87	1.12	22.16	74.35	1.12
14	250	30	4	22.26	72.07	1.12	22.14	75.11	1.12
15	200	30	5	20.62	89.82	1.04	20.60	89.61	1.03
16	300	75	4	24.32	68.43	1.22	24.27	69.79	1.23
17	250	75	5	22.29	71.97	1.12	22.16	74.35	1.12

Table 4.4. Experimental design and responses for the solvolysis process.

				Experimental values			Model values		
Run	Temp: X_1 (°C)	Time: X_2 (min)	LSR: X_3 (-)	HHV (MJ/kg)	Mass Yield (%)	EEF (-)	HHV (MJ/kg)	Mass Yield (%)	EEF (-)
1	200	30	5	22.12	75.46	1.12	21.60	77.86	1.09
2	200	75	6	21.72	70.43	1.10	21.70	72.01	1.09
3	250	75	5	23.38	69.56	1.18	23.65	72.53	1.19
4	250	120	6	23.91	55.52	1.21	23.75	56.86	1.19
5	250	30	6	23.12	67.14	1.18	22.85	69.64	1.15
6	250	75	5	23.71	68.43	1.20	23.65	72.53	1.19
7	300	30	5	24.16	65.31	1.22	24.80	69.26	1.25
8	200	75	4	22.53	73.31	1.14	22.40	73.75	1.13
9	250	120	4	24.12	59.05	1.22	24.45	61.14	1.23
10	250	75	5	23.73	70.62	1.20	23.65	72.53	1.19
11	250	75	5	23.73	71.21	1.20	23.65	72.53	1.19
12	300	75	6	25.01	51.03	1.26	24.90	55.56	1.25
13	250	75	5	23.86	71.06	1.21	23.65	72.53	1.19
14	300	75	4	26.42	59.79	1.33	25.60	63.10	1.29
15	250	30	4	23.52	71.45	1.19	23.55	74.64	1.19
16	300	120	5	26.13	48.93	1.32	25.70	51.17	1.29
17	200	120	5	22.43	68.71	1.13	22.50	69.67	1.13

An Analysis of Variance (ANOVA) test was done to determine the statistical significance of the experimental results and the developed models. The developed models for both torrefaction and solvolysis process were statistically significant, as indicated by the F-values reported in Table 4.5 and Table 4.6, respectively. This statistical significance implied that to a satisfactory confidence level of 95 %, the model was adequate to describe the experimental results. It was also observed that the HHV and EEF both had the same ANOVA table and consequently, similar statistical conclusions. This observation was due to the linear relationship between the HHV and the EEF, as shown in Equation 3.4 from Chapter 3 (i.e. showing high collinearity). A process variable is considered significant if the P-value is less than 0.05. However, as seen in Table 4.5 and Table 4.6, only a few terms were insignificant. These terms were not removed from the model because they did not significantly improve the models.

Furthermore, the coefficient of determination (R^2) of the responses explained by the process variables and the Lack of Fit, were analyzed to support the F-test's inferences. For Inference sake, Keivani *et al*. (2018) suggested that an R^2 greater than 0.85 can be considered a reliable model. An R^2 of 0.85 means that the process variables can explain 85 % of the variation in the responses. The R^2 for the HHV and MY model during torrefaction were 0.9979 and 0.9920, as shown in Table 4.5. The R^2 for the HHV and MY model during solvolysis were 0.9301 and 0.9915, as shown in Table 4.6. Hence, these coefficients of determination validate the significance of the developed models.

Although the R^2 can be overestimated while increasing the number of terms in the model, the Adjusted R^2 (Adj.R^2) gives a better view of its significance. All Adjusted R^2s were higher than 0.91, supporting the significance of the models. The accuracy of the developed regression models for torrefaction and solvolysis was also verified by plotting the predicted values against the actual values shown in Figures 4.2 and 4.3, respectively. The predicted R^2 reported in Table 4.5 and Table 4.6 also show values higher than 0.85. Additionally, the adjusted and predicted

R^2s were within a difference of less than 0.2, indicating an adequate agreement level (Okolie *et al.,* 2020).

Table 4.5. Analysis of Variance (ANOVA) of the torrefaction models.

Source	DF	F-Value	P-Value	Comment
HHV and EEF: Higher Heating Value and Energy Enhancement Factor				
Model	9	362.28	< 0.0001	Significant
X_1: Temp.	1	2877.83	< 0.0001	
X_2: Time	1	248.51	< 0.0001	
X_3: NSR	1	12.77	0.0091	
X_1X_2	1	3.86	0.0901	
X_1X_3	1	5.05	0.0595	
X_2X_3	1	3.65	0.0979	
X_1^2	1	27.91	0.0011	
X_2^2	1	38.50	0.0004	
X_3^2	1	31.04	0.0008	
Lack of Fit	3	1.46	0.3523	Not significant

R^2 = 0.9979; Adj.R^2 = 0.9951; Pred.R^2 = 0.9805; Adeq.Precision = 63.9923

MY: Mass Yield				
Model	9	165.60	< 0.0001	Significant
X_1: Temp.	1	1189.01	< 0.0001	
X: Time	1	63.62	0.0005	
X_3: NSR	1	9.92	0.0473	
X_1X_2	1	44.16	0.0014	
X_1X_3	1	1.88	0.3308	
X_2X_3	1	0.0462	0.8744	
X_1^2	1	161.80	< 0.0001	
X_2^2	1	22.73	0.0083	
X_3^2	1	4.83	0.1376	
Lack of Fit	3	3.23	0.0655	Not Significant
R^2 = 0.9920; Adj.R^2 = 0.9817; Pred.R^2 = 0.8942; Adeq.Precision = 32.0294				

Table 4.6. Analysis of Variance (ANOVA) of the solvolysis models.

Source	DF	F-Value	P-Value	Comment
HHV and EEF: Higher Heating Value and Energy Enhancement Factor				
Model	3	57.67	< 0.0001	Significant
X_1: Temp.	1	153.30	< 0.0001	
X_2: Time	1	12.37	0.0038	
X_3: LSR	1	7.36	0.0178	
Lack of Fit	9	5.69	0.0548	Not significant
R^2 = 0.9301; Adj.R^2 = 0.9140; Pred.R^2 = 0.8593; Adeq.Precision = 23.1757				
MY: Mass Yield				
Model	9	110.70	< 0.0001	Significant
X_1: Temp.	1	493.77	< 0.0001	
X_2: Time	1	277.89	< 0.0001	
X_3: LSR	1	47.43	0.0004	
X_1X_2	1	23.18	0.0033	

X_1X_3	1	8.64	0.0321	
X_2X_3	1	0.1521	0.7338	
X_1^2	1	28.72	0.0018	
X_2^2	1	36.93	0.0009	
X_3^2	1	64.84	0.0002	
Lack of Fit	3	3.02	0.5830	Not Significant
$R^2 = 0.9915$; Adj.$R^2 = 0.9807$; Pred.$R^2 = 0.9434$; Adeq.Precision = 32.5437				

The Lack of Fitness test was used to check the acceptability of the models. This test compares the residuals associated with the model and the pure error, estimated by the center points of the design. While employing a 95 % confidence level, the P-values of the LOF for all models were found to be higher than 0.05, indicating its non-significance. There was a 35.2 % and 6.6 % chance that a Lack of Fit F-value this large for HHV model and mass yield model could occur due to noise during torrefaction. Similarly, there was a 5.5 % and 58.3 % chance that a Lack of Fit F-value this large for HHV model and mass yield model could occur due to noise during solvolysis. The LOF should not be significant to ensure the model's fitness (Kumar *et al*., 2020).

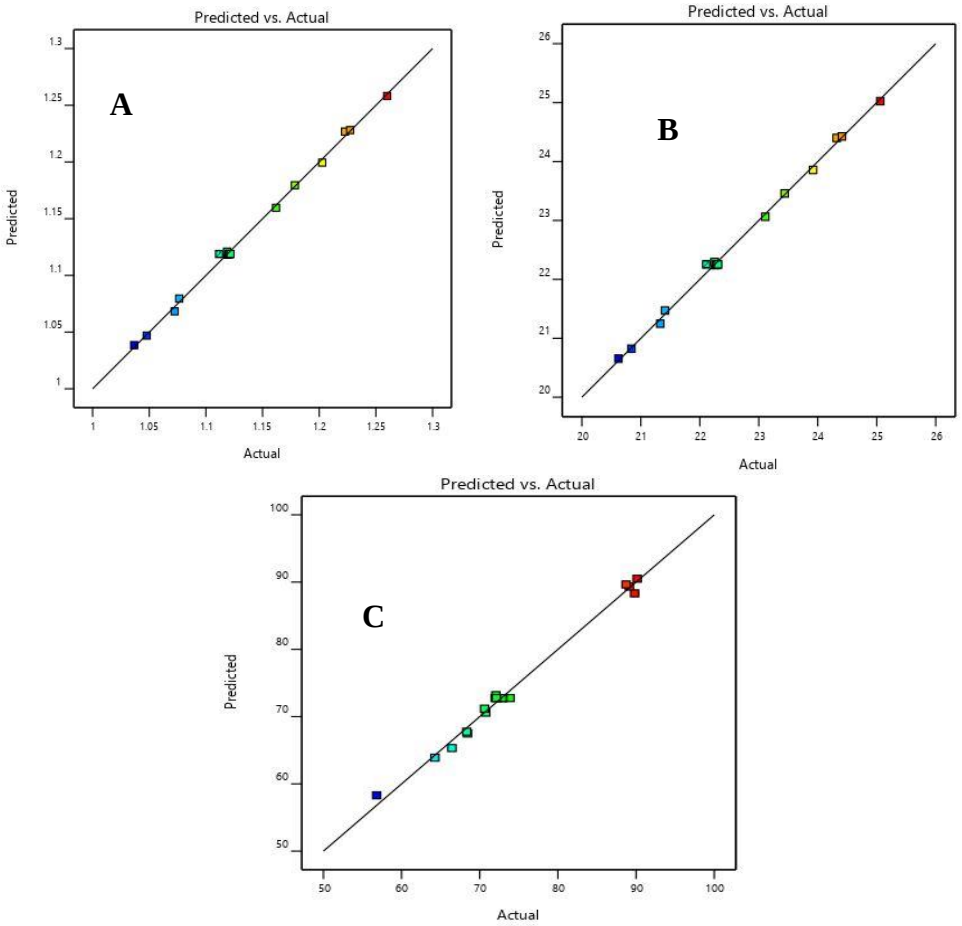


Figure 4.2. Predicted responses against actual responses of (a) EEF (b) HHV and (c) MY for torrefaction process

All models were found to have a ratio greater than 4, indicating an adequate signal, as shown in Table 4.5 and 4.6. The homoscedasticity of the residuals was studied to ascertain that the

normality assumption for a regression model was observed. This study was done using the normal probability plots of the residuals. It can be confirmed that the normality assumption was observed as the residuals between the actual and predicted values were normally distributed at random exhibited by the straight-line graph as shown in Figures 4.4 and 4.5 for torrefaction and solvolysis process respectively.

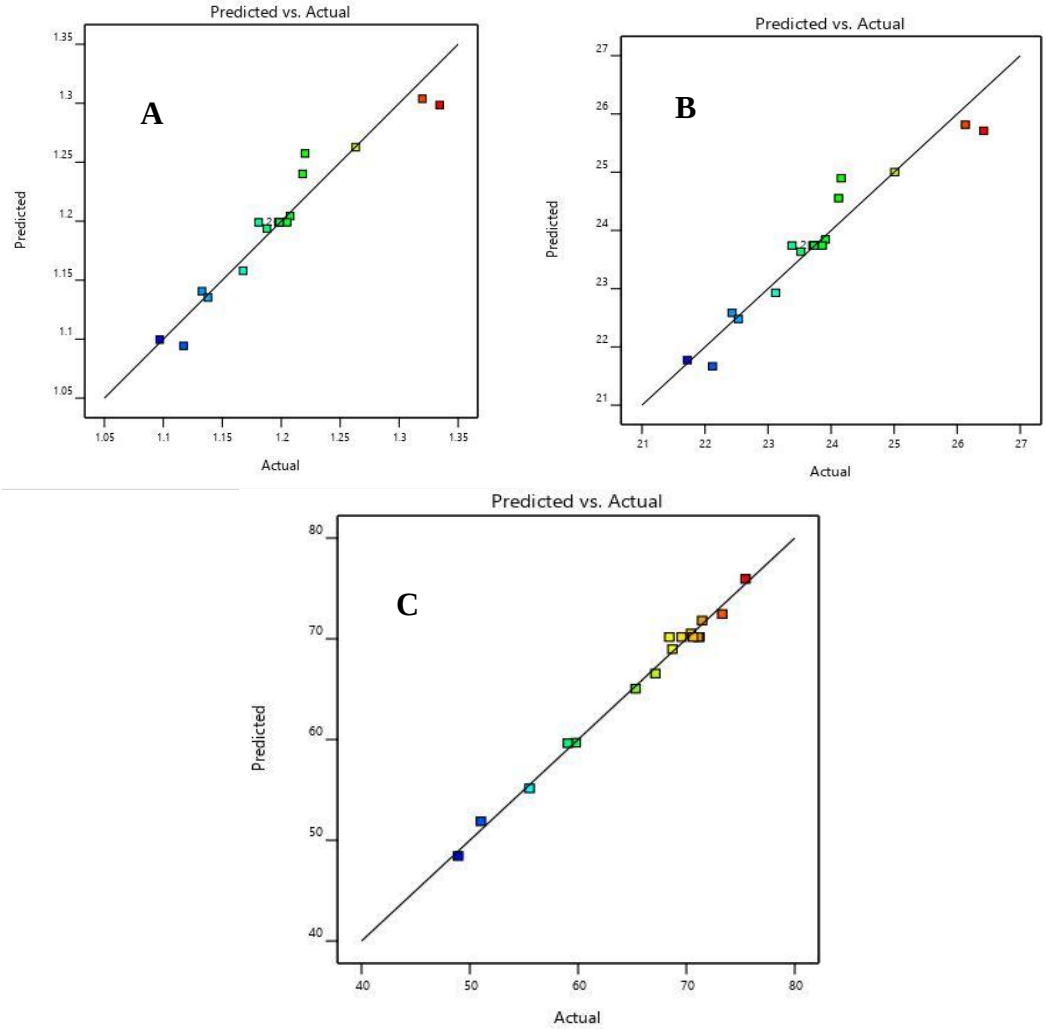


Figure 4.3. Predicted responses against actual responses of (a) EEF (b) HHV and (c) MY for solvolysis process

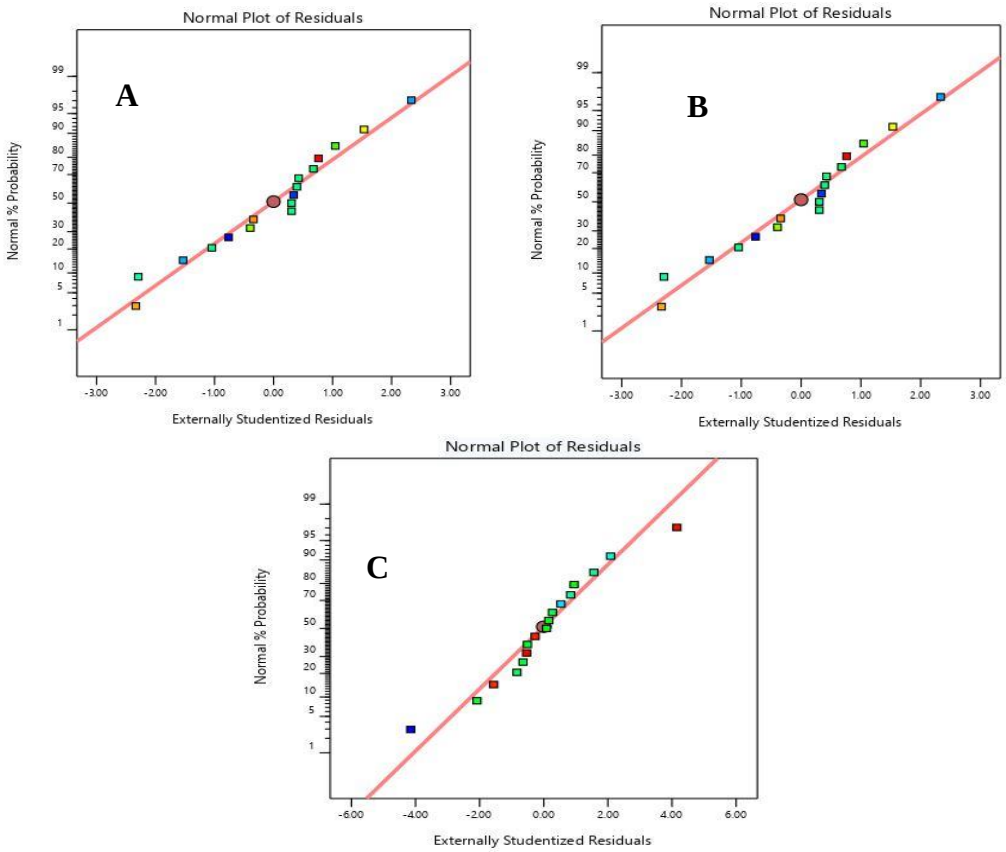


Figure 4.4. Normal plot of residual for (a) HHV (b) EEF and (c) MY for torrefaction process

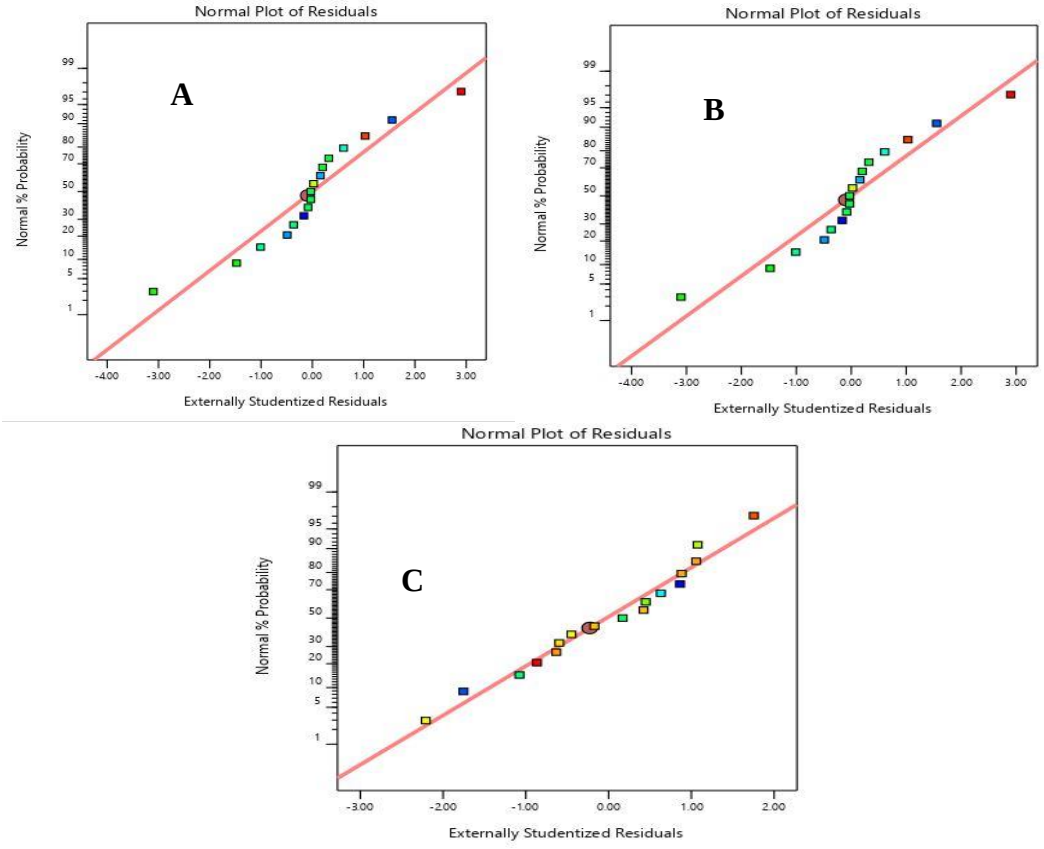


Figure 4.5. Normal plot of residual for (a) HHV (b) EEF and (c) MY for solvolysis process

4.3.3. Comparative analysis of the effect of process conditions on torrefaction and solvolysis process

Three responses were used to study and compare the effect of process conditions on torrefaction and solvolysis process. 3-dimensional response surface plots shown in Figures 4.6 and 4.7 were used to study these effects for torrefaction and solvolysis, respectively. The 3D surface plots show the effect of any two process conditions on individual responses, keeping the third condition constant (usually the mid-point value). These plots made it possible to study how each response changes while varying process conditions simultaneously, i.e. avoiding considering OFAT (One Factor at a Time).

4.3.3.1. Effect of process conditions on HHV and EEF

The 3D surface plots describing the effect of all three process conditions (i.e. Temperature: X_1, Time: X_2 and NSR/LSR: X_3) on the higher heating value of pre-treated PSD are shown in Figures 4.6 and 4.7. It is shown that HHV of biomass was highly significantly (i.e. P-value < 0.0001) influenced by the reaction temperature. From the 3D plots, it can be concluded that there is a linear correlation between the HHV and temperature of biomass. The analysis of variance of the torrefaction model suggests that only the independent and the squared effects of the process conditions were significant in explaining the HHV of PSD (as seen in Table 4.5). Also, only the independent process conditions were the significant terms in explaining the HHV of PSD during solvolysis process (as seen in Table 4.6).

Unlike other developed models, the HHV and EEF models for solvolysis process only contained the independent terms. This observation was in agreement with the result reported by Gan *et al*. (2019) for the pretreatment of palm kernel shell via solvolysis. Like the torrefaction process, the independent temperature term showed the most significance on the HHV of PSD during solvolysis process. Also, the temperature and residence time significantly affected the HHV than LSR/NSR for both pretreatments.

From the coded equations for torrefaction process (see Equation 4.1 and 4.3), an increase in the temperature, time, and NSR (i.e. reduction of mass feed) increase the HHV and EEF of PSD. This observation agrees with the literature results (Barbanera & Muguerza, 2020; Kanwal *et al.*, 2019; Kumar *et al.*, 2020; Lee & Lee, 2014; Siyal *et al*., 2020; Wang *et al.*, 2017). Due to the low conductivity property of biomass, it has been reported that there is a limitation in the transference of heat from the heating source of the torrefier to the biomass sample (Ceylan, 2015; Gajera *et al.*, 2020). As a result of this limitation, higher temperatures will be required to ensure uniform decomposition of the lignocellulosic components throughout the biomass sample, translating into an increase in the HHV. This phenomenon is responsible for increasing HHV and EEF as the mass feed reduces (i.e. increase in NSR).

Furthermore, as indicated by the coded equations for solvolysis process (see Equation 4.4 and 4.6), unlike LSR, an increase in the reaction temperature and time increases the HHV and EEF. Similar observations have been reported by Bach *et al*., (2016); Chen *et al.*, (2012); Gong *et al*., (2016); He *et al*., (2018). The full quadratic coded equation for torrefaction also shows that the squared effects of each independent process conditions positively affects the HHV of PSD. These significant terms also suggest that the squared time and NSR term has more effect than the squared temperature term.

While comparing torrefaction and solvolysis using similar process condition, it was observed that there was a 26 % increase in HHV recorded by torrefaction. In comparison, a 31.37 % increase in HHV was recorded after solvolysis. This observation can be seen by comparing run 6 of Table 4.3 and run 16 of Table 4.4.

Similarly, comparing run 15 of Table 4.3 and run 1 of Table 4.4 (i.e. having similar process conditions), torrefaction improved the HHV of PSD by 3.76 % while solvolysis improved the HHV of PSD by 11.21 %.

Therefore, it can be concluded that solvolysis tends to improve the HHV of PSD higher than the torrefaction process. Similar observations were made by Bach and Skreiberg (2016); Yan *et al*. (2017).

4.3.3.2. Effect of process conditions of mass yield

The graphical representations of the effect of process conditions on the mass yield of fuel are shown in Figure 4.6 and Figure 4.7 during torrefaction and solvolysis, respectively. It can be observed that the pretreatment of PSD resulted in a continuous mass loss as the severity of the operating conditions increased. The removal of the methoxy group from the lignin component of PSD and eliminating the carboxyl group from the hemicellulose component of PSD can be attributed to these observed mass losses. The removal of both the carbonyl and carboxyl groups from the cellulose component of PSD could also be responsible for the observed mass loss during pretreatment (Nhuchhen *et al*., 2018).

Torrefaction and solvolysis study indicated that temperature was the most influential variable on the char's mass yield. The order of influence on the mass yield was Temperature>Time>NSR/LSR, as indicated by the P-values, as shown in Table 4.5 and Table 4.6. Nizamuddin *et al*. (2019) and Kumar *et al.* (2020) also reported that the severity (which is most influenced by the reaction temperature) of the pretreatment process significantly affects the mass yield of char. As shown in Table 4.5 and Table 4.6, and from the interactional terms, the temperature-time relationship was significant (P-value < 0.05) for torrefaction. In contrast, both the temperature-time and temperature-LSR relationship were found to be significant for solvolysis. Only the time-LSR term was found to be insignificant for the solvolysis process. This observation indicates that the LSR relies more on the operating temperature of the process than residence time to affect the mass yield of hydrochar. All linear terms have negative signs, as shown in Equation (4.2) and Equation (4.5), indicating a negative effect on the mass yield

of both biochar and hydrochar. As explained earlier, smaller mass feed of biomass (i.e. increase in NSR) results in a negative effect on biomass's mass yield.

The mass yield of hydrochar reduces as the LSR increases. This phenomenon was attributed to water behaviour at the subcritical temperature region, which readily decomposes the lignocellulosic components (Ahmed *et al*., 2019). Aside from the quadratic temperature term, all other terms negatively affect the mass yield of biochar. This observation suggests that the negative effect of temperature on mass yield at extremely high temperatures tends to reduce at extremely high temperatures. This observation could be attributed to the reduced effect of temperature on the conversion of fixed carbon formed after the volatilization process.

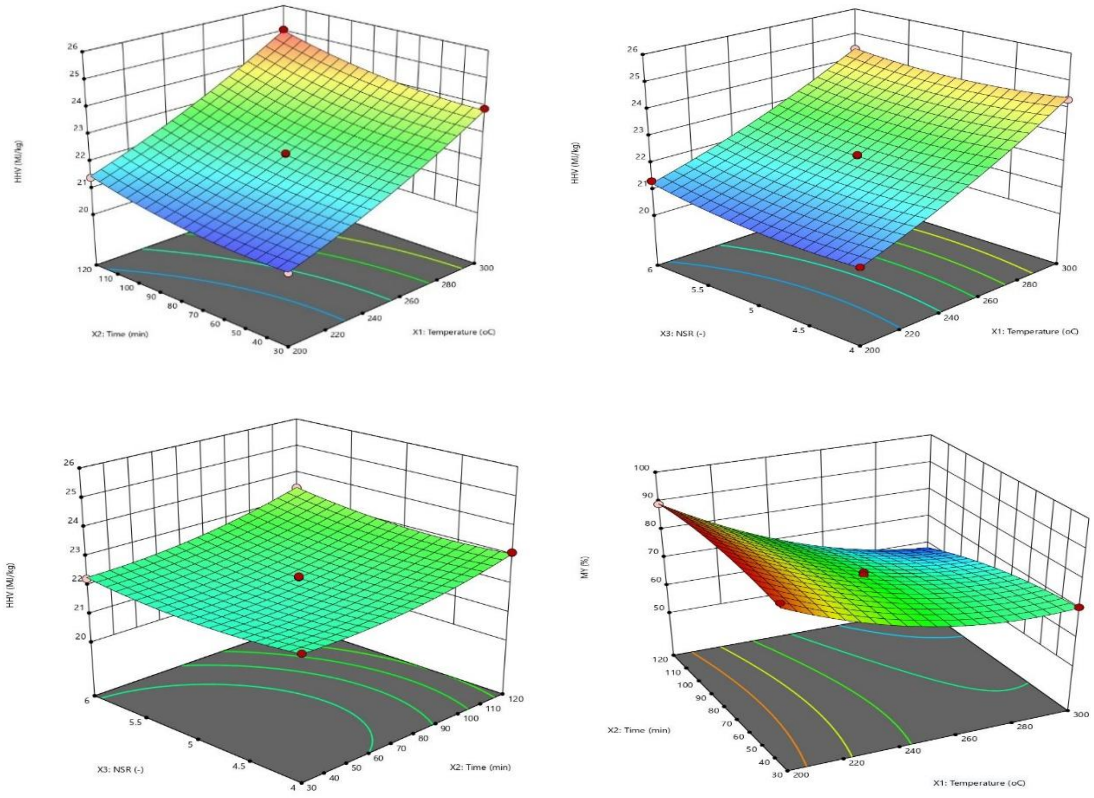


Figure 4.6. 3D response surface plots of HHV, MY and EEF for torrefaction process

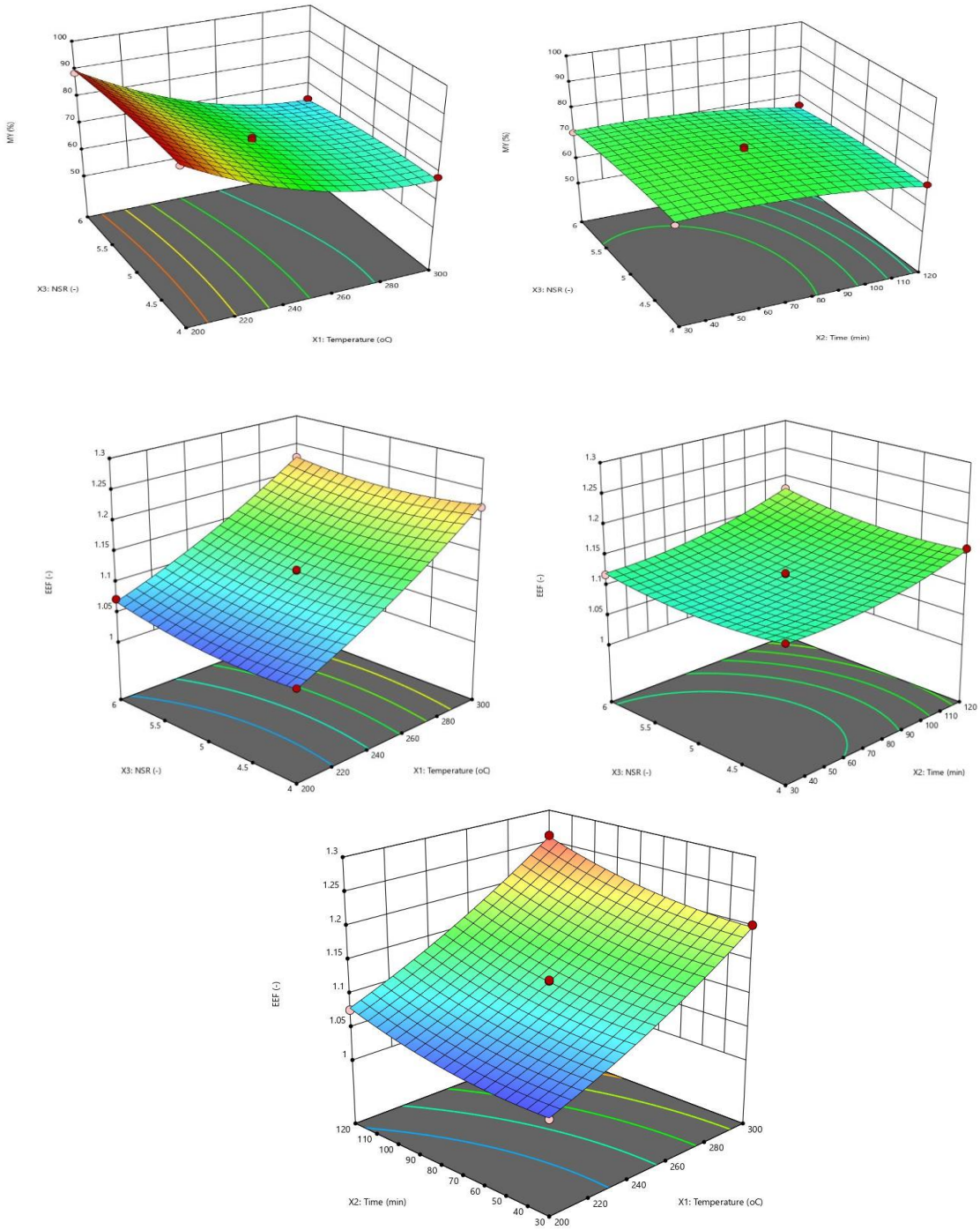


Figure 4.6. (continued)

Furthermore, both pretreatments' residence time exhibit adverse effects on the mass yield of the char produced. This observation is because longer residence time means longer time spent by the biomass in the reactor to form more oxygenated volatile compounds, resulting in a lower mass yield (Mundike *et al.*, 2016)**.**

Tables 4.3 and 4.4 show that solvolysis negatively affects the mass yield of char than the torrefaction process. To compare torrefaction and solvolysis process in terms of mass yield, two similar process conditions were used (i.e. run 6 of Table 4.3 and run 16 of Table 4.4). It can be observed that torrefaction yielded a mass of 56.81 % while solvolysis yielded a mass of 48.93 %. Similarly, comparing similar process conditions employed in run 15 of Table 4.3 and run 1 of Table 4.4, torrefaction recorded a higher mass yield of 89.82 % than solvolysis of 75.46 %. This comparison indicates that the solvolysis process negatively affected the mass yield of biomass than the torrefaction process at lower temperature regions.

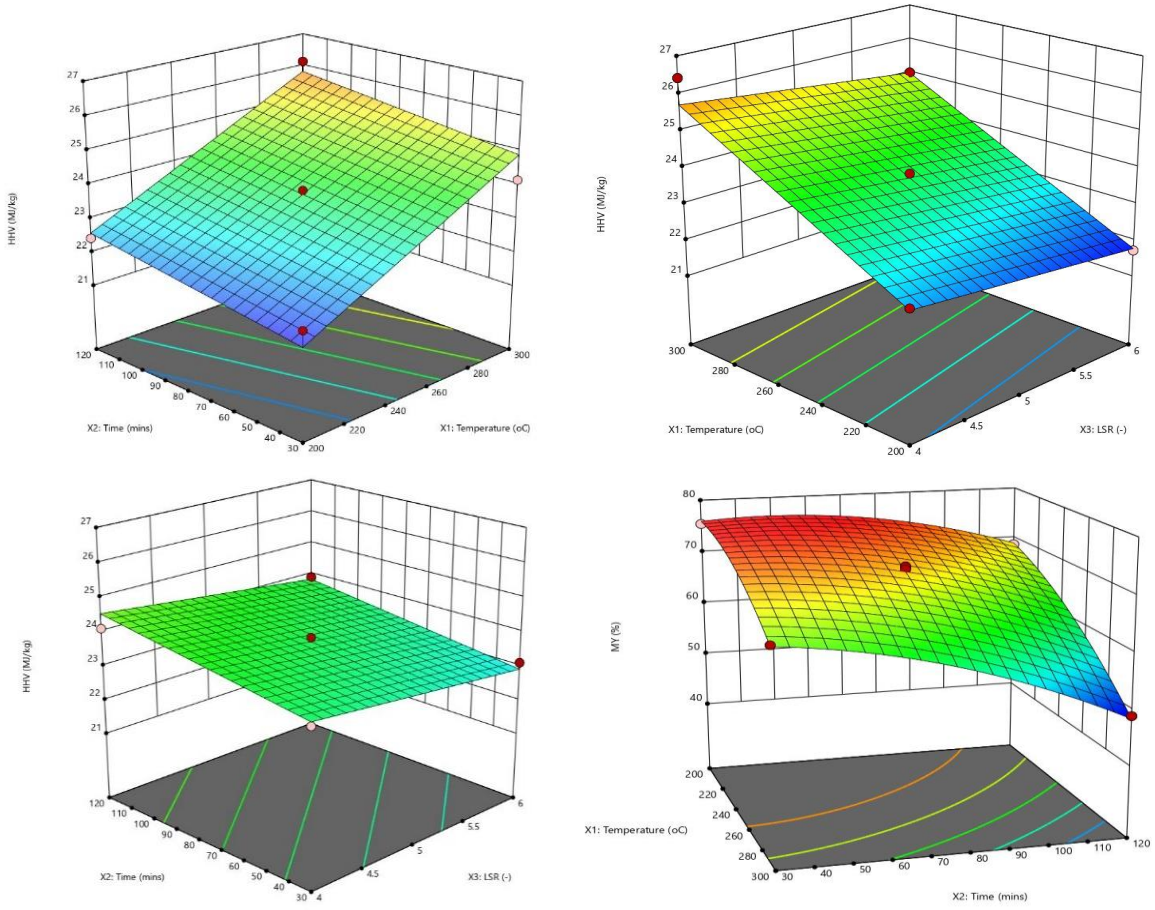


Figure 4.7. 3D response surface plots of HHV, MY and EEF for solvolysis process

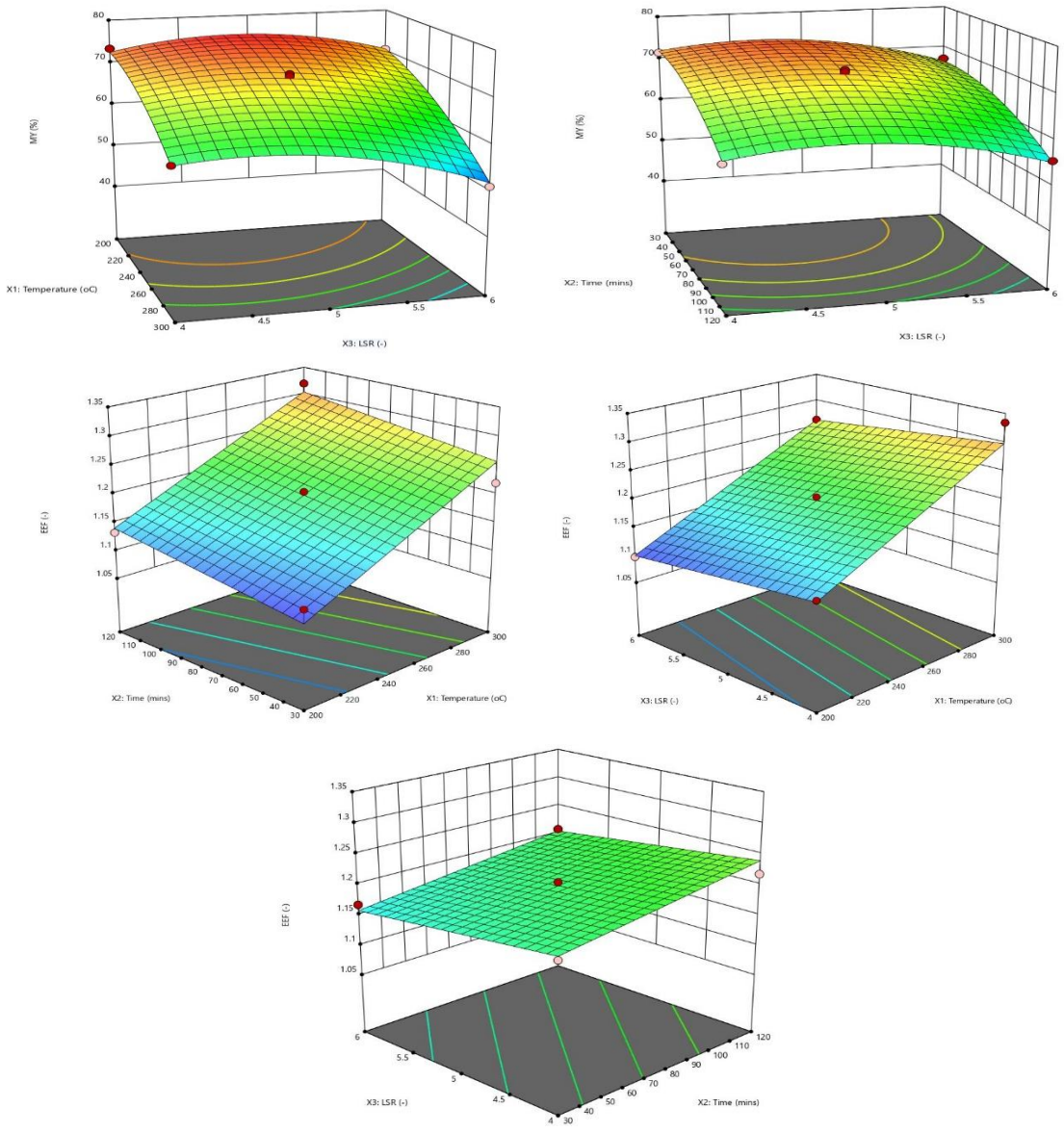


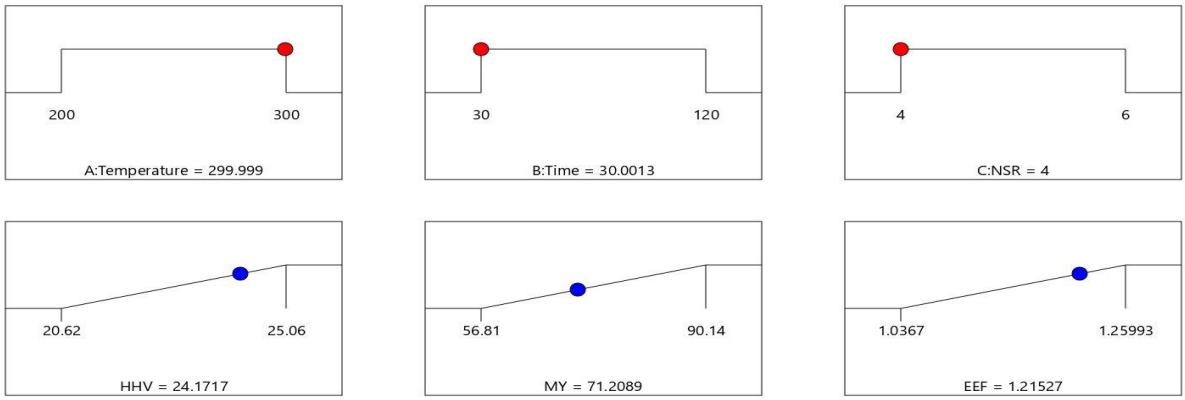
Figure 4.7. (continued)

4.3.4. Optimization of process conditions

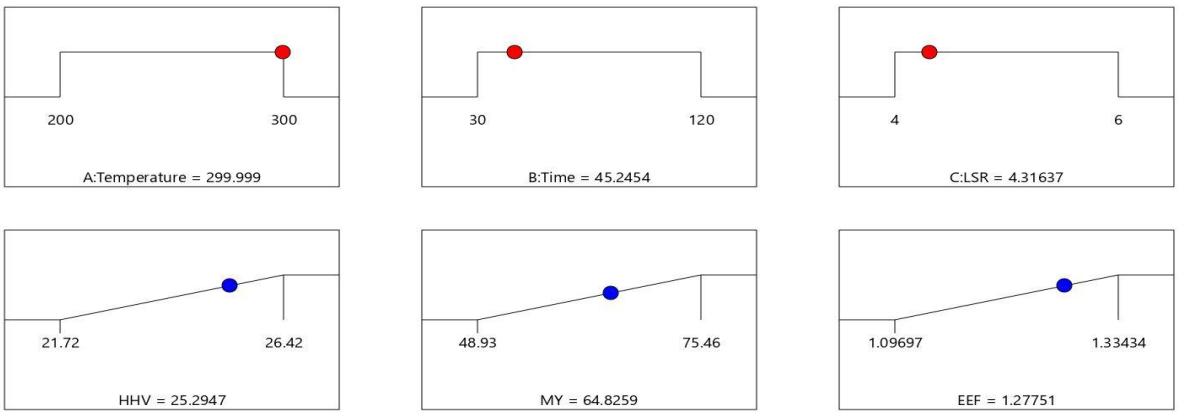
Several methods have been employed in carrying out the optimization of torrefaction and solvolysis process. One of these methods is to evaluate the energy yield of biochar/hydrochar, a function of the HHV and the mass yield. However, this method has been considered inefficient in determining the optimal conditions because the energy yield decreases with an increase in the severity of the pretreatment process (Lee and Lee, 2014). Hence, an ideal method to estimate the optimal conditions is by simultaneously increasing the mass yield and HHV of biochar/hydrochar.

4.3.4.1. Optimization using desirability function

As described in Section 3.1.5 of Chapter 3, equal weights of 1 and equal importance, were assigned to all responses to determine the optimal conditions within the range of the process conditions. As shown in Figure 4.8, based on the desirability function approach, the optimal process conditions based on the responses for solvolysis process were at 299.99 °C, 45.25 min and 4.32 LSR while torrefaction process was at 299.99 °C, 30.00 min and 4.00 NSR. At the optimal conditions, the desirability for torrefaction and solvolysis were 0.651 and 0.702, respectively. These desirability values indicate that 65.1 % and 70.02 % of all responses reached their respective torrefaction and solvolysis process targets, respectively.



(a)

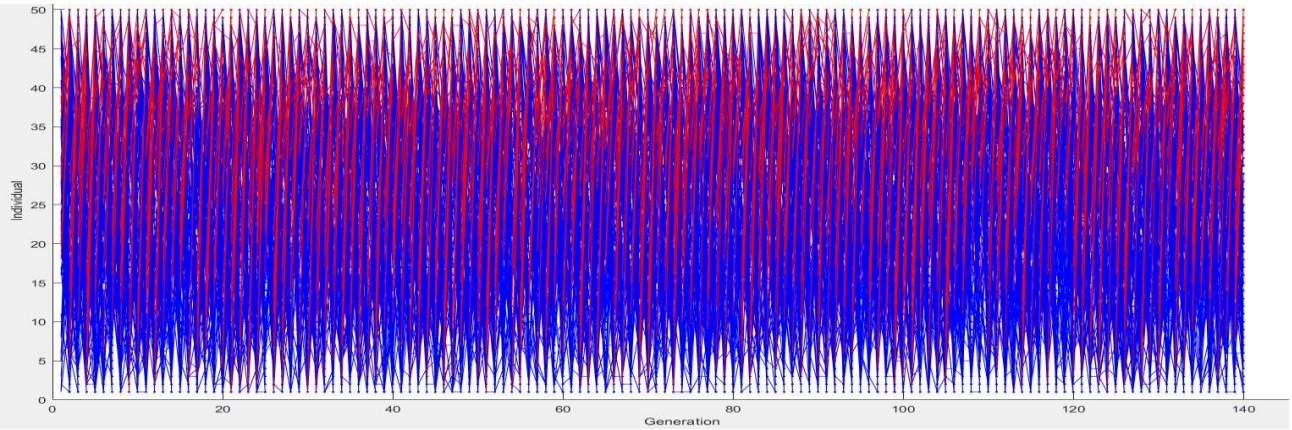


(b)

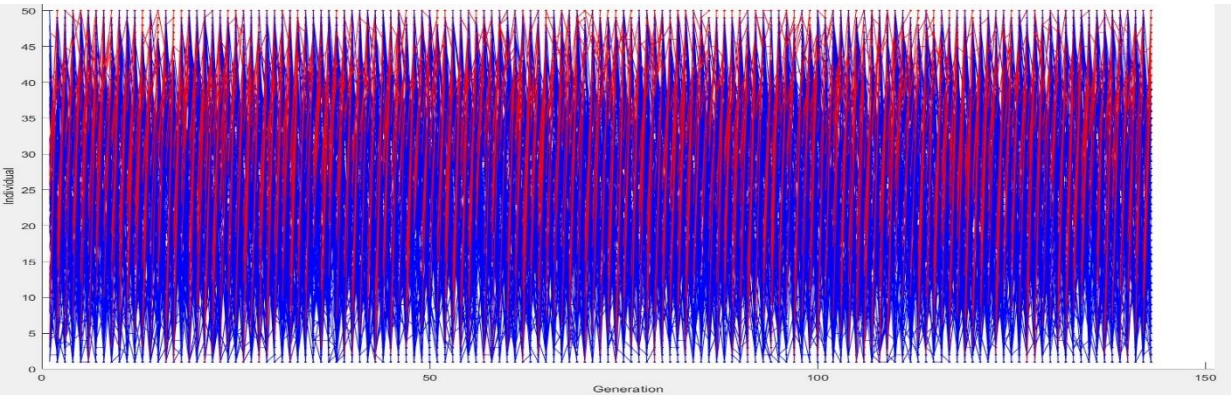
Figure 4.8. Optimal conditions for (a) torrefaction and (b) solvolysis pretreatment process

4.3.4.2. Optimization using genetic algorithm (GA)

Although the genetic algorithm has been broadly applied in the industry to optimize processes, using the genetic algorithm to optimise torrefaction and solvolysis process is scarce in the literature. It is required that before the use of a genetic algorithm for optimization, the objective functions are transformed into minimizing functions. The HHV and MY predictive models developed using the Box-Behnken were used as the objective functions 1 and 2, respectively. The EEF model was excluded because it is directly proportional to the HHV (i.e., optimising the HHV translates to an optimization in the EEF). Figure 4.9 shows the genealogy of the optimization process, which illustrates how genes are reproduced from generation to generation.



(a)



(b)

Figure 4.9. Genealogy of the optimization: (a) Torrefaction and (b) Solvolysis process

The errors existing in the optimal conditions were reduced after each generation. The optimization was terminated when the average change in the Pareto solutions' spread was less than the function tolerance. It was observed that for both torrefaction and solvolysis optimisation, the reproduction terminated at the 140th generation. The Pareto plot, as shown in Figure 4.10, gives the various optimal conditions that can be possibly estimated depending on the importance given to a response. However, for this study, the optimum conditions were chosen based on the closest values with the optimized values estimated using the desirability function.

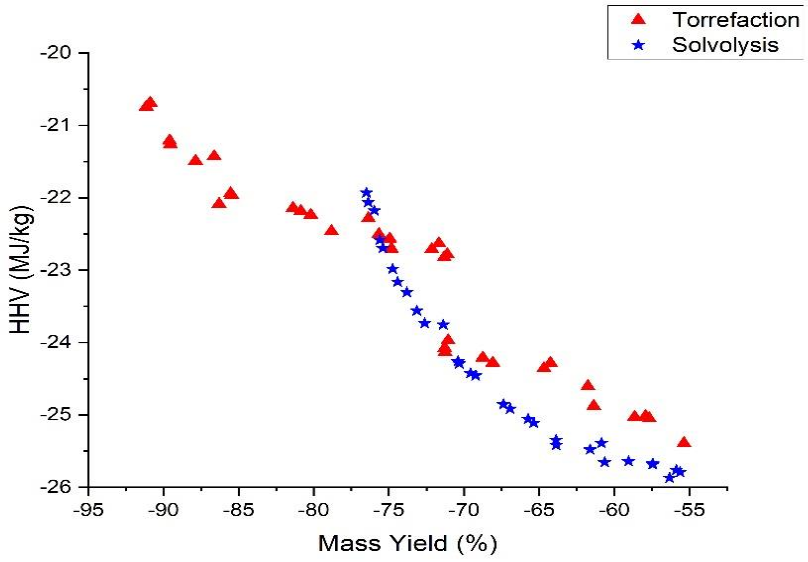


Figure 4.10. Pareto plots showing the optimal responses for torrefaction and solvolysis

Hence, the optimum conditions estimated using genetic algorithm for torrefaction and solvolysis process were at 299.83 °C, 30.07 min, 4.12 NSR and 295.10 °C, 50.85 min, 4.55 LSR, respectively.

4.3.4.3. Comparison of optimization technique: (RSM and GA)

Comparing the optimization techniques used in this study was done by validating the optimal responses predicted by both the response surface methodology (RSM) and genetic algorithm

(GA) with the developed models' expected responses. As shown in Table 4.7, the predicted values are the optimized responses obtained from the RSM and GA optimization technique. In contrast, the calculated values are the responses expected to be obtained via the developed regression model equations for the different optimal process conditions.

Table 4.7. Comparison between the predicted and calculated values of the responses at optimum process conditions.

Process	Technique	X_1 (°C)	X_2 (min)	X_3 (-)	HHV (MJ/kg)			MY (%)		
					Predicted	Calculated	Error (%)	Predicted	Calculated	Error (%)
Torrefaction	RSM	299.99	30.00	4.00	24.17	24.20	-0.12	71.21	71.24	-0.04
	GA	299.83	30.07	4.12	24.13	24.13	0.00	71.27	71.27	0.00
Solvolysis	RSM	299.99	45.25	4.32	25.29	25.28	0.04	64.83	64.80	0.05
	GA	295.10	50.85	4.55	25.11	25.11	0.00	65.36	65.36	0.00

As seen in Table 4.7, the error values indicate genetic algorithm to show a higher level of accuracy than response surface methodology. This accuracy is attributed to GA's principle, which involves a natural genetic system of coding each optimization solutions as chromosomes and therefore reproducing generations that reduced the error to the bare minimum. Furthermore, although the desirability function approach based on RSM helps assign importance to responses before optimization, GA also offers a series of optimized solutions and allows the user to pick the best conditions based on the most important response.

4.3.4.4. Results compared with literature

Having explained the results obtained during this study and the possible mechanisms responsible for the observation made during the pretreatments, it is essential to validate these observations with pre-existing results obtained by other authors in literature. Several authors have investigated pine wood's torrefaction for different purposes such as: enhancing grindability, the effect of milling technique on torrefied pine wood, and energy densification of briquettes made from torrefied pine wood.

The changes in the pine's ultimate analysis after torrefaction performed by some authors are reported in Table 4.8. As can be seen from Table 4.8, the variation in the ultimate analysis of biochar from pine can be obviously attributed to the variation in the process conditions studied. However, common trends are noticed. It can be observed that as temperature increases, the carbon content increases accompanied by a reduction in the oxygen content. Taking a closer look at the carbon content of the fuel produced by Phanphanich & Mani (2011) and this study, it can be seen that at a shorter time of 30 min at 300 °C, Phanphanich and Mani produced fuel with higher carbon content than the fuel produced in this study at that same temperature but longer time (120 min). This discrepancy could be due to other process conditions employed, the reactor design, and the pinewood's origin and type. The same disparity was observed in the carbon content reported by Keivani *et al*. (2018) at 300 °C.

Table 4.8. Percentage changes in ultimate analysis of torrefied fuel (Pine wood).

Temp (°C)	Time (min)	NSR	% Change					Ref.
			C	H	O	N	S	
200	30	5	+2.41	-27.26	-2.54	-7.14	-38.60	This study
250	120	6	+21.37	-41.67	-18.03	-13.33	-56.14	
300	120	5	+29.71	-44.92	-27.56	-13.33	-59.65	
220	30	-	+3.52	+3.48	-6.34	+68.57	+133.33	Chen *et al*. (2016)
250	30	-	+11.64	-10.76	-14.92	+182.56	+94.44	
280	30	-	+15.13	-14.72	-18.71	+242.86	+72.22	
225	30	-	+20.00	-6.80	-18.96	+134.38	+700.00	Keivani *et al*. (2018)
250	30	-	+24.08	-7.14	-19.48	-40.63	+33.33	
300	30	-	+54.84	-34.86	-45.93	+103.13	-10.00	
230	30	-	+4.73	-3.40	-5.51	0.00	+16.67	Gong *et al.* (2016)
260	60	-	+15.75	-11.00	-20.91	+7.14	+25.00	
290	60	-	+31.08	-19.90	-42.86	+28.57	+29.17	
225	30	-	+4.79	-8.58	-3.78	-11.76	-	Phanphanich & Mani
250	30	-	+9.00	-11.75	-8.17	-17.65	-	(2011)
300	30	-	+34.87	+12.66	-0.34	+17.65	-	

(+) – Increase; (-) – Reduction.

Furthermore, it can be observed from Table 4.8 that the hydrogen content trend was not consistent. This inconsistent trend could be because neither de-hydrogenation nor hydrogenation represents the primary reaction taking place during torrefaction. Hence, the decarboxylation, decarbonylation and deoxygenation reactions tend to increase or decrease the fractional percentage of the hydrogen content by reducing the percentage oxygen content in the fuel.

Considering the properties of the fuel produced in this study at 250 ° for 120 min and the fuel produced by Chen *et al*. (2016) at 280 °C for 30 min, there is a similar percentage reduction in the oxygen content. Although the latter is slightly higher than the former, the long residence time covered up for the 30 °C difference in temperature. Therefore, employing a longer residence time can allow make-up or the use of a milder operating temperature.

Unlike torrefaction, few authors have studied the effect of solvolysis on pine wood. Lynam *et al*. (2015) carried out the solvolysis pretreatment of loblolly pine. However, the elemental changes in the fuel were not reported. The fuel's energy yields were reported, and the results indicated an improvement in the HHV of the fuel, which is proportional to an increase in the carbon content of the fuel. Similar observations were reported in this study.

The mass yield and the HHV of fuel after pretreatment are vital in determining any pretreatment process's efficiency. Several authors have studied the effect of torrefaction and solvolysis on the mass yield and HHV of pre-treated fuel. Some of the results obtained by these authors are reported in Table 4.9 and are compared with the results obtained in this study. For easy comparison, at most two process conditions each are tabulated. Due to the variation in the initial energy content of different biomass, the use of HHV to compare the extent of pretreatment on different types of biomass is not efficient. Hence, the use of the Energy Enhancement Factor provides more possibility for comparison.

Table 4.9. Comparison of mass yield and energy yield from this study with literature.

Pretreatment	Biomass	Temp. (°C)	Time (min)	NSR/LSR (-)	Mass Yield (%)	HHV (MJ/kg)	Ref.
Torrefaction	Pine*	300	120	5	57.00	25.06 (1.26)	This study
	sawdust	200	30	5	90.00	20.62 (1.04)	
	Sugarcane	300	5	-	90.00	(1.13)	Anukam *et al*.
	bagasse						(2017)
	Corncob	220	30	-	87.00	16.55 (1.02)	Li *et al*. (2018)
		260	30	-	80.00	19.00 (1.17)	
	Spruce	200	45	-	90.00	19.90 (1.01)	Grycova *et al*.
		300	45	-	30.00	24.30 (1.23)	(2020)
	Straw	200	45	-	85.00	17.40 (1.01)	
		300	45	-	25.00	23.20 (1.35)	
	Mango	300	30	-	70.00	(1.18)	Rago *et al*. (2020)
	branches						
	Pine sawdust	230	30	-	93.00	20.73 (1.05)	Gong *et al*. (2016)
		290	60	-	48.00	26.02 (1.32)	
	Pine chips	225	30	-	89.00	19.48 (1.06)	Phanphanich *et al*.
		300	30	-	52.00	25.38 (1.37)	(2011)
	Spruce stem	225	30	-	92.40	20.03 (1.01)	Wang *et al*. (2018)
		300	60	-	57.50	23.61 (1.20)	
	Spruce stump	225	30	-	92.70	19.84 (1.02)	

		300	60	-	46.20	23.49 (1.20)	
	Spruce bark	225	30	-	90.40	21.11 (1.05)	
		300	60	-	60.50	24.35 (1.21)	
Solvolysis	Bamboo	150	15	10	90.00	18.27 (1.03)	Dai *et al*. (2018)
	sawdust	210	35	10	70.00	20.77 (1.18)	
	Norway	200	30	5	73.61	22.95 (1.10)	Bach *et al.* (2016)
	spruce	200	60	5	69.54	23.09 (1.11)	
	Birch	200	30	5	62.17	21.09 (1.08)	
		200	60	5	60.25	21.42 (1.10)	
	Pine*	200	30	5	75.46	22.12 (1.11)	This study
	sawdust	200	120	5	68.71	22.43 (1.13)	
	Loblolly pine	260	20	5	50.00	25.56 (1.42)	Lynam *et al*. (2015)
		260	20	10	42.00	26.64 1.48)	
	Empty fruit	200	5	8	69.45	(1.04)	Gong *et al*. (2019)
	bunch						
	Sugarcane	200	5	8	73.62	(1.05)	
	bagasse						

* – This study; Numbers in bracket – Energy Enhancement Factor.

As shown throughout Table 4.9, the HHV of biomass increases as the temperature and time increase while the mass yield reduces as the temperature and time increase. A similar observation was made in this study. As explained earlier, this mass loss is due to the loss of moisture content, devolatilization of light compounds and breaking of the lignocellulosic component in the biomass during torrefaction. Likewise, the HHV enhancement of biomass was attributed to removing free moisture, the de-oxygenation reaction taking place, and the increase in biomass's carbon content.

Anukam *et al*. (2017) studied the torrefaction of sugarcane bagasse using one process condition. The results reported that torrefaction at 300 °C for 5 min resulted in a high mass yield of 90 %. As compared to the result obtained from this study, from Table 4.9, it can be seen that while using the same temperature of 300 °C but for a much longer residence time, the mass yield drastically dropped to 57 %. This observation suggests that a longer residence time gives more opportunity for the resistive lignocellulosic components to depolymerize. Furthermore, the HHV for this study at 300 °C for 120 min, saw a higher EEF of 1.26 than the EEF of 1.13 obtained by Anukam *et al.* by using the process conditions of 300 °C for 5 min.

From Table 4.9, a high mass yield was obtained in this study at a temperature of 200 °C for 30 min. Similar mass yield values were reported by Li *et al*. (2018) for corncob; Grycova *et al*. (2020) for spruce and straw biomass; Gong *et al*. (2016) for pine sawdust; and Phanphanich *et al*. (2011) for pine wood chips. The energy enhancement factors at 200 °C for 30 min reported in this study agree with those reported by the authors mentioned above.

Considering the EEF of pinewood studied by Gong *et al*. (2016) and Phanphanich *et al*. (2011) compared to that reported in this study, at similar operating conditions of about 200 °C for 30 min, different EEF were reported but were within a difference of 0.01. This little difference suggests that the results obtained in this study support those reported in the literature. However,

studying the HHV of the spruce biomass from different parts of the same tree as seen in Table 4.9, Wang *et al*. (2018) suggest that one of the reasons why the fuel properties of the same type of biomass could differ can be because of the part of the tree from which the biomass species were obtained. This suggestion makes biomass one of the most inconsistent fuel known to man.

Table 4.9 also contains the mass yield and HHV of different types of fuels studied by different authors. It can be noticed at low-temperature regions, and the EEF are as high as the EEF of torrefaction pretreatment. However, solvolysis suffers a more significant mass loss than torrefaction. At similar process conditions of 200 °C, 30 min and 5 LSR, the EEF reported by Bach *et al.* (2016) for Norway spruce biomass and Birch biomass were 0.01 less than Pine sawdust reported in this study. This difference could be because of the relatively smaller amount of the PSD hemicellulose component than the other two biomasses. Hence, being able to depolymerize most of the hemicellulose and initiate other reactions during the pretreatment. The results obtained by Lynam *et al*. (2015) on the solvolysis pretreatment of Loblolly pine at a higher temperature of 260 °C suggests that if the solvolysis temperature is increased, the HHV of biomass can be significantly raised. However, it will cause a drastic mass loss which will affect the energy yield of the hydrochar.

Several authors have employed different optimization techniques to optimize torrefaction and solvolysis pretreatments. The optimization of a process depends on the range of process conditions studied, the optimization techniques, and the importance given to each variable. The optimization of solvolysis within the temperature range of 200 – 300 °C and time range 30 – 120 min has not been reported in the literature. Table 4.10 contains the existing optimum conditions of torrefaction and solvolysis pretreatments of different types of biomass obtained by different authors.

Table 4.10. Optimum conditions for torrefaction and solvolysis pretreatment from this study and literature.

Pretreatment	Biomass	Optimization technique	Optimum condition	Ref.
Torrefaction	Eucalyptus	Energy gain and mass loss	245.3 °C	Lee & Lee (2014)
			60 min	
	Larch		250.5 °C	
			60 min	
	Yellow poplar		245.3 °C	
			60 min	
	Mesocarp		246.8 °C	
			60 min	
	Acacia		247.8 °C	
			60 min	
	Albasia		248.2 °C	
			60 min	
	Mixed softwood		256.0 °C	

		60 min	
Acacia nilotica	RSM (FCCD)	252.0 °C	Singh *et al.* (2019)
		60 min	
Eucalyptus	RSM (FCCD)	280.0 °C	Kumar *et al.* (2020)
		60 min	
Pinewood	RSM (FCCD)	299.7 °C	Keivani *et al.* (2018)
		28 min	
Coffee chaff	RSM (BBD)	271.1 °C	Buratti *et al.* (2018)
		20 min	
Spent coffee grounds	RSM (BBD)	256.0 °C	
		20 min	
Pine sawdust	RSM (BBD)	299.9 °C	This study
		30 min	
	GA	299.83 °C	
		30 min	

Solvolysis	Palm kernel shell	RSM (CCD)	220.0 °C 30 min	Gan *et al*. (2019)
	Rice straw	RSM (CCD)	180.0 °C 20 min	Nizamuddin *et al*. (2019)
	Shrimp waste	RSM (CCD)	180.0 °C 112 min	Kannan *et al*. (2017)
	Cornstalk	RSM (CCD)	181.9 °C 40 min	Kang *et al*. (2019)
	Pine sawdust	RSM (BBD)	299.9 °C 45 min	This study
		GA	295.1 °C 51 min	

RSM – Response Surface Methodology; FCCD – Face Central Composite Design; CCD – Central Composite Design; BBD – Box-Behnken Design; SFED – Single Factor Experimental Design; GA – Genetic Algorithm.

As shown in Table 4.10, the optimum conditions obtained for Pinewood by Keivani *et al*. (2018) and those reported from this study for the torrefaction process are approximately 300 °C and 30 min. Optimum conditions derived using the genetic algorithm were also close to that reported in the literature. However, GA offers more accurate estimation and provides a series of optimum conditions depending on the level of importance of each process variable. Due to the non-existence of the optimum conditions for solvolysis within a process conditions range of 200 – 300 °C and 30 – 120 min in the literature, proper comparison cannot be made.

The results obtained during this study has shown good correlations with those reported in the literature. Therefore, the results reported in this study can be considered reliable and can, therefore, be used to validate future claims in this research field.

4.4 Conclusion

Two pretreatment tests; torrefaction and solvolysis were carried out using PSD to understand the effect of process conditions such as temperature, time, and NSR/LSR on biochar/hydrochar's fuel properties, respectively. The RSM (Box-Behnken design) method was used to design the experiments. The desirability function and Genetic Algorithm (GA) were employed for modelling and optimization processes. From this study, the following conclusions can be made:

- RSM was efficient in developing regression models that could explain the interactional effect of process conditions during the process. The ANOVA gave an informed conclusion on the statistical significance of the developed regression models.
- The most influential variables on the responses (HHV, mass yield and energy enhancement factor) for the pre-treated PSD were of the order: operating temperature > residence time > NSR/LSR

- The effect of the liquid-to-solid ratio on mass yield during solvolysis process was highly dependent on the operating temperature than the time.
- Although solvolysis pretreatment recorded a higher energy enhancement factor than torrefaction, torrefaction pretreatment process recorded a higher mass yield than solvolysis process.
- The desirability function approach and GA showed close optimum conditions for torrefaction and solvolysis methods. However, the GA gave more accurate responses compared to the calculated values using the regression models.

In this study, the results obtained from the torrefaction and solvolysis processes are promising. However, it is recommended that more studies should be done on solvolysis process, to exploit its promising future. The design of a torrefier should be considered to achieve more uniform heating when the biomass mass loading is increased. Furthermore, GA should be adopted as an optimization technique in this field of study to obtained accurate results which can be implemented in an automated energy/coal-fired plants in the industry.

CHAPTER FIVE

5. KINETIC STUDY OF ISOTHERMAL DEGRADATION OF PINE SAWDUST (PSD) DURING TORREFACTION PROCESS

5.1. Introduction

The combustion of fossil fuels and other carbon content materials without proper control has contributed to the emission of Green House Gases (GHG), leading to global warming and climate change worldwide. The energy insecurity posed by the rapid depletion of fossil fuels and the environmental impact of using the fuels has motivated researchers to study biomass as an alternative fuel source for energy production (Li *et al*., 2018).

Several thermochemical conversion technologies such as; pyrolysis, combustion, and gasification have been regarded as promising routes for converting waste biomass to biofuels. The utilization of raw biomass against fossil fuel such as coal is faced with challenges including; its low bulk energy density, grindability, hydrophobicity, and low combustion properties (Bates and Ghoniem, 2013).

A pretreatment technology such as torrefaction has proved to be an efficient thermal process for the improvement of the quality of raw biomass, and an application of this process will help solve the challenges mentioned above (Nhuchhen *et al*., 2018; Stelt *et al*., 2011; Chen *et al*., 2015; Gil *et al.*, 2015; Phanphanich & Mani, 2011). Torrefaction is a thermal pretreatment process whereby a known quantity of biomass is subjected to a mild temperature between 200 and 300 ^{o}C for a residence time of around 2 hours. During this process, the bulk energy density of a lignocellulosic biomass increases and is accompanied by mass loss of the fuel. Mass loss is characterised by the removal of water content, release of volatile matter, and depolymerisation of the lignocellulosic components (Barbanera and Muguerza, 2020; Cahyanti

et al., 2020a; Jagodzińska *et al*., 2020). This technology fosters the utilization of torrefied biomass as a replacement for coal in coal-firing plants.

Several researchers including; Dorde *et al*. (2011); Acharjee *et al*. (2011), Singh *et al*. (2019); and Wang *et al*. (2017) have studied the effect of process conditions on the improved fuel properties of torrefied biomass. Fluidized bed reactors, batch reactors, continuous reactors. (Brachi *et al*., 2019; Severy *et al*., 2018; Shang *et al.*, 2014) were employed for the process. Understanding the mass loss of solid fuel is necessary because it helps design a gasification or pyrolysis reactor. Mass loss is related to the degree of torrefaction and is measured by the degradation of biomass (Almeida *et al*., 2010; Lee & Lee, 2014; Pathomrotsakun *et al*., 2020; Rago *et al.*, 2020). The authors mentioned above concluded that the solid mass loss of biomass can estimate the severity of the torrefaction process.

The thermogravimetric analyzer (TGA) has been the most commonly used experimental technique for studying biomass's thermal degradation. It is also used to study the solid distribution during torrefaction process. The analyzer determines the thermal degradation rate of solid fuel. Two main methods have been extensively used to describe the thermal degradation of biomass. These methods are the isothermal method (steady-state conditions) and the non-isothermal method (unsteady-state conditions). The main advantage of estimating kinetic parameters using the non-isothermal method (i.e. Friedman method, Kissinger-Akahira-Sunose method, Flynn-Wall-Ozawa) is: it is easier to account for the mass loss during the non-isothermal period. However, results reported by Kumar *et al.* (2020); Sharma *et al*. (2019) and Yan *et al*. (2019) while employing the non-isothermal method suggested that multiple reactions are present during the torrefaction and pyrolysis of biomass. Therefore, using the non-isothermal method leads to a wrong estimation of the kinetic parameters, and based on this fact, the isothermal method is considered.

Isothermal degradation of biomass is the rate at which biomass decomposes when subjected to a fixed temperature without any heat loss or gain during the process. Modelling this process is vital because it enhances the design of an efficient torrefaction reactor, estimates the mass and energy balance of the fuel conversion system, estimates and improves the biochar's fuel properties. It has been reported in the literature that torrefaction occurs within the temperature range of 200 ^{o}C to 300 ^{o}C. This temperature range is attributed to the degradation of the hemicellulose component in biomass (Li *et al*., 2018).

A variety of kinetic models have been employed in modelling the isothermal degradation of biomass (Broido & Nelson, 1975; Blasi & Lanzetta, 1997). Over the years, two models have been proposed for studying the kinetic process, namely; the detailed model and the pseudo-components model. The detailed model considered the individual decomposition of three different biopolymer components; the hemicellulose, the cellulose and lignin, in the biomass. This model was first introduced by Ranzi *et al.* (2008) and was later modified and improved by Blondeau & Jeanmart (2012) and Anca-Couce *et al.* (2014), respectively. However, due to the difficulty in extending this method to the torrefaction of various biomass species, the pseudo-component model is therefore adopted due to its simplicity. This model describes the overall anhydrous weight loss (AWL) of biomass during the reaction. It has been adopted based on a one-reaction scheme (Repellin *et al*., 2010), several reactions steps scheme in parallel (Ratte *et al.*, 2011), as well as several reaction steps scheme in series by Peduzzi *et al.* (2014).

The use of the two-step reaction mechanism requires that the fuel degradation be demarcated into two stages namely; the first stage (i.e. characterised by rapid mass loss rate) and the second stage (i.e. characterised by a slower mass loss rate). Several kinetic studies have been carried out employing the two-step kinetic model technique. For example; the kinetics of the isothermal degradation of pure xylan during pyrolysis was first studied by Blasi & Lanzetta,

(1997), and the activation energies of the decomposition steps were found to be 76.57 kJ/mol for the first stage and 54.81 kJ/mol for the second stage.

Shang *et al*. (2013), also carried out a kinetic study on the isothermal degradation of wheat straw biomass, employing the 2-step reaction scheme and reported activation energies of 71 and 76.6 kJ/mol for the char formation at stage one and stage two respectively. It was also reported that this model technique was efficient in predicting the residual mass of the biomass during torrefaction on a bench-scale batch reactor.

Edgar (2019) carried out a similar study on poplar biomass and obtained the char's activation energies as 104.42 and 97.60 kJ/mol for stage one and two, respectively. Bach *et al.* (2016) also studied the isothermal degradation of spruce and birch biomass using a similar reaction mechanism. Activation energies of 20.79 kJ/mol and 70.61 kJ/mol for spruce biomass were reported for the first and second stages. In contrast, 87.71 kJ/mol and 93.51 kJ/mol for birch biomass were recorded for the first and second stages.

Prins *et al*. (2006), reported the activation energies of the first and second stage of the torrefaction of willow biomass using the same kinetic model technique as 76.0 and 151.7 kJ/mol, respectively. It was also suggested that the first stage of the degradation process is attributed to depolymerising the hemicellulose, accompanied by the removal of free moisture content in the biomass and light compounds in the form of volatiles. Whereas, the second stage of the degradation process is mainly attributed to the depolymerization of the cellulose and a fraction of the lignin. Due to the more resistive behaviour of the cellulosic components than the hemicellulose, the second stage's activation energy has been estimated to be higher than the first stage.

Similarly, Shang *et al*. (2014) considered the mass loss during the heating period when estimating the kinetic parameters. The study showed that it is difficult to model the non-

isothermal degradation phase of the process. This conclusion was reflected by the low correlation between the estimated kinetic parameters and the Arrhenius equation. Similar observations have been reported by Bach *et al.* (2016). Hence, while carrying out the kinetic study of the process, the non-isothermal period was not included. It was assumed that the mass when the set temperature was reached, to be the initial mass and initial time. A similar procedure was employed in this study.

While estimating the kinetic parameters using the two-step reaction technique, a demarcation time must be determined to separate the two steps and estimate the reactions' overall rate constants. However, Prins *et al.* (2006) suggested that it is difficult to identify a demarcation time as the two stages co-occur. Subsequent kinetic studies either went ahead to use only the demarcation method or used previously estimated kinetic parameters as initial guesses to estimate the correct kinetic parameters using MATLAB. Based on this fact, the fitness of experimental results with modelled results has not exhibited a perfect correlation.

Previous studies have focused on the incomplete degradation of biomass existent within the torrefaction region. However, in this study, the complete degradation of ash-free biomass, which allows for further degradation of biomass beyond the torrefaction region is assumed. The demarcation time methods and the iteration methods are used to study the kinetics of isothermal degradation of PSD during torrefaction process. Mathematical modelling of the isothermal degradation of the fuel (PSD) following the intrinsic two-step kinetic reaction scheme in series was carried out. When comparing the experimental results to the modelled results, the model's accuracy was improved via this approach. The outcome of the study will provide information for the development of efficient torrefaction and energy production plants based on the mechanism of fuel reaction and its activation energy.

5.2. Experimental and Modelling Procedure

A thermogravimetric analyzer was used to study the isothermal degradation of fuel (PSD) during torrefaction pretreatment. A 2-step reaction mechanism was employed to develop a kinetic model to describe the degradation process. The procedures taken to prepare the biomass sample is described in section 3.1.1.1. The experimental procedure taken for the thermogravimetric analysis is detailed in section 3.2.2. subsequent sections give the modelling procedures take such as the model formulation and model solution.

5.2.1. Kinetic model formulation

A two-step reaction in series was first adopted to describe pure xylan (hemicellulose) decomposition during an isothermal pyrolysis process by Blasi and Lanzetta (1997). The assumptions using this model are based on two things; conversion occurs purely under kinetic control, and a semi-global reaction mechanism is applicable. These steps as shown in Figure 5.1, indicates that during torrefaction, an initial mass of biomass when heated to a specific temperature within 200 ^{o}C and 300 ^{o}C from an initial time (t_i) to a time (t*) produces an intermediate solid *B* accompanied by the first release of volatiles V_1. When further heated to a final time (t_f), a final solid char *C* is produced accompanied by the second release of volatiles V_2.

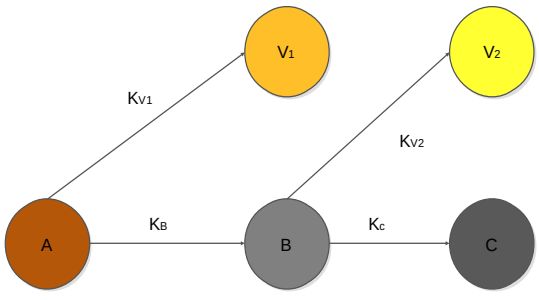


Figure 5.1. Two-step kinetic model

A first-order kinetic reaction is assumed for the degradation of biomass (Braga *et al.*, 2014). Based on this hypothesis, and from Figure 5.1, the differential Equations (5.1) – (5.5) are developed from the rate equations of the individual steps;

$$\frac{dM_A}{dt} = -(K_{V1} + K_B)M_A = -K_1 M_A \tag{5.1}$$

$$\frac{dM_B}{dt} = K_B M_A - (K_{V2} + K_C)M_B = K_B M_A - K_2 M_B \tag{5.2}$$

$$\frac{dM_C}{dt} = K_C M_B \tag{5.3}$$

$$\frac{dM_{V1}}{dt} = K_{V1} M_A \tag{5.4}$$

$$\frac{dM_{V2}}{dt} = K_{V2} M_B \tag{5.5}$$

M_i is the mass fraction of the pseudo-components (A, B, C, V_1, and V_2) and K_i is the rate constant for each of the equations. As illustrated in Figure 5.1, the mathematical expression describing the overall rate constants for the first and second stages of the torrefaction reaction are expressed in Equation (5.6) and can be estimated from the relationship between the mass loss and time as shown in Equation (5.7) and Equation (5.8):

$$K_1 = K_{V1} + K_B;\ K_2 = K_{V2} + K_C \tag{5.6}$$

$$\ln\left(1 - \frac{M_0 - W}{M_0 - M_B^*}\right) = \log X_1 = -K_1 t \tag{5.7}$$

$$\ln\left(1 - \frac{M_B^* - W}{M_B^* - M_{C\infty}}\right) = \log X_2 = -K_2(t - t^*) \tag{5.8}$$

Where M_0 is the initial mass of solid, W is the mass of solid char remaining at any time t after the torrefaction process obtained from TGA results, M^*_B is the mass at the demarcation time t^*. The demarcation time will be the point on the TGA graph where there is a significant mass loss indicated by a shoulder on the curve. After estimating the rate constants, the linearized Arrhenius equation plots are then used to estimate the activation energies, E_i, and the pre-exponential factors, A_i;

$$K_i = A_i exp\left({}^{-E_i}/_{RT}\right) \quad (5.9)$$

5.2.2. Kinetic model solution

Integrating Equations (5.1 – 5.5) yields Equation (5.10 – 5.14), with boundary conditions at when time $t = 0$; $M_{A(0)} = M_0, M_{B(0)} = M_{V1(0)} = M_{V2(0)} = M_{C(0)} = 0$

$$M_A = M_0 e^{-K_1 t} \quad (5.10)$$

$$M_B = \frac{K_B M_0}{(K_2 - K_1)} e^{-K_1 t} - \frac{K_B M_0}{(K_2 - K_1)} e^{-K_2 t} \quad (5.11)$$

$$M_C = \frac{K_C K_B M_0}{(K_2 - K_1) K_1} [1 - e^{-K_1 t}] + \frac{K_C K_B M_0}{(K_2 - K_1) K_2} [e^{-K_2 t} - 1] \quad (5.12)$$

$$M_{V1} = \frac{K_{V1} M_0}{K_1} [1 - e^{-K_1 t}] \quad (5.13)$$

$$M_{V2} = \frac{K_{V2} K_B M_0}{(K_2 - K_1) K_1} [1 - e^{-K_1 t}] + \frac{K_{V2} K_B M_0}{(K_2 - K_1) K_2} [e^{-K_2 t} - 1] \quad (5.14)$$

Where W/M_o is the solid char remaining after the torrefaction process, Equation (5.16) is obtained;

$$\frac{W}{M_0} = M_A + M_B + M_C \quad (5.15)$$

$$\frac{W}{M_0} = \left[\frac{(K_2 - K_1) K_1 + K_B K_1 - K_C K_B}{(K_2 - K_1) K_1}\right] e^{-K_1 t} - \left[\frac{K_B K_2 - K_C K_B}{(K_2 - K_1) K_2}\right] e^{-K_2 t} + \frac{K_C K_B}{K_1 K_2} \quad (5.16)$$

However, because the ash content is unreactive during the torrefaction process, the experimental fractional mass loss is represented by Equation (5.17):

$$\left(\frac{W}{M_0}\right)_{TGA} = \frac{m_S - m_{ash}}{m_0 - m_{ash}} \quad (5.17)$$

Where m_0 is the initial mass of biomass, m_s is the mass of solid remaining recorded by TGA, and m_{ash} is the mass of ash contained in PSD, as shown in Table 5.1.

Integrating Equation (5.3) with boundary conditions; $M_{C(0)} = 0, M_{C(\infty)} = M_{C\infty}$ (when there is sufficient time for the formation of final char, *C*) results in Equation (5.18) and Equation (5.19):

$$\frac{M_{C\infty}}{M_0} = \frac{K_C K_B}{K_1 K_2} \tag{5.18}$$

$$\frac{W - M_{C\infty}}{M_0} = \left[\frac{(K_2 - K_1)K_1 + K_B K_1 - K_C K_B}{(K_2 - K_1)K_1}\right] e^{-K_1 t} - \left[\frac{K_B K_2 - K_C K_B}{(K_2 - K_1)K_2}\right] e^{-K_2 t} \tag{5.19}$$

The detailed steps on how these equations were derived are documented in section B of the appendices.

Table 5.1. Lignocellulosic and proximate analysis of air-dried pine sawdust (PSD).

Lignocellulosic composition (%)[a]			Proximate analysis (%)			
Hemicellulose	Cellulose	Lignin	Moisture	Volatile	Fixed carbon	Ash
10.5	48.6	25.3	8.55	71.80	19.06	0.59

[a] – adapted from Shi and Wang (2014).

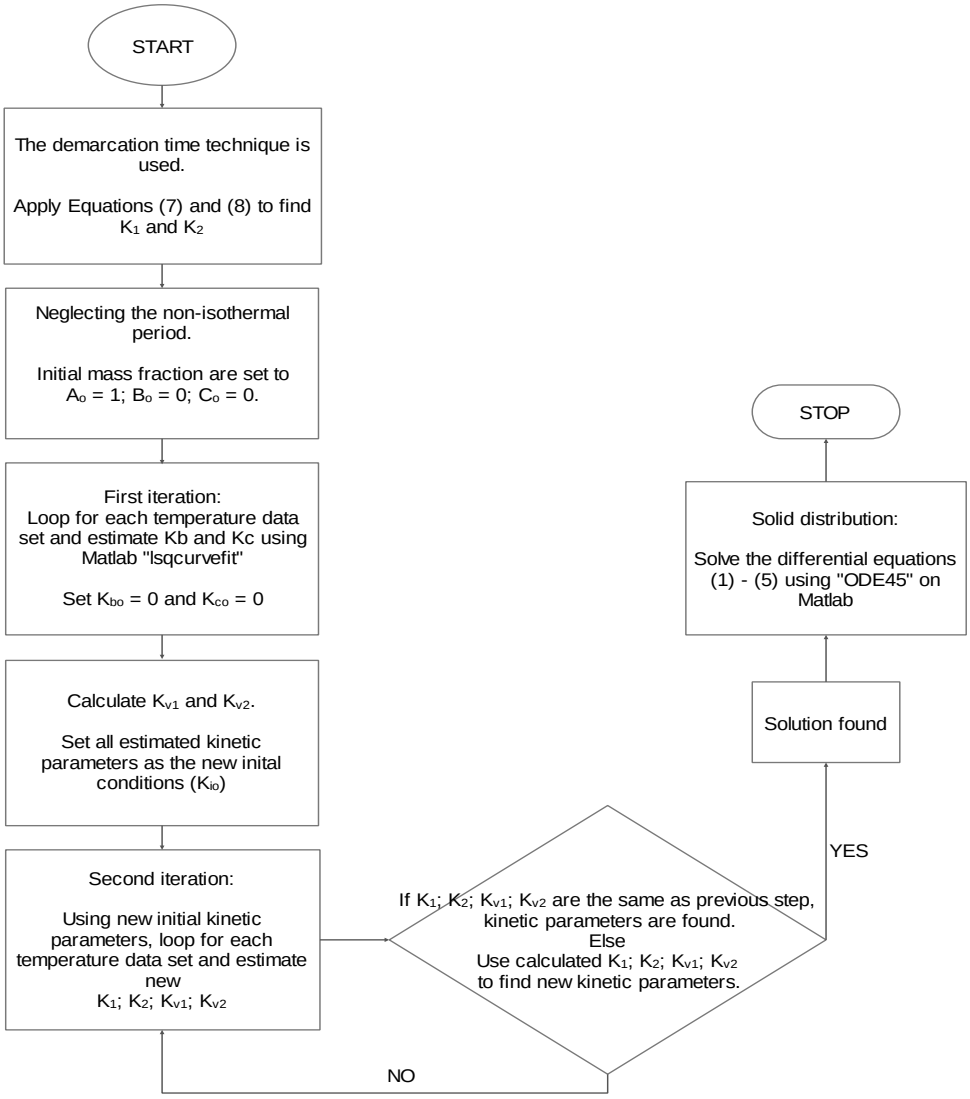


Figure 5.2. Flowchart algorithm used in MATLAB for estimating the kinetic parameters and the solid distribution during the torrefaction of PSD

A flowchart diagram describing the MATLAB algorithm used in determining the kinetic parameters of the torrefaction of PSD while employing both demarcation time techniques and numerical solution techniques is shown in Figure 5.2. First of all, the demarcation time method as used by Prins *et al*. (2006) was employed to determine the kinetic parameters.

It was reported that due to the inaccuracy of estimating the demarcation time, the kinetic parameters derived using this technique was unable to predict the mass loss obtained experimentally adequately. Hence, the kinetic parameters derived using the demarcation time

technique was used as initial conditions for the numerical solution method known as nonlinear optimization using MATLAB software version R2020b.

In this study, "lsqcurvefit" is used as the function. The "lsqcurvefit" function operates under the principle of Niedler-Mead optimization algorithm. It is used to minimize the residual sum of squares between the modelled and TGA data, as shown in Equation (5.20). The "lsqcurvefit" process was therefore iterated till the initial conditions for the kinetic parameters became the estimated kinetic parameters, indicating an optimum solution. Presented in Figure A.4 and A.5 of the appendices are the kinetic modelling script file and function file, respectively, generated from MATLAB software.

$$E = \sum_T \left[\left(\frac{W}{M_0}\right)_{TGA,T} - \left(\frac{W}{M_0}\right)_{model,T} \right]^2 \quad (5.20)$$

T indicates each isothermal temperature, $(W/M_o)_{TGA}$ is the weight loss recorded experimentally by the TGA and $(W/M_o)_{model}$ is the calculated weight loss from the model.

5.3. Results and Discussion

5.3.1. Isothermal degradation of PSD during torrefaction in a TGA

The mass loss rate during the torrefaction of pine sawdust using a thermogravimetric analyzer is shown in Figure 5.3. The figure contains a plot of the fractional mass loss of the fuel against time. The non-isothermal period (heating period) was removed by assuming the mass yield at each set temperature to be the initial mass ($Y_{s,\,T\,°C} = 1$), and the time was recorded as the initial time ($t = 0$).

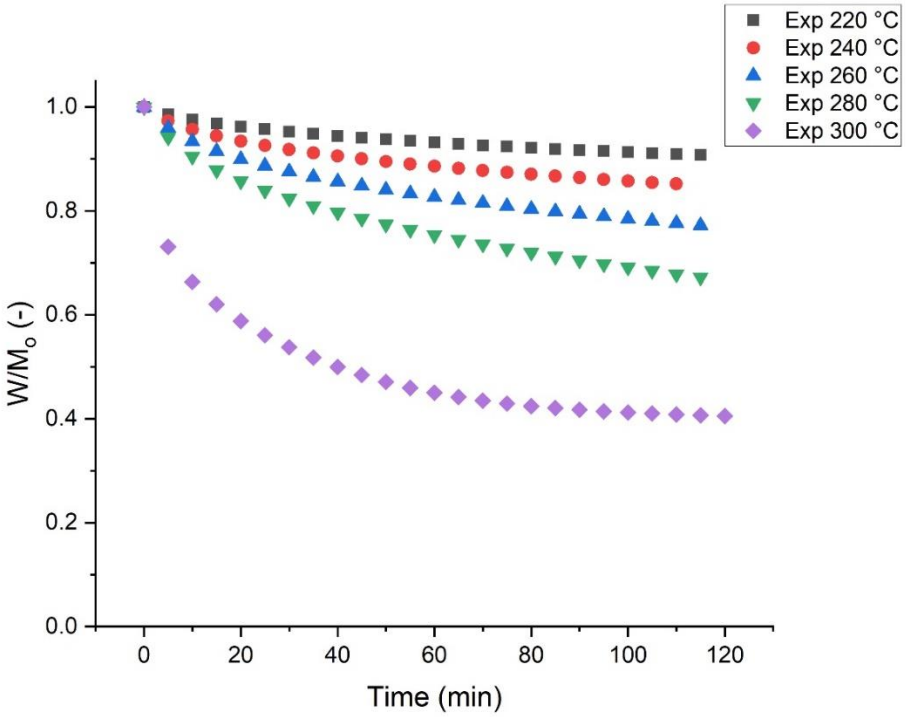


Figure 5.3. Mass loss curves during the torrefaction of PSD using a TGA

Figure 5.3 shows a continuous mass loss as the severity (i.e. temperature and time) of the torrefaction process increased. The result agrees with the results reported by Anca-Couce *et al*. (2020); and Gajera *et al*. (2020) during thermal degradation of biomass using a TGA. Furthermore, it can be observed that there was a drastic mass loss only when the temperature was increased to 300 °C. This observation could be because the hemicellulose is mainly decomposed at lower temperatures, resulting in a marginal mass loss due to the low fractional composition of hemicellulose in pine, as shown in Table 5.1. Similarly, Xiao *et al*. (2020) studied the thermal degradation of pine sawdust in a TGA. They observed that cellulose's depolymerisation, though overlaps with the depolymerisation of hemicellulose, is more evident between 260 °C and 380 °C.

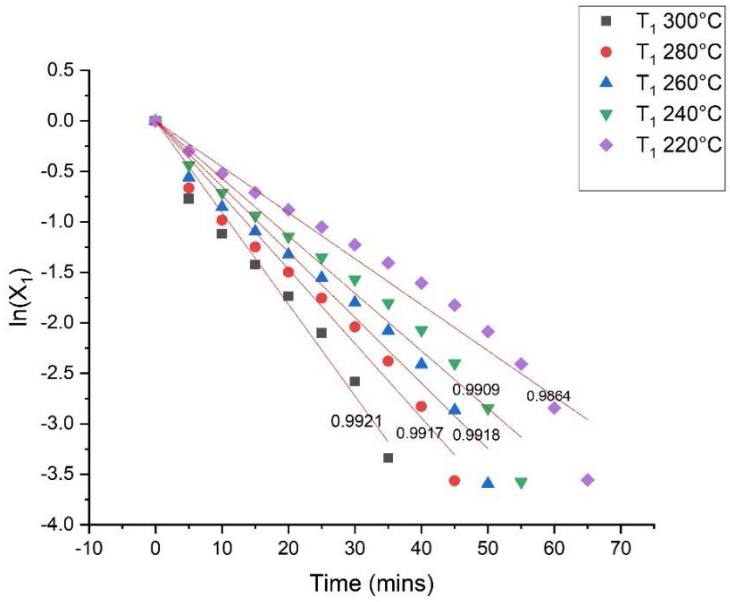
Evidently, there seem to be higher slopes within the first 10 to 20 min of the mass loss curves from the TGA curves, which indicates a rapid mass loss rate within the first period than the

second period. Previous studies have shown that the rapid mass loss in the first stage is due to the depolymerisation of hemicellulose accompanied by the loss of water, light compounds, CO_2, and acetic acid. The slow mass loss rate evident in the second stage is mainly caused by the difficulty in depolymerising the cellulosic component which happens to be a more crystalline compound than hemicellulose (Bach *et al*., 2016; Bates & Ghoniem, 2013; Shang *et al*., 2013).

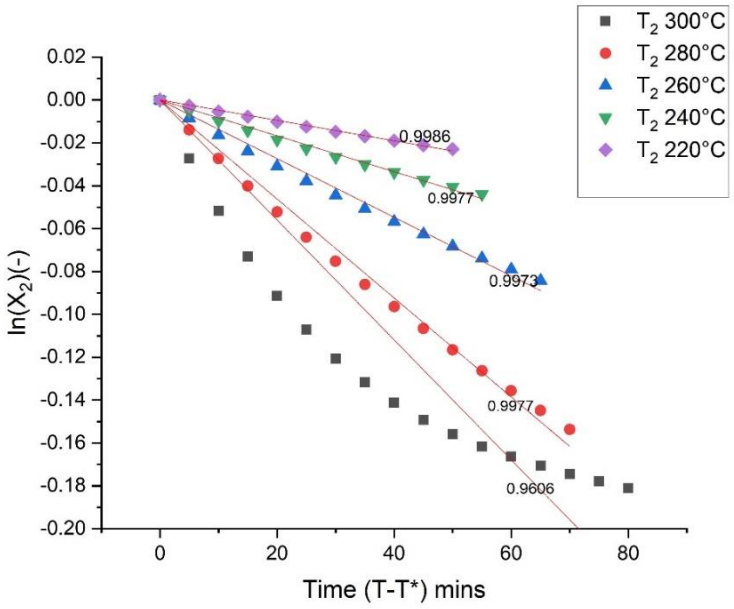
5.3.2. Estimation of kinetic parameters

The demarcation time technique was applied to achieve the initial kinetic parameters from which the torrefaction kinetic parameters were estimated. After that, the model was validated using the experimental mass loss curves. In this study, the presence of two stages (fast and slow mass loss stages) during the isothermal degradation of PSD was determined and, a demarcation time was assumed. In this case, Equations (5.7) and (5.8) were applied. Figures 5.4 (a) and (b) shows plots of Equations (5.7) and (5.8) respectively. The slopes of the straight-line graphs were estimated as the overall rate constants for the first stage and second stage of the isothermal degradation during the torrefaction process. The R-square values indicated on the plots show that the equations could explain the mass loss during the stages.

Table 5.2 shows the torrefaction kinetic parameter estimated in this study. These parameters were estimated based on five torrefaction temperature regimes that were studied (220, 240, 260, 280 and 300 °C) while employing different heating rates (23, 27, 31, 35 and 39 °C/min) such that only 10 minutes was the allowable time for the solid to rise from room temperature to each pre-set temperature. The Arrhenius equation, as illustrated in Equation (5.9), was used to determine the activation energies and pre-exponential for each stage of the degradation process. The plots are shown in Figure 5.5.



(a)



(b)

Figure 5.4. Logarithmic plots of the mass loss for the (a) first stage and (b) second stage

Table 5.2. Estimated kinetic parameters for the torrefaction of pine sawdust.

Rate constant (min^{-1})	Arrhenius equations
k_b	$5.954 \times 10^{-1} \exp\left(\frac{-10.293}{RT}\right)$
k_c	$3.96 \times 10^{8} \exp\left(\frac{-141.280}{RT}\right)$
k_{v1}	$7.19 \times 10^{5} \exp\left(\frac{-80.291}{RT}\right)$
k_{v2}	$7.086 \times 10^{-1} \exp\left(\frac{-13.736}{RT}\right)$

k_b, k_c, k_{v1}, k_{v2} – rate constant for the formation of intermediate char b, final char c, first volatiles v_1 and second volatile v_2; R = 0.008314 kJ K^{-1} mol^{-1}; T – torrefaction temperature (K).

The coefficient of determination (R^2), as shown in Figure 5.5, shows that the estimated kinetic parameters follow the Arrhenius equation. As seen in Table 5.2, in agreement with the literature, the mass loss in the first stage occurs faster than the mass loss in the second stage. The table also shows that the activation energy required for forming the intermediate solid in the first step ($E_{a,b}$) is lower than the activation energy need to form the solid char in the second stage ($E_{a,c}$). This difference in activation energy is because less energy is required to depolymerise the hemicellulose component and remove water and light compounds in the first stage than to depolymerise cellulose in the second stage. These results agree with the result of the degradation of spruce and birch wood reported by Bach *et al*. (2016). Furthermore, the activation energy required to form the first volatiles was higher than the energy required to form the second volatile. These observations are equally in agreement with the results of the degradation of pine sawdust reported by Shang *et al.* (2014).

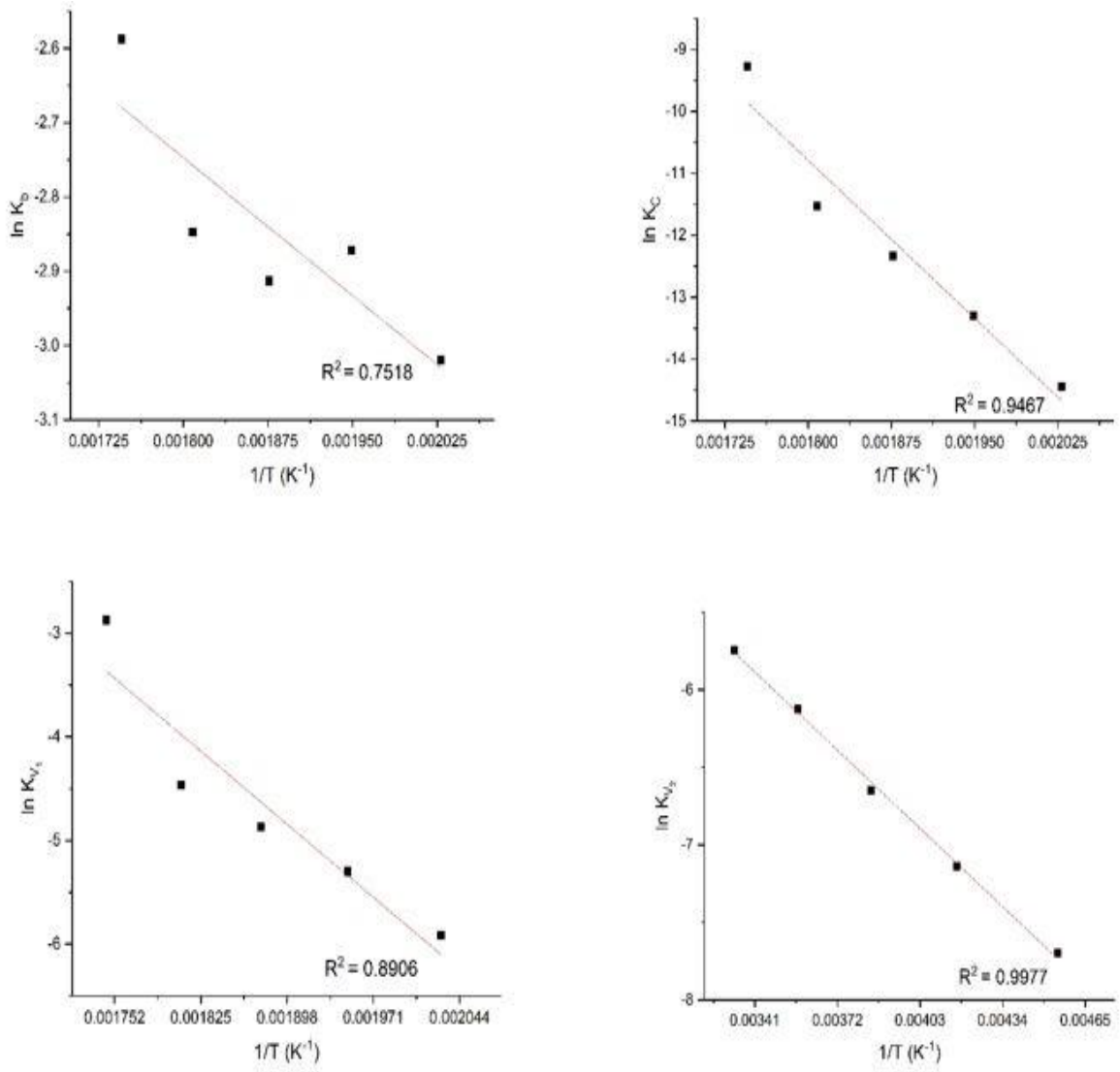


Figure 5.5. Arrhenius plots for the determination of activation energies and pre-exponential factors for each pseudo-component (kb, kc, kv1, kv2)

5.3.3. Kinetic model validation

To validate the kinetic model, the predicted mass loss was compared to the experimental plots using the model for each isothermal temperature period, as shown in Figure 5.6. The residual sum of squares (RSS), coefficient of determination (R^2) and the Pearson correlation coefficient (r) values as reported in Table 5.3 was used to check the goodness of fit of the model. As shown in Figure 5.6, the predicted mass loss using the kinetic model is close to the experimental

values. It can be seen that the predicted curves overlap with the experimental curves. Likewise, the low RSS and high coefficient of determination (R^2) support the goodness of fit as seen graphically.

It can also be observed that the mass loss at lower temperature had better fit than higher temperatures. This observation could be because of the drastic mass loss within the first ten minutes at 300 °C. Hence, the model overestimated the mass loss at the end of the process. A similar observation was made by Shang *et al.* (2014). The predicted mass loss curves also suggest that there will be a continuous mass loss as the temperature and time increase. Hence, this model can be further applied to the isothermal degradation of biomass during pyrolysis temperature region.

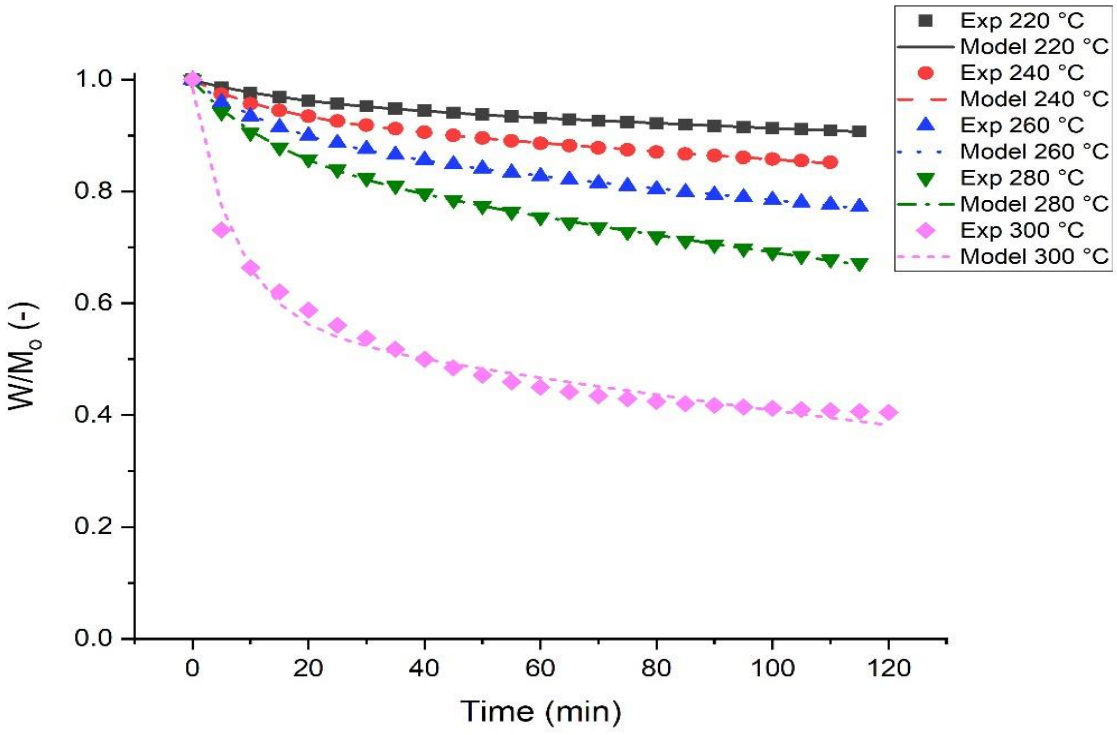


Figure 5.6. Experimental and modelled mass loss of PSD torrefaction at different temperatures

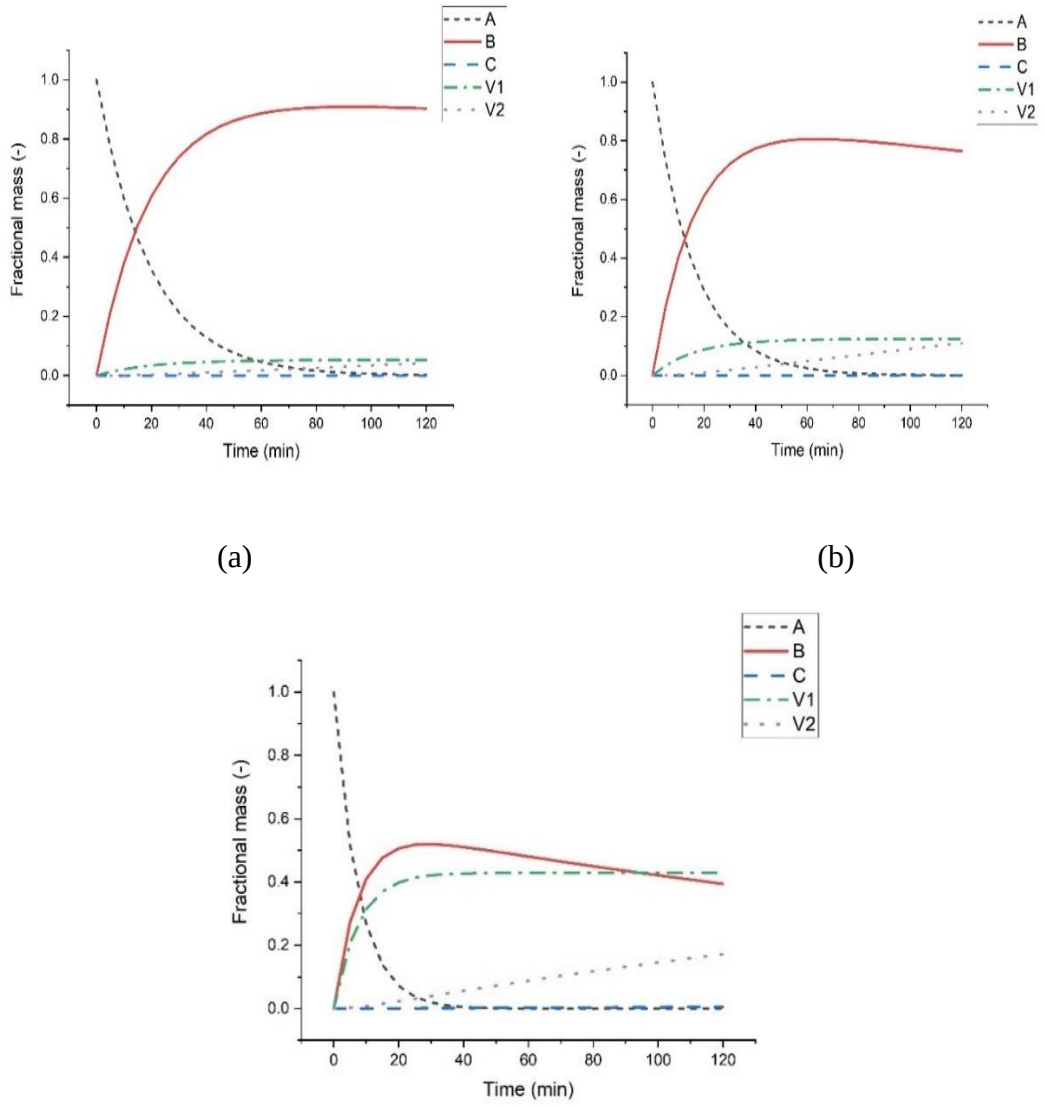
Table 5.3. Statistical test of kinetic model for prediction of mass loss.

Temperature (°C)	RSS	R^2	r
220	0.0000068	0.9996	0.9998
240	0.0000253	0.9993	0.9997
260	0.0000607	0.9993	0.9997
280	0.0001190	0.9993	0.9997
300	0.0067100	0.9847	0.9923

5.3.4. Predicted solid and gas distribution

The kinetic parameters estimated from this study were used to predict the solid distribution using Equations (5.1) – (5.5) during pine sawdust torrefaction. The MATLAB function files that were generated to plot the solid distribution during torrefaction, as shown in Figure A.6 and Figure A.7 of the appendices. Although five torrefaction temperatures were studied, three selected temperatures 220 °C, 260 °C and 300 °C were presented for discussion, as shown in Figures 5.7 (a), (b) and (c) respectively. The solid distribution curves at 240 °C and 280 °C are presented in Figure A.10 and Figure A.11 of the appendix.

Figures 5.7 show the conversion of the initial solid (A) into an intermediate solid (B) and finally into a solid char (C). The formation of the first and second volatile are also presented in Figure 5.7. As shown in Figure 5.7, the conservation of mass is obeyed such that the sum of the fraction composition of each component at any given time is always equal to 1.



(a) (b)

(c)

Figure 5.7. Solid and gas distribution during torrefaction of PSD at (a) 220 °C, (b) 260 °C and (c) 300 °C

The degradation of the initial solid biomass has been discovered to be significantly influenced by the operating temperature. In particular, it can be observed that at 220 °C, 260 °C and 300 °C, it takes about 90 min, 80 min and 40 min, for the initial biomass to get converted, respectively. Similarly, the conversion of the intermediate solid (B) is also dependent on temperature. This dependency is observed as the intermediate solid curve decreases earlier at higher temperatures than lower temperatures. These results agreed with the kinetic parameters

reported in Table 5.2, indicating lower activation energy in the first stage than the second stage of the degradation process. Figure 5.7 also supports Prins' *et al*. (2006) claim that the first and second stage co-occur. Hence, making it difficult to establish an accurate demarcation time between the stages.

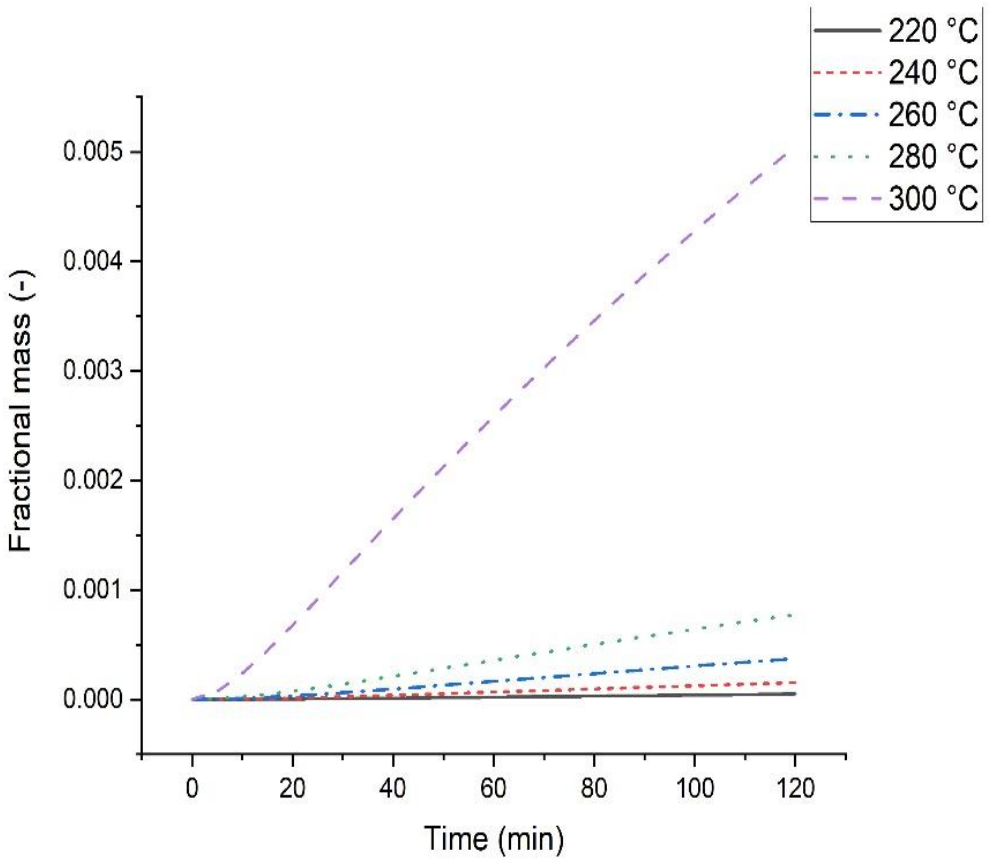


Figure 5.8. Formation of final char at different temperatures

Furthermore, the formation of the final char was considerable at higher temperatures. As seen at 220 °C, the total mass loss is mainly occupied by the degradation of the initial biomass and the intermediate solid formation. Figure 5.8 shows the final char's formation, which was extracted from the solid distribution curve at different temperatures. It can be observed that the formation of the final char only becomes evident at 300 °C. In essence, after torrefaction, the char produced often contains more of the intermediate solid, little of untreated biomass and a

fraction of the final char if sufficient time is given for the process. It can also be observed that higher temperatures favour the formation of volatiles.

Furthermore, it can be seen that as the temperature increases, the fractional composition of the first volatiles significantly increases as compared to the second volatiles. Therefore, it can be said that the formation of the second volatiles is dependent on the formation of the first volatile which is responsible for the higher activation energy needed for the formation of the first volatiles as reported in Table 5.2. Conclusively, an increase in the severity of the torrefaction process fosters the final char (C) formation and vice versa.

5.3.5. Results compared with literature

While employing this 2-step reaction mechanism for the isothermal degradation of different types of biomass as reviewed in the literature, various estimated kinetic parameters are shown in Table 5.4. The kinetic parameters estimated in this study are also tabulated and compared with those in literature.

As discussed early, the results obtained in this study agree with those reported in the literature. However, the difference in parameters for different types of biomass can be attributed to the different lignocellulosic structures. The kinetic parameters for pine reported by Shang *et al*. (2014) are different from this those estimated in this study because the non-isothermal heating period was not considered in this study.

Table 5.4. Kinetic parameters for different types of biomass reported in the literature

Biomass	Kinetic parameters	Pseudo-Components				Ref.
		B	C	V_1	V_2	
Xylan	Ea (kJ mol^{-1})	66.23	56.35	91.47	52.59	Blasi and Lanzetta
	A (s^{-1})	1.74 x 10^4	3.43 x 10^2	3.31 x 10^6	58.7	(1997)
Spruce	Ea (kJ mol^{-1})	76.00	151.70	11.40	11.40	Repellin *et al*. (2010)
	A (s^{-1})	2.47 x 10^4	1.10 x 10^{10}	1.95 x 10^7	1.10 x 10^6	
Willow	Ea (kJ mol^{-1})	75.98	151.71	114.21	151.71	Prins *et al.* (2006)
	A (s^{-1})	2.48 x 10^4	1.1 10^{10}	3.23 x 10^7	1.59 x 10^{10}	
Wheat	Ea (kJ mol^{-1})	41.00	76.57	139.46	118.62	Shang *et al*. (2013)
	A (s^{-1})	3.48 x 10^3	4.34 x 10^3	3.91 x 10^{10}	3.48 x 10^7	
Poplar	Ea (kJ mol^{-1})	104.42	97.60	125.10	111.57	Edgar (2019)
	A (s^{-1})	4.80 x 10^8	3.2 x 10^6	9.65 x 10^9	2.75 x 10^7	

Spruce	Ea (kJ mol^{-1})	20.79	40.61	90.26	93.47	Bach *et al.* (2016)
	A (s^{-1})	1.04 x 10^{1}	2.76 x 10^{4}	1.26 x 10^{7}	3.84 x 10^{6}	
Birch	Ea (kJ mol^{-1})	87.71	93.51	119.85	109.62	
	A (s^{-1})	2.25 x 10^{7}	2.39 x 10^{1}	1.02 x 10^{10}	1.03 x10^{8}	
Pine	Ea (kJ mol^{-1})	46.85	6.1 x 10^{-6}	122.11	94.40	Shang *et al*. (2014)
	A (s^{-1})	77.14	1 x 10^{-5}	2.68 x 10^{8}	5.75 x 10^{4}	
Pine	Ea (kJ mol^{-1})	10.29	141.28	80.29	13.74	This study
	A (s^{-1})	5.95 x 10^{-1}	3.96 x 10^{8}	7.19 x 10^{5}	7.09 x 10^{-1}	

Ea – Activation Energy; A – Pre-exponential factor.

As a result of Shang modelling the non-isothermal period, the model reported was not accurate enough to describe the degradation process. Furthermore, in accounting for the non-isothermal period by Shang, the kinetic parameters failed to fit the Arrhenius equation. Hence, due to the difficulty in modelling the non-isothermal period, only the isothermal period should be considered while employing this reaction mechanism scheme. A similar suggestion was made by Bach *et al.* (2016).

5.4. Conclusion

A kinetic study on the isothermal degradation of pine sawdust during torrefaction was carried out employing a two-step first-order reaction mechanism in series. A thermogravimetric analyzer was used to carry out the torrefaction process. The demarcation technique was used to determine the initial conditions for the rate constants. An iteration technique was then employed to estimate the actual kinetic parameters that will efficiently predict pine sawdust's mass loss during torrefaction. The model results obtained from this study agree with the experimental results. Different and slow heating rates were employed to reduce the effect of the non-isothermal period on the mass loss and to neglect the heat transfer within the biomass sample, respectively. The activation energies of the pseudo-components (k_b, k_c, k_{v1}, k_{v2}) obtained at the different stages of the degradation process were 10.29, 141.28, 80.29and 13.74 kJ mol^{-1}, respectively. The introduction of the pseudo-components helped to establish a better understanding of the torrefaction process by showing the degradation and formation of the intermediate products. The estimation of the pseudo-components' activation energy will also help in estimating the overall activation energy of the process. The solid distribution of components during torrefaction via kinetics can pave the way for implementing the torrefaction process in the industry. Therefore, based on the results obtained from this study, the combined demarcation time and iteration technique are recommended to study the reaction kinetics of similar waste biomass.

CHAPTER SIX

6. GENERAL CONCLUSION AND RECOMMENDATION

This chapter presents the general conclusions drawn from this study. The contributions of this study to this field are also highlighted. The challenges faced during this study's execution and possible measures to take for further studies to enhance the quality of the results reported in this study are documented in this chapter.

6.1. General Conclusions

This study aimed to understand the effect of process condition on pine sawdust (PSD) pretreatment during torrefaction and solvolysis. Three specific objectives were developed to achieve this aim based on the research questions that were developed.

Firstly, the first objective was to develop a predictive empirical model that can describe the effect of operating temperature, residence time, Liquid-to-Solid ratio/Nitrogen-to-Solid ratio during torrefaction and solvolysis pretreatment of PSD. This objective was achieved by carrying out the torrefaction and solvolysis pretreatments on a bench scale. Simultaneously, response surface methodology (RSM) based on Box-Behnken Design (BBD) was used to design the experiments. The process conditions studied, were benchmarked between 200 °C – 300 °C, 30 – 120 min and 4 – 6 NSR/LSR for easy comparison between the char produced from both pretreatments. 3D-plots, developed based on RSM, were used to establish the interactional effect of the process conditions on the fuel properties of char produced from torrefaction (biochar) and char produced from solvolysis (hydrochar). BBD was sufficient to develop predictive models that could explain the effect of process conditions during the process. The predictive models developed were all significant at a 95 % confidence level. The P-values, F-tests, Lack of Fitness test (LOF) and the coefficient of determination (R^2) all suggested that the models well significant and reliable. The 3D-plot surface plots indicated that

the order of influence of process conditions on the fuel properties of pre-treated PSD from highest to lowest was; Temperature>Time>NSR/LSR. However, the increase in LSR during the solvolysis pretreatment significantly reduced the mass yield of the char. The fuel quality of the biochar and hydrochar were also compared. Based on the higher heating value (HHV), oxygen-to-carbon (O:C) ratio and hydrogen-to-carbon (H:C) ratio, solvolysis was noticed to improve the fuel properties of PSD than torrefaction significantly. However, the mass yield during torrefaction was significantly higher.

Secondly, for the execution of the second objective, a genetic algorithm was to be used as an optimization tool to optimize the pretreatment processes. Desirability function based on RSM was also used to optimize the processes, and the two optimization techniques were qualitatively and quantitively compared. Design expert software and MATLAB were used to carry out this optimization while employing a desirability function approach and genetic algorithm, respectively. Similar optimum values were obtained using both methods; GA and desirability function. However, the genetic algorithm exhibited a higher level of accuracy when compared using the developed predictive models. Furthermore, the optimum process conditions obtained for torrefaction and solvolysis pretreatment processes were; 299 °C, 30.07 min, 4.12 NSR and 295.1 °C, 50.85 min, 4.55 LSR, respectively.

Lastly, the third objective of this study was to develop a 2-step kinetic model that will be capable of explaining the isothermal degradation of PSD during torrefaction. A TGA was used to carry out the torrefaction experiment between 200 °C – 300 °C for 120 min in achieving this objective. The experiment was done in a Nitrogen inert atmosphere. Five experimental runs were done for five different temperatures. Each experiment was carried out isothermally, and the different heating rates were employed to maintain a non-isothermal period of 10 mins. Before the model development and solution, the non-isothermal heating periods were ignored due to the difficulty in modelling it. The 2-step reaction mechanism was adequate in describing

the isothermal degradation of PSD during torrefaction as it was observed that the modelled mass loss showed a high correlation with the recorded experimental mass loss obtained from the TGA graphs. The estimated kinetic parameters significantly fitted the Arrhenius equation. The activation energies required for the formation of the four pseudo-components were estimated to be; 10.29 kJ mol^{-1} (B), 141.28 kJ mol^{-1} (C), 80.29 kJ mol^{-1} (V_1) and 13.74 kJ mol^{-1} (V_2).

Hence, the realisation of this study has shown that a predictive empirical model can be developed to predict the fuel properties (mass yield (MY), higher heating value (HHV), and energy enhancement factor (EEF)) of PSD. The developed model can also explain the effect of process conditions during torrefaction and solvolysis pretreatment processes. The completion of this study has suggested that the genetic algorithm can accurately optimize torrefaction and solvolysis process. Furthermore, this study has indicated that implementing a 2-step reaction mechanism to describe the isothermal degradation of PSD during torrefaction pretreatment is highly efficient and can be extended to other similar biomass types.

Having completed this study, the scientific contributions of this study to this research field are as follows:

- Optimum process variables that can be used on a commercial scale for the pretreatment of pine wood have been established for torrefaction and solvolysis methods.
- This study provides, for the first time, the comparison between the quality of biochar and hydrochar produced from torrefaction and solvolysis pe-treatments.
- The kinetic data provided in this study can be used to evaluate the efficiency of a torrefaction pretreatment and help simulate the process using industrial simulating software while considering the minimum energy required to form intermediate products during torrefaction.

- The kinetic data provided in this study can also be used to design an efficient torrefaction reactor, design an efficient process and control the pretreatment process.

6.2. Recommendations

Torrefaction and solvolysis pretreatment were done on a laboratory scale. As a result of this, when the experimental time elapsed, there was still a continuous mass loss as the reactor was cooling from the operating temperature to the room temperature. Hence, it is recommended that a cooling medium is provided to reduce the cooling time, thereby not losing significant mass during cooling.

Also, after torrefaction pretreatment, it was difficult to account for the total mass yield because some of the char got stuck around the internal walls of the torrefier.

It was also noticed that water and biomass did not easily mix before solvolysis pretreatment. Although proper mixing was achieved during the process, better results could be achieved by initially using a magnetic stirrer to mix the de-ionized water and biomass before pretreatment.

One of the challenges faced during this study's experimental stage was that some of the solid char was lost on the filter paper during the solvolysis process while filtering the water from the biomass solution. This challenge could have affected the measured mass yield of the hydrochar.

Also, while carrying out the TGA analysis on PSD, it was not easy to measure 10 mg of feed accurately. Although the variation in the mass of feed was reasonably considered to about ±0.2 mg, this could affect the true mass loss of PSD in the TGA with respect to the mass of the initial feed.

REFERENCES

Abou Hussein, S.D., Sawan, O.M., 2010. The utilization of agricultural waste as one of the environmental issues in Egypt (a case study). J. Appl. Sci. Res. 6, 1116–1124.

Acharjee, T.C., Coronella, C.J., Vasquez, V.R., 2011. Effect of thermal pretreatment on equilibrium moisture content of lignocellulosic biomass. Bioresour. Technol. 102, 4849–4854. https://doi.org/10.1016/j.biortech.2011.01.018

Acharya, B., Dutta, A., Minaret, J., 2015. Review on comparative study of dry and wet torrefaction. Sustain. Energy Technol. Assessments 12, 26–37. https://doi.org/10.1016/j.seta.2015.08.003

Adib, R., Murdock, H.E., Appavou, F., Brown, A., Epp, B., Leidreiter, A., Lins, C., Musolino, E., Petrichenko, K., Farrell, T.C., 2015. Renewables 2015 Global Status Report Distrbuted Renewable Energy for Energy Access. Paris REN21 Secr.

Aguado, R., Cuevas, M., Pérez-Villarejo, L., Martínez-Cartas, M.L., Sánchez, S., 2020. Upgrading almond-tree pruning as a biofuel via wet torrefaction. Renew. Energy 145, 2091–2100. https://doi.org/10.1016/j.renene.2019.07.142

Ahmed, T., Sajidah, A., Jamari, S.S., Hasbi, M., Rahim, A., Park, J., Kim, H., 2019. Biomass and Bioenergy Hydrothermal carbonization of lignocellulosic biomass for carbon rich material preparation : A review. Biomass and Bioenergy 130, 105384. https://doi.org/10.1016/j.biombioe.2019.105384

Akbari, M., Oyedun, A.O., Kumar, A., 2020. Techno-economic assessment of wet and dry torrefaction of biomass feedstock. Energy 207, 118287. https://doi.org/10.1016/j.energy.2020.118287

Ali, I., Naqvi, S.R., Bahadar, A., 2018. Kinetic analysis of Botryococcus braunii pyrolysis

using model-free and model fitting methods. Fuel 214, 369–380. https://doi.org/10.1016/j.fuel.2017.11.046

Almeida, G., Brito, J.O., Perré, P., 2010. Alterations in energy properties of eucalyptus wood and bark subjected to torrefaction: The potential of mass loss as a synthetic indicator. Bioresour. Technol. 101, 9778–9784. https://doi.org/10.1016/j.biortech.2010.07.026

Anca-Couce, A., Mehrabian, R., Scharler, R., Obernberger, I., 2014. Kinetic scheme to predict product composition of biomass torrefaction. Chem. Eng. Trans. 37, 43–48. https://doi.org/10.3303/CET1437008

Anca-Couce, A., Tsekos, C., Retschitzegger, S., Zimbardi, F., Funke, A., Banks, S., Kraia, T., Marques, P., Scharler, R., de Jong, W., Kienzl, N., 2020. Biomass pyrolysis TGA assessment with an international round robin. Fuel 276, 118002. https://doi.org/10.1016/j.fuel.2020.118002

Antonio Erias, Cansu Karaka, Corinna Grajetzki, James Carton, Mekalia Paulos, Pirjo Jantunen, Prajwal Baral, Samal Bex, J.M.V., 2016. World Energy Resources 2016. World Energy Counc. 2016 6–46. https://doi.org/http://www.worldenergy.org/wp-content/uploads/2013/09/Complete_WER_2013_Survey.pdf

Anukam, A., Mamphweli, S., Okoh, O., Reddy, P., 2017. Influence of Torrefaction on the Conversion Efficiency of the Gasification Process of Sugarcane Bagasse. https://doi.org/10.3390/bioengineering4010022

ASTM International, 2015a. ASTM E1755-01, Standard Test Method for Ash in Biomass. West Conshohocken, PA.

ASTM International, 2015b. ASTM E1756-08, Standard Test Method for Determination of Total Solids in Biomass. West Conshohocken, PA. https://doi.org/10.1520/E1756-08R15

ASTM International, 2013. ASTM E872-82, Standard Test Method for Volatile Matter in the Analysis of Particulate Wood Fuels. West Conshohocken, PA.

ASTM standards-D3176-89, 2002. standard practice for ultimate analysis of coal and coke.

Atienza-Martínez, M., Rubio, I., Fonts, I., Ceamanos, J., Gea, G., 2017. Effect of torrefaction on the catalytic post-treatment of sewage sludge pyrolysis vapors using γ-Al2O3. Chem. Eng. J. 308, 264–274. https://doi.org/10.1016/j.cej.2016.09.042

Bach, Q., Skreiberg, Ø., 2016. Upgrading biomass fuels via wet torrefaction : A review and comparison with dry torrefaction. Renew. Sustain. Energy Rev. 54, 665–677. https://doi.org/10.1016/j.rser.2015.10.014

Bach, Q.V., Chen, W.H., Chu, Y.S., Skreiberg, Ø., 2016a. Predictions of biochar yield and elemental composition during torrefaction of forest residues. Bioresour. Technol. 215, 239–246. https://doi.org/10.1016/j.biortech.2016.04.009

Bach, Q.V., Tran, K.Q., Skreiberg, Ø., 2016b. Hydrothermal pretreatment of fresh forest residues: Effects of feedstock pre-drying. Biomass and Bioenergy 85, 76–83. https://doi.org/10.1016/j.biombioe.2015.11.019

Barbanera, M., Muguerza, I.F., 2020. Effect of the temperature on the spent coffee grounds torrefaction process in a continuous pilot-scale reactor. Fuel 262, 116493. https://doi.org/10.1016/j.fuel.2019.116493

Barskov, S., Zappi, M., Buchireddy, P., Dufreche, S., Guillory, J., Gang, D., Hernandez, R., Bajpai, R., Baudier, J., Cooper, R., Sharp, R., 2019. Torrefaction of biomass: A review of production methods for biocoal from cultured and waste lignocellulosic feedstocks. Renew. Energy 142, 624–642. https://doi.org/10.1016/j.renene.2019.04.068

Barzegar, R., Yozgatligil, A., Olgun, H., Atimtay, A.T., 2020. TGA and kinetic study of

different torrefaction conditions of wood biomass under air and oxy-fuel combustion atmospheres. J. Energy Inst. 93, 889–898. https://doi.org/10.1016/j.joei.2019.08.001

Bates, R.B., Ghoniem, A.F., 2013. Biomass torrefaction: Modeling of reaction thermochemistry. Bioresour. Technol. 134, 331–340. https://doi.org/10.1016/j.biortech.2013.01.158

Bello, J.O., Danjuma, M.N., Ahmed, A.S., 2016. Decontamination of Textile Effluent Using Cation Exchange Derived From Agricultural Waste. J. Niger. Soc. Chem. Eng.

Blondeau, J., Jeanmart, H., 2012. Biomass pyrolysis at high temperatures: Prediction of gaseous species yields from an anisotropic particle. Biomass and Bioenergy 41, 107–121. https://doi.org/10.1016/j.biombioe.2012.02.016

Bogale, W., 2010. Preparation Of Charcoal Using Agricultural Wastes. Ethiop. J. Educ. Sci. 5. https://doi.org/10.4314/ejesc.v5i1.56314

Brachi, P., Chirone, R., Miccio, M., Ruoppolo, G., 2019. Fluidized bed torrefaction of biomass pellets: A comparison between oxidative and inert atmosphere. Powder Technol. 357, 97–107. https://doi.org/10.1016/j.powtec.2019.08.058

Braga, R.M., Costa, T.R., Freitas, J.C.O., Barros, J.M.F., Melo, D.M.A., Melo, M.A.F., 2014. Pyrolysis kinetics of elephant grass pretreated biomasses. J. Therm. Anal. Calorim. 117, 1341–1348. https://doi.org/10.1007/s10973-014-3884-2

Broido, A., Nelson, M.A., 1975. Char yield on pyrolysis of cellulose. Combust. Flame 24, 263–268. https://doi.org/10.1016/0010-2180(75)90156-X

Buratti, C., Barbanera, M., Lascaro, E., Cotana, F., 2018. Optimization of torrefaction conditions of coffee industry residues using desirability function approach. Waste Manag. 73, 523–534. https://doi.org/10.1016/j.wasman.2017.04.012

Cahyanti, M.N., Doddapaneni, T.R.K.C., Kikas, T., 2020a. Biomass torrefaction: An overview on process parameters, economic and environmental aspects and recent advancements. Bioresour. Technol. 301, 122737. https://doi.org/10.1016/j.biortech.2020.122737

Cahyanti, M.N., Doddapaneni, T.R.K.C., Kikas, T., 2020b. Biomass torrefaction: An overview on process parameters, economic and environmental aspects and recent advancements. Bioresour. Technol. 301, 122737. https://doi.org/10.1016/j.biortech.2020.122737

Ceylan, S., 2015. Kinetic analysis on the non-isothermal degradation of plum stone waste by thermogravimetric analysis and integral Master-Plots method. Waste Manag. Res. 33, 345–352. https://doi.org/10.1177/0734242X15574590

Cha, J.S., Park, S.H., Jung, S.C., Ryu, C., Jeon, J.K., Shin, M.C., Park, Y.K., 2016. Production and utilization of biochar: A review. J. Ind. Eng. Chem. 40, 1–15. https://doi.org/10.1016/j.jiec.2016.06.002

Chen, D., Li, Y., Deng, M., Wang, J., Chen, M., Yan, B., Yuan, Q., 2016. Effect of torrefaction pretreatment and catalytic pyrolysis on the pyrolysis poly-generation of pine wood. Bioresour. Technol. 214, 615–622. https://doi.org/10.1016/j.biortech.2016.04.058

Chen, W.H., Peng, J., Bi, X.T., 2015. A state-of-the-art review of biomass torrefaction, densification and applications. Renew. Sustain. Energy Rev. 44, 847–866. https://doi.org/10.1016/j.rser.2014.12.039

Chen, W.H., Ye, S.C., Sheen, H.K., 2012. Hydrothermal carbonization of sugarcane bagasse via wet torrefaction in association with microwave heating. Bioresour. Technol. 118, 195–203. https://doi.org/10.1016/j.biortech.2012.04.101

Chen, Z., Wang, M., Jiang, E., Wang, D., Zhang, K., Ren, Y., Jiang, Y., 2018. Pyrolysis of Torrefied Biomass. Trends Biotechnol. 36, 1287–1298.

https://doi.org/10.1016/j.tibtech.2018.07.005

Cotana, F., Buratti, C., Barbanera, M., Lascaro, E., 2015. Bioresource Technology Optimization of the steam explosion and enzymatic hydrolysis for sugars production from oak woods. Bioresour. Technol. 198, 470–477. https://doi.org/10.1016/j.biortech.2015.09.047

Dai, L., He, C., Wang, Y., Liu, Y., Ruan, R., Yu, Z., Zhou, Y., Duan, D., Fan, L., Zhao, Y., 2018. Hydrothermal pretreatment of bamboo sawdust using microwave irradiation. Bioresour. Technol. 247, 234–241. https://doi.org/10.1016/j.biortech.2017.08.104

Derringer, G., Suich, R., 1980. Simultaneous Optimization of Several Response Variables. J. Qual. Technol. 12, 214–219. https://doi.org/10.1080/00224065.1980.11980968

Di Blasi, C., Lanzetta, M., 1997. Intrinsic kinetics of isothermal xylan degradation in inert atmosphere. J. Anal. Appl. Pyrolysis 40–41, 287–303. https://doi.org/10.1016/S0165-2370(97)00028-4

Dorde Medic, Matthew Darr, Benjamin Potter, Ajay Shah, 2011. Effect of Torrefaction Process Parameters on Biomass Feedstock Upgrading, in: 2010 Pittsburgh, Pennsylvania, June 20 - June 23, 2010. American Society of Agricultural and Biological Engineers, St. Joseph, MI. https://doi.org/10.13031/2013.29898

Dowaki, K., Mori, S., 2005. Biomass energy used in a sawmill. Appl. Energy 80, 327–339. https://doi.org/10.1016/j.apenergy.2004.04.006

Duan, H., Zhang, Z., Rahman, M., Guo, X., Zhang, X., Cai, J., 2020. Insight into torrefaction of woody biomass : Kinetic modeling using pattern search method. Energy 201, 117648. https://doi.org/10.1016/j.energy.2020.117648

Edgar, A., 2019a. ScienceDirect ScienceDirect ScienceDirect Prediction of higher heating

values (HHVs) and energy yield during Prediction of higher heating Symposium values (HHVs) and energy yield during torrefaction via kinetics torrefaction via kinetics Assessing the. Energy Procedia 158, 111–116. https://doi.org/10.1016/j.egypro.2019.01.054

Edgar, A., 2019b. ScienceDirect ScienceDirect ScienceDirect Prediction of higher heating values (HHVs) and energy yield during Prediction of higher heating Symposium values (HHVs) and energy yield during torrefaction via kinetics torrefaction via kinetics Assessing the. Energy Procedia 158, 111–116. https://doi.org/10.1016/j.egypro.2019.01.054

Energy Information Administration, 2008. COAL -- A Fossil Fuel Mining the Coal Processing the Coal. Dev. Proj. Intermed. Energy Infob.

Falcon, R., 2013. Coal geology, types, ranks and grades. Johannesburg.

Felfli, F.F., Luengo, C.A., Suárez, J.A., Beatón, P.A., 2005. Wood briquette torrefaction. Energy Sustain. Dev. 9, 19–22. https://doi.org/10.1016/S0973-0826(08)60519-0

Funke, A., Ziegler, F., Berlin, T.U., 2010. Hydrothermal carbonization of biomass : A summary and discussion of chemical mecha- nisms for process engineering 160–177. https://doi.org/10.1002/bbb

Gai, C., Zhang, Y., Chen, W.T., Zhang, P., Dong, Y., 2013. Thermogravimetric and kinetic analysis of thermal decomposition characteristics of low-lipid microalgae. Bioresour. Technol. 150, 139–148. https://doi.org/10.1016/j.biortech.2013.09.137

Gajera, Z.R., Verma, K., Tekade, S.P., Sawarkar, A.N., 2020. Kinetics of co-gasification of rice husk biomass and high sulphur petroleum coke with oxygen as gasifying medium via TGA. Bioresour. Technol. Reports 11, 100479.

https://doi.org/10.1016/j.biteb.2020.100479

Gan, M.J., Lim, W.S., Ng, H.X., Ong, M.H., Gan, S., Lee, L.Y., Thangalazhy-Gopakumar, S., 2019. Enhancement of Palm Kernel Shell Fuel Properties via Wet Torrefaction: Response Surface, Optimization, and Combustion Studies. Energy and Fuels. https://doi.org/10.1021/acs.energyfuels.9b02229

Gil, M. V., García, R., Pevida, C., Rubiera, F., 2015. Grindability and combustion behavior of coal and torrefied biomass blends. Bioresour. Technol. 191, 205–212. https://doi.org/10.1016/j.biortech.2015.04.117

Gong, C., Huang, J., Feng, C., Wang, G., Tabil, L., Wang, D., 2016. Effects and mechanism of ball milling on torrefaction of pine sawdust. Bioresour. Technol. 214, 242–247. https://doi.org/10.1016/j.biortech.2016.04.062

Gong, S.H., Im, H.S., Um, M., Lee, H.W., Lee, J.W., 2019. Enhancement of waste biomass fuel properties by sequential leaching and wet torrefaction. Fuel 239, 693–700. https://doi.org/10.1016/j.fuel.2018.11.069

Gordillo, M.C., Mart, J., 2001. Hydrogen bonding in supercritical water confined in carbon nanotubes 341, 250–254.

Grycova, B., Pryszcz, A., Krzack, S., Klinger, M., Lestinsky, P., 2020. Torrefaction of biomass pellets using the thermogravimetric analyser. Biomass Convers. Biorefinery. https://doi.org/10.1007/s13399-020-00621-4

Gucho, E.M., Shahzad, K., Bramer, E.A., Akhtar, N.A., Brem, G., 2015. Experimental study on dry torrefaction of beech wood and miscanthus. Energies 8, 3903–3923. https://doi.org/10.3390/en8053903

Hartnady, C.J.H., 2010. South Africa's diminishing coal reserves. S. Afr. J. Sci. 106, 1–5.

https://doi.org/10.4102/sajs.v106i9/10.369

Hashemi, S.S., Karimi, K., Mirmohamadsadeghi, S., 2019. Hydrothermal pretreatment of safflower straw to enhance biogas production. Energy 172, 545–554. https://doi.org/10.1016/j.energy.2019.01.149

Hassan, S.S., Williams, G.A., Jaiswal, A.K., 2018. Bioresource Technology Emerging technologies for the pretreatment of lignocellulosic biomass. Bioresour. Technol. 262, 310–318. https://doi.org/10.1016/j.biortech.2018.04.099

He, C., Tang, C., Li, C., Yuan, J., Tran, K.Q., Bach, Q.V., Qiu, R., Yang, Y., 2018. Wet torrefaction of biomass for high quality solid fuel production: A review. Renew. Sustain. Energy Rev. 91, 259–271. https://doi.org/10.1016/j.rser.2018.03.097

He, L., Huang, H., Zhang, Z., Lei, Z., 2015. A Review of Hydrothermal Pretreatment of Lignocellulosic Biomass for Enhanced Biogas Production 437–446.

Hernández, J.J., Lapuerta, M., Monedero, E., Pazo, A., 2018. Biomass quality control in power plants: Technical and economical implications. Renew. Energy 115, 908–916. https://doi.org/10.1016/j.renene.2017.09.026

Jagodzińska, K., Czerep, M., Kudlek, E., Wnukowski, M., Pronobis, M., Yang, W., 2020. Torrefaction of Agricultural Residues: Effect of Temperature and Residence Time on the Process Products Properties. J. Energy Resour. Technol. 142, 1–8. https://doi.org/10.1115/1.4046275

Jin, S., Zhang, G., Zhang, P., Li, F., Fan, S., Li, J., 2016. Bioresource Technology Thermo-chemical pretreatment and enzymatic hydrolysis for enhancing saccharification of catalpa sawdust. Bioresour. Technol. 205, 34–39. https://doi.org/10.1016/j.biortech.2016.01.019

Kambo, H.S., Dutta, A., 2014. Strength , storage , and combustion characteristics of densified

lignocellulosic biomass produced via torrefaction and hydrothermal carbonization. Appl. Energy 135, 182–191. https://doi.org/10.1016/j.apenergy.2014.08.094

Kang, K., Nanda, S., Sun, G., Qiu, L., Gu, Y., Zhang, T., Zhu, M., Sun, R., 2019. Microwave-assisted hydrothermal carbonization of corn stalk for solid biofuel production: Optimization of process parameters and characterization of hydrochar. Energy 186, 115795. https://doi.org/10.1016/j.energy.2019.07.125

Kannan, S., Gariepy, Y., Raghavan, G.S.V., 2017. Optimization and Characterization of Hydrochar Derived from Shrimp Waste. Energy and Fuels 31, 4068–4077. https://doi.org/10.1021/acs.energyfuels.7b00093

Kanwal, S., Chaudhry, N., Munir, S., Sana, H., 2019. Effect of torrefaction conditions on the physicochemical characterization of agricultural waste (sugarcane bagasse). Waste Manag. 88, 280–290. https://doi.org/10.1016/j.wasman.2019.03.053

Kaushal, P., Tyagi, R., 2017. Advanced simulation of biomass gasification in a fluidized bed reactor using ASPEN PLUS. Renew. Energy 101, 629–636. https://doi.org/10.1016/j.renene.2016.09.011

Keivani, B., Gultekin, S., Olgun, H., Atimtay, A.T., 2018. Torrefaction of pine wood in a continuous system and optimization of torrefaction conditions. Int. J. Energy Res. 42, 4597–4609. https://doi.org/10.1002/er.4201

Kharagpur, I.I.T., Web, N., 2019. Module 2 : Solid Fossil Fuel (Coal) Lecture 7 : Coal classification , composition and basis 1–6.

Kruse, A., Karlsruhe, F., 2008. Supercritical water gasifi cation 415–437. https://doi.org/10.1002/bbb

Kruse, A, Dinjus, E., Kruse, Andrea, 2011. Hydrothermale Karbonisierung : 1 . Einfluss des

Lignins in Lignocellulosen 1734–1741. https://doi.org/10.1002/cite.201100092

Kumar, M., Kumar, S., Upadhyay, S.N., Mishra, P.K., 2020. Bioresource Technology Analysis of thermal degradation of banana (Musa balbisiana) trunk biomass waste using iso-conversional models. Bioresour. Technol. 310, 123393. https://doi.org/10.1016/j.biortech.2020.123393

Kumar, R., Sarkar, A., Prasad, J., 2020. Effect of torrefaction on the physicochemical properties of eucalyptus derived biofuels : estimation of kinetic parameters and optimizing torrefaction using response surface methodology (RSM). Energy 198, 117369. https://doi.org/10.1016/j.energy.2020.117369

Lee, S.M., Lee, J.W., 2014. Optimization of biomass torrefaction conditions by the Gain and Loss method and regression model analysis. Bioresour. Technol. 172, 438–443. https://doi.org/10.1016/j.biortech.2014.09.016

Lei, H., Cybulska, I., Julson, J., 2013. Hydrothermal Pretreatment of Lignocellulosic Biomass and Kinetics 2013, 250–259.

Lei, Y., Tian, R., 2016. RSC Advances Morphology evolution , formation mechanism and adsorption properties of hydrochars prepared by hydrothermal carbonization of corn stalk † 107829–107835. https://doi.org/10.1039/c6ra21607b

Li, H., Wang, S., Yuan, X., Xi, Y., Huang, Z., Tan, M., 2018. Bioresource Technology The e ff ects of temperature and color value on hydrochars ' properties in hydrothermal carbonization. Bioresour. Technol. 249, 574–581. https://doi.org/10.1016/j.biortech.2017.10.046

Li, S.X., Chen, C.Z., Li, M.F., Xiao, X., 2018. Torrefaction of corncob to produce charcoal under nitrogen and carbon dioxide atmospheres. Bioresour. Technol. 249, 348–353.

https://doi.org/10.1016/j.biortech.2017.10.026

Lopez, J.L., Abt, R.C., Dvorak, W.S., Hodge, G.R., Phillips, R., 2018. Tree breeding model to assess financial performance of pine hybrids and pure species: deterministic and stochastic approaches for South Africa. New For. 49, 123–142. https://doi.org/10.1007/s11056-017-9609-1

Louwes, A.C., Basile, L., Yukananto, R., Bhagwandas, J.C., Bramer, E.A., Brem, G., 2017. Torrefied biomass as feed for fast pyrolysis: An experimental study and chain analysis. Biomass and Bioenergy 105, 116–126. https://doi.org/10.1016/j.biombioe.2017.06.009

Lu, K.M., Lee, W.J., Chen, W.H., Liu, S.H., Lin, T.C., 2012. Torrefaction and low temperature carbonization of oil palm fiber and eucalyptus in nitrogen and air atmospheres. Bioresour. Technol. 123, 98–105. https://doi.org/10.1016/j.biortech.2012.07.096

Lu, Q., Li, W., Zhang, X., Liu, Z., Cao, Q., Xie, X., Yuan, S., 2020. Experimental study on catalytic pyrolysis of biomass over a Ni/Ca-promoted Fe catalyst. Fuel 263, 116690. https://doi.org/10.1016/j.fuel.2019.116690

Lynam, J.G., Reza, M.T., Yan, W., Vásquez, V.R., Coronella, C.J., 2015. Hydrothermal carbonization of various lignocellulosic biomass. Biomass Convers. Biorefinery 5, 173–181. https://doi.org/10.1007/s13399-014-0137-3

Ma, M., Su, M., Li, S., Jiang, F., Li, R., 2018. Predicting coal consumption in South Africa based on linear (Metabolic Grey Model), nonlinear (Non-Linear Grey Model), and combined (Metabolic Grey Model-Autoregressive Integrated Moving Average Model) models. Sustain. 10. https://doi.org/10.3390/su10072552

Mahawar, N., Goyal, P., Lakhiwal, S., Jain, S., 2015. Agro Waste: A New Eco-Friendly Energy Resource. Int. Res. J. Environ. Sci. Int. Sci. Congr. Assoc. 4, 47–49.

https://doi.org/10.7251/AGSY1203393S

Mäkelä, M., Benavente, V., Fullana, A., 2015. Hydrothermal carbonization of lignocellulosic biomass: Effect of process conditions on hydrochar properties. Appl. Energy 155, 576–584. https://doi.org/10.1016/j.apenergy.2015.06.022

Martín-Lara, M.A., Ronda, A., Zamora, M.C., Calero, M., 2017. Torrefaction of olive tree pruning: Effect of operating conditions on solid product properties. Fuel 202, 109–117. https://doi.org/10.1016/j.fuel.2017.04.007

Mohan, D., Pittman, C.U., Steele, P.H., 2006. Pyrolysis of wood/biomass for bio-oil: A critical review. Energy and Fuels 20, 848–889. https://doi.org/10.1021/ef0502397

Mohlala, L.M., Bodunrin, M.O., Awosusi, A.A., Daramola, M.O., Cele, N.P., Olubambi, P.A., 2016. Beneficiation of corncob and sugarcane bagasse for energy generation and materials development in Nigeria and South Africa: A short overview. Alexandria Eng. J. 55, 3025–3036. https://doi.org/10.1016/j.aej.2016.05.014

Mundike, J., Collard, F.X., Görgens, J.F., 2016. Torrefaction of invasive alien plants: Influence of heating rate and other conversion parameters on mass yield and higher heating value. Bioresour. Technol. 209, 90–99. https://doi.org/10.1016/j.biortech.2016.02.082

Nakason, K., 2017. Hydrothermal Carbonization of Oil Palm Pressed Fiber : Effect of Reaction Parameters on Product Characteristics 17, 47–56.

Ness, J., Moghtaderi, B., 2003. Biomass and bio-energy. Fuel Energy Abstr. 44, 158. https://doi.org/10.1016/s0140-6701(03)81796-4

Nhuchhen, D.R., Abdul Salam, P., 2012. Estimation of higher heating value of biomass from proximate analysis: A new approach. Fuel 99, 55–63. https://doi.org/10.1016/j.fuel.2012.04.015

Nhuchhen, D.R., Afzal, M.T., 2017. HHV predicting correlations for torrefied biomass using proximate and ultimate analyses. Bioengineering 4. https://doi.org/10.3390/bioengineering4010007

Nhuchhen, D.R., Afzal, M.T., Parvez, A.M., 2018. Effect of torrefaction on the fuel characteristics of timothy hay. Biofuels 7269, 1–14. https://doi.org/10.1080/17597269.2018.1479135

Nizamuddin, S., Qureshi, S.S., Baloch, H.A., Siddiqui, M.T.H., Takkalkar, P., Mubarak, N.M., Dumbre, D.K., Griffin, G.J., Madapusi, S., Tanksale, A., 2019. Microwave hydrothermal carbonization of rice straw: Optimization of process parameters and upgrading of chemical, fuel, structural and thermal properties. Materials (Basel). 12. https://doi.org/10.3390/ma12030403

Nunes, L.J.R., Matias, J.C.O., Catalão, J.P.S., 2014. A review on torrefied biomass pellets as a sustainable alternative to coal in power generation. Renew. Sustain. Energy Rev. 40, 153–160. https://doi.org/10.1016/j.rser.2014.07.181

Ohliger, A., Förster, M., Kneer, R., 2013. Torrefaction of beechwood: A parametric study including heat of reaction and grindability. Fuel 104, 607–613. https://doi.org/10.1016/j.fuel.2012.06.112

Okolie, J.A., Nanda, S., Dalai, A.K., Kozinski, J.A., 2020. Optimization and modeling of process parameters during hydrothermal gasification of biomass model compounds to generate hydrogen-rich gas products. Int. J. Hydrogen Energy 45, 18275–18288. https://doi.org/10.1016/j.ijhydene.2019.05.132

Olugbade, T.O., Ojo, O.T., 2020. Biomass Torrefaction for the Production of High-Grade Solid Biofuels: a Review. Bioenergy Res. https://doi.org/10.1007/s12155-020-10138-3

Ozonoh, M., Aniokete, T.C., Oboirien, B.O., Udeh, B.C., Yoro, K.O., Daramola, M.O., 2019. Prediction of Emissions and Profits from a Biomass, Tyre, and Coal Fired Co-Gasification CHP Plant Using Artificial Neural Network: Nigerian and South African Perspectives. J. Phys. Conf. Ser. 1378. https://doi.org/10.1088/1742-6596/1378/2/022021

Park, J.H., Choi, Y.C., Lee, Y.J., Kim, H.T., 2020. Characteristics of miscanthus fuel by wet torrefaction on fuel upgrading and gas emission behavior. Energies 13. https://doi.org/10.3390/en13102669

Pathak, H., Bhatia, A., Jain, N., Aggarwal, P.K., 2010. ING Bulletins on Regional Assessment of Reactive Nitrogen Greenhouse Gas Emission and Mitigation in Indian Agriculture – A Review.

Pathomrotsakun, J., Nakason, K., Kraithong, W., Khemthong, P., Panyapinyopol, B., Pavasant, P., 2020. Fuel properties of biochar from torrefaction of ground coffee residue: effect of process temperature, time, and sweeping gas. Biomass Convers. Biorefinery 10, 743–753. https://doi.org/10.1007/s13399-020-00632-1

Paulien Harmsen, Wouter Huijgen, Laura Bermudez, R.B., 2010. Literature review of physical and chemical pretreatment processes for lignocellulosic biomass, Wageningen UR Food & Biobased Research, institute within the legal entity Stichting Dienst Landbouwkundig Onderzoek.

Peduzzi, E., Boissonnet, G., Haarlemmer, G., Dupont, C., Maréchal, F., 2014. Torrefaction modelling for lignocellulosic biomass conversion processes. Energy 70, 58–67. https://doi.org/10.1016/j.energy.2014.03.086

Pérez, J.F., Raul, M., Samaniego, P., Garcia, M., 2019. Torrefaction of Fast-Growing Colombian Wood Species. Waste and Biomass Valorization 10, 1655–1667. https://doi.org/10.1007/s12649-017-0164-y

Phanphanich, M., Mani, S., 2011. Impact of torrefaction on the grindability and fuel characteristics of forest biomass. Bioresour. Technol. 102, 1246–1253. https://doi.org/10.1016/j.biortech.2010.08.028

Piotrowska, P., Zevenhoven, M., Davidsson, K., Hupa, M., Åmand, L.E., Barišić, V., Coda Zabetta, E., 2010. Fate of alkali metals and phosphorus of rapeseed cake in circulating fluidized bed boiler part 2: Cocombustion with coal. Energy and Fuels 24, 4193–4205. https://doi.org/10.1021/ef100482n

Prins, M.J., Ptasinski, K.J., Janssen, F.J.J.G., 2006. Torrefaction of wood. Part 1. Weight loss kinetics. J. Anal. Appl. Pyrolysis 77, 28–34. https://doi.org/10.1016/j.jaap.2006.01.002

Rackemann, D.W., Bartley, J.P., Doherty, W.O.S., 2019. Solvolysis of Sugarcane Bagasse: Strategy To Increase the Yields of Secondary Fuel Precursors. https://doi.org/10.1021/acs.iecr.9b03711

Radovic, L.R., 1997. Energy and Fuels in Society: Analysis of Bills and Media Reports, in: Energy and Fuels in Society: Analysis of Bills and Media Reports.

Rafein, M., Hirata, S., Fujimoto, S., Ali, M., 2015. Bioresource Technology Combined pretreatment with hot compressed water and wet disk milling opened up oil palm biomass structure resulting in enhanced enzymatic digestibility. Bioresour. Technol. 193, 128–134. https://doi.org/10.1016/j.biortech.2015.06.074

Rago, Y.P., Collard, F.X., Görgens, J.F., Surroop, D., Mohee, R., 2020. Torrefaction of biomass and plastic from municipal solid waste streams and their blends: Evaluation of interactive effects. Fuel 277, 118089. https://doi.org/10.1016/j.fuel.2020.118089

Ranzi, E., Cuoci, A., Faravelli, T., Frassoldati, A., Migliavacca, G., Pierucci, S., Sommariva, S., 2008. Chemical kinetics of biomass pyrolysis. Energy and Fuels 22, 4292–4300.

https://doi.org/10.1021/ef800551t

Ratte, J., Fardet, E., Mateos, D., Héry, J.S., 2011. Mathematical modelling of a continuous biomass torrefaction reactor: TORSPYD^{TM} column. Biomass and Bioenergy 35, 3481–3495. https://doi.org/10.1016/j.biombioe.2011.04.045

Raymundo, L.M., Espindola, J.S., Borges, F.C., Lazzari, E., Trierweiler, J.O., Trierweiler, L.F., 2020. Continuous fast pyrolysis of rice husk in a fluidized bed reactor with high feed rates. Chem. Eng. Commun. 0, 1–11. https://doi.org/10.1080/00986445.2020.1798937

Raza, S., Tariq, R., Hameed, Z., Ali, I., Naqvi, M., Chen, W., Ceylan, S., Rashid, H., Ahmad, J., Taqvi, S.A., Shahbaz, M., 2019. Pyrolysis of high ash sewage sludge : Kinetics and thermodynamic analysis using Coats-Redfern method. Renew. Energy 131, 854–860. https://doi.org/10.1016/j.renene.2018.07.094

Repellin, V., Govin, A., Rolland, M., Guyonnet, R., 2010. Modelling anhydrous weight loss of wood chips during torrefaction in a pilot kiln. Biomass and Bioenergy 34, 602–609. https://doi.org/10.1016/j.biombioe.2010.01.002

Ribeiro, J.M.C., Godina, R., Matias, J.C. de O., Nunes, L.J.R., 2018. Future perspectives of biomass torrefaction: Review of the current state-of-the-art and research development. Sustain. 10, 1–17. https://doi.org/10.3390/su10072323

Sanwal Hussain, Suhail A. Soomro, Shaheen Aziz, Ahsan Ali, N.A., 2018. Ultimate and Proximate Coal Analysis Ultimate and Proximate Coal Analysis. Eng. Sci. Technol. Int. Res. J. 2, 7.

Savage, P.E., 1999. Organic Chemical Reactions in Supercritical Water. https://doi.org/10.1021/cr9700989

Şensöz, S., 2003. Slow pyrolysis of wood barks from Pinus brutia Ten. and product

compositions. Bioresour. Technol. 89, 307–311. https://doi.org/10.1016/S0960-8524(03)00059-2

Sermyagina, E., Saari, J., Kaikko, J., Vakkilainen, E., 2015. Hydrothermal carbonization of coniferous biomass: Effect of process parameters on mass and energy yields. J. Anal. Appl. Pyrolysis 113, 551–556. https://doi.org/10.1016/j.jaap.2015.03.012

Serowik, M., Figiel, A., Nejman, M., Pudlo, A., Chorazyk, D., Kopec, W., 2017. Drying characteristics and some properties of spouted bed dried semi-refined carrageenan. J. Food Eng. 194, 46–57. https://doi.org/10.1016/j.jfoodeng.2016.09.007

Severy, M.A., Chamberlin, C.E., Eggink, A.J., Jacobson, A.E., 2018. Demonstration of a Pilot-Scale Plant for Biomass Torrefaction and Briquetting. Appl. Eng. Agric. 34, 85–98. https://doi.org/10.13031/aea.12376

Shang, L., Ahrenfeldt, J., Holm, J.K., Bach, L.S., Stelte, W., Henriksen, U.B., 2014. Kinetic model for torrefaction of wood chips in a pilot-scale continuous reactor. J. Anal. Appl. Pyrolysis 108, 109–116. https://doi.org/10.1016/j.jaap.2014.05.010

Shang, L., Ahrenfeldt, J., Holm, J.K., Barsberg, S., Zhang, R.Z., Luo, Y.H., Egsgaard, H., Henriksen, U.B., 2013. Intrinsic kinetics and devolatilization of wheat straw during torrefaction. J. Anal. Appl. Pyrolysis 100, 145–152. https://doi.org/10.1016/j.jaap.2012.12.010

Sharma, P., Pandey, O.P., Diwan, P.K., 2019. Non-isothermal kinetics of pseudo-components of waste biomass. Fuel 253, 1149–1161. https://doi.org/10.1016/j.fuel.2019.05.093

Shen, Y., 2020. A review on hydrothermal carbonization of biomass and plastic wastes to energy products. Biomass and Bioenergy 134, 105479. https://doi.org/10.1016/j.biombioe.2020.105479

Shi, X., Wang, J., 2014. A comparative investigation into the formation behaviors of char, liquids and gases during pyrolysis of pinewood and lignocellulosic components. Bioresour. Technol. 170, 262–269. https://doi.org/10.1016/j.biortech.2014.07.110

Sikarwar, V.S., Zhao, M., Fennell, P.S., Shah, N., Anthony, E.J., 2017. Progress in biofuel production from gasification. Prog. Energy Combust. Sci. 61, 189–248. https://doi.org/10.1016/j.pecs.2017.04.001

Singh, S., Chakraborty, J.P., Mondal, M.K., 2019a. Optimization of process parameters for torrefaction of Acacia nilotica using response surface methodology and characteristics of torrefied biomass as upgraded fuel. Energy 186, 115865. https://doi.org/10.1016/j.energy.2019.115865

Singh, S., Chakraborty, J.P., Mondal, M.K., 2019b. Optimization of process parameters for torrefaction of A cacia nilotica using response surface methodology and characteristics of torre fi ed biomass as upgraded fuel. Energy 186, 115865. https://doi.org/10.1016/j.energy.2019.115865

Siyal, A.A., Mao, X., Liu, Y., Ran, C., Fu, J., Kang, Q., Ao, W., Zhang, R., Dai, J., Liu, G., 2020. Torrefaction subsequent to pelletization: Characterization and analysis of furfural residue and sawdust pellets. Waste Manag. 113, 210–224. https://doi.org/10.1016/j.wasman.2020.05.037

South Africa, D., 2016. Innovation & Knowledge 1–14.

Stelte, W., 2012. Torrefaction of unutilized biomass resources and characterization of torrefaction gasses 3–4.

Tran, K.Q., Luo, X., Seisenbaeva, G., Jirjis, R., 2013. Stump torrefaction for bioenergy application. Appl. Energy 112, 539–546. https://doi.org/10.1016/j.apenergy.2012.12.053

Tumuluru, J.S., 2015. High moisture corn stover pelleting in a flat die pellet mill fitted with a 6 mm die: Physical properties and specific energy consumption. Energy Sci. Eng. 3, 327–341. https://doi.org/10.1002/ese3.74

U.S. Department of Energy (DOE) and U.S. Department of Agriculture (USDA)., 2009. Chapter 2. What is Biomass ?, Woody Biomass Desk Guide & Toolkit. Washington, DC.

Uemura, Y., Omar, W.N., Tsutsui, T., Bt, S., 2011. Torrefaction of oil palm wastes. Fuel 90, 2585–2591. https://doi.org/10.1016/j.fuel.2011.03.021

Ul, N., Baroutian, S., Sarmah, A.K., 2018. Bioresource Technology Physicochemical , structural and combustion characterization of food waste hydrochar obtained by hydrothermal carbonization. Bioresour. Technol. 266, 357–363. https://doi.org/10.1016/j.biortech.2018.06.112

Umeda, K., Nakamura, S., Lu, D., Yoshikawa, K., 2019. Biomass gasification employing low-temperature carbonization pretreatment for tar reduction. Biomass and Bioenergy 126, 142–149. https://doi.org/10.1016/j.biombioe.2019.05.002

United States Environmental Protection Association, 2020. The Renewable Fuel Standard (RFS) 2014.

van der Stelt, M.J.C., Gerhauser, H., Kiel, J.H.A., Ptasinski, K.J., 2011. Biomass upgrading by torrefaction for the production of biofuels: A review. Biomass and Bioenergy 35, 3748–3762. https://doi.org/10.1016/j.biombioe.2011.06.023

Vassilev, S. V., Baxter, D., Andersen, L.K., Vassileva, C.G., 2010. An overview of the chemical composition of biomass. Fuel 89, 913–933. https://doi.org/10.1016/j.fuel.2009.10.022

Vasudev, V., Ku, X., Lin, J., 2020. Bioresource Technology Pyrolysis of algal biomass :

Determination of the kinetic triplet and thermodynamic analysis. Bioresour. Technol. 317, 124007. https://doi.org/10.1016/j.biortech.2020.124007

Wang, G.J., Luo, Y.H., Deng, J., Kuang, J.H., Zhang, Y.L., 2011. Pretreatment of biomass by torrefaction. Chinese Sci. Bull. 56, 1442–1448. https://doi.org/10.1007/s11434-010-4143-y

Wang, L., Barta-Rajnai, E., Skreiberg, Khalil, R., Czégény, Z., Jakab, E., Barta, Z., Grønli, M., 2018. Effect of torrefaction on physiochemical characteristics and grindability of stem wood, stump and bark. Appl. Energy 227, 137–148. https://doi.org/10.1016/j.apenergy.2017.07.024

Wang, T., Zhai, Y., Zhu, Y., Li, C., Zeng, G., 2018. A review of the hydrothermal carbonization of biomass waste for hydrochar formation : Process conditions , fundamentals , and physicochemical properties. Renew. Sustain. Energy Rev. 90, 223–247. https://doi.org/10.1016/j.rser.2018.03.071

Wang, Z., Lim, C.J., Grace, J.R., Li, H., Parise, M.R., 2017. Effects of temperature and particle size on biomass torrefaction in a slot-rectangular spouted bed reactor. Bioresour. Technol. 244, 281–288. https://doi.org/10.1016/j.biortech.2017.07.097

Whitley, D., 1994. A genetic algorithm tutorial.

Winjobi, O., Shonnard, D.R., Zhou, W., 2017. Production of Hydrocarbon Fuel Using Two-Step Torrefaction and Fast Pyrolysis of Pine. Part 1: Techno-economic Analysis. ACS Sustain. Chem. Eng. 5, 4529–4540. https://doi.org/10.1021/acssuschemeng.7b00372

Wu, S., Zhang, S., Wang, C., Mu, C., Huang, X., 2018. High-strength charcoal briquette preparation from hydrothermal pretreated biomass wastes. Fuel Process. Technol. 171, 293–300. https://doi.org/10.1016/j.fuproc.2017.11.025

Xiao, R., Yang, W., Cong, X., Dong, K., Xu, J., Wang, D., Yang, X., 2020. Thermogravimetric analysis and reaction kinetics of lignocellulosic biomass pyrolysis. Energy 201, 117537. https://doi.org/10.1016/j.energy.2020.117537

Yan, J., Jiao, H., Li, Z., Lei, Z., Wang, Z., Ren, S., Shui, H., Kang, S., Yan, H., Pan, C., 2019. Kinetic analysis and modeling of coal pyrolysis with model-free methods. Fuel 241, 382–391. https://doi.org/10.1016/j.fuel.2018.12.079

Yan, W., Perez, S., Sheng, K., 2017. Upgrading fuel quality of moso bamboo via low temperature thermochemical treatments: Dry torrefaction and hydrothermal carbonization. Fuel 196, 473–480. https://doi.org/10.1016/j.fuel.2017.02.015

Yang, W., Shimanouchi, T., Iwamura, M., Takahashi, Y., Mano, R., Takashima, K., Tanifuji, T., Kimura, Y., 2015. Elevating the fuel properties of Humulus lupulus , Plumeria alba and Calophyllum inophyllum L . through wet torrefaction. FUEL 146, 88–94. https://doi.org/10.1016/j.fuel.2015.01.005

Yılgın, M., Duranay, N., Pehlivan, D., 2019. Torrefaction and combustion behaviour of beech wood pellets. J. Therm. Anal. Calorim. 138, 819–826. https://doi.org/10.1007/s10973-019-08250-4

Yu, C., Thy, P., Wang, L., Anderson, S.N., Vandergheynst, J.S., Upadhyaya, S.K., Jenkins, B.M., 2014. In fl uence of leaching pretreatment on fuel properties of biomass 128, 43–53. https://doi.org/10.1016/j.fuproc.2014.06.030

Yu, F., Zhu, X., Jin, W., Fan, J., Clark, J.H., Zhang, S., 2020. Optimized synthesis of granular fuel and granular activated carbon from sawdust hydrochar without binder. J. Clean. Prod. 276, 122711. https://doi.org/10.1016/j.jclepro.2020.122711

Yu, S., Park, J., Kim, M., Kim, H., Ryu, C., Lee, Y., Yang, W., Jeong, Y., 2019. Improving

Energy Density and Grindability of Wood Pellets by Dry Torrefaction. Energy & Fuels 33, 8632–8639. https://doi.org/10.1021/acs.energyfuels.9b01086

Yu, Y., Fu, X., Yu, L., Liu, R., Cai, J., 2016. Combustion kinetics of pine sawdust biochar: Data smoothing and isoconversional kinetic analysis. J. Therm. Anal. Calorim. 124, 1641–1649. https://doi.org/10.1007/s10973-016-5296-y

Yue, Y., Singh, H., Singh, B., Mani, S., 2017. Torrefaction of sorghum biomass to improve fuel properties. Bioresour. Technol. 232, 372–379. https://doi.org/10.1016/j.biortech.2017.02.060

Zafar, S., 2018. Analysis of Agro Biomass Projects. BioEnergy Consult.

Zhang, S., Chen, T., Xiong, Y., Dong, Q., 2017. Effects of wet torrefaction on the physicochemical properties and pyrolysis product properties of rice husk. Energy Convers. Manag. 141, 403–409. https://doi.org/10.1016/j.enconman.2016.10.002

Zhang, X., Gao, B., Zhao, S., Wu, P., Han, L., Liu, X., 2020. Optimization of a “coal-like” pelletization technique based on the sustainable biomass fuel of hydrothermal carbonization of wheat straw. J. Clean. Prod. 242, 118426. https://doi.org/10.1016/j.jclepro.2019.118426

APPENDICES

A. Figures



Figure A.1. Log of pine wood



Figure A.2. Pine wood chips



Figure A.3. Muffle furnace

```
%% Declaration of variables
t = 0:5:120;
W = []; %% input the mass loss data from TGA
%% Plot of mass loss against time
figure
plot (t,W,'b*')
grid on
%% Declaration of kinetic paramters anc call the kinetic fucntion
const = lsqcurvefit(@Kinetic, [initial conditions], t, W);
%% Store the kinetic paramters
K1 = const(1);
K2 = const(2);
Kb = const(3);
Kc = const(4);
%% Plot the fitted data and the experimental plots from TGA
tfit = 0:5:120;
Wfit = Kinetic(const,tfit);
figure
plot(t,W,'b*')
hold on
plot(tfit,Wfit,'r','linewidth',2)
grid on
%% Export the fitted data as excel file
xlswrite('model_data.xlsx',[tfit(:),Wfit(:)]);
```

Figure A.4. Kinetic modelling script file

```
%% Create function
function W = Kinetic(const,t)
W = (((const(2) - const(1))*const(1) + const(3)*const(1) - ...
        const(4)*const(3))/((const(2) - const(1))*const(1)))...
        *exp(-const(1)*t) - ((const(3)*const(2) - const(4)*const(3))/...
            ((const(2) - const(1))*const(2)))*exp(-const(2)*t);
end
```

Figure A.5. Kinetic modelling function file

```
%% Create function
function [Ddv_Div] = differential(I,D)
%% Declare variables and assign values to them
 K1 = 0.1317;
 K2 = 0.0033;
 Kb = 0.0752;
 Kc = 0.0000942;
 Kv1 = K1 - Kb;
 Kv2 = K2 - Kc;
 %% Assign each elements of the dependent variable D to each ...
 %% pseudo-component
 A = D(1);
 B = D(2);
 C = D(3);
 V1 = D(4);
 V2 = D(5);
 %% Arrange the obatained data in an array format
 Ddv_Div = [ -K1*A;
            Kb*A - K2*B;
               Kc*B;
                Kv1*A;
                    Kv2*B];
end
```

Figure A.6. Ordinary differential equation function file

```
%% declare the time range and the initial values of the pseudo-components
t = 0:5:120;
Ao = 1; %% Assume 100 % of component A
Bo = 0; %% Assume no B is initially formed
Co = 0; %% Assume no C is initially formed
V1o = 0; %% Assume no V1 is initially formed
V2o = 0; %% Assume no V2 is initially formed
%% Assign the inital values to an array
IC = [Ao Bo Co V1o V2o];
%% call ODE45 to solve the differential equations
[IVsol, DVsol] = ode45('differential', t, IC);
%% Plots of the solid distribution using the differential solutions
plot(IVsol, DVsol(:,1), 'k')
hold on
plot(IVsol, DVsol(:,2), 'r')
hold on
plot(IVsol, DVsol(:,3), 'b')
hold on
plot(IVsol, DVsol(:,4), 'g')
hold on
plot(IVsol, DVsol(:,5), 'c')
hold off
%% Export the data to an excel file
xlswrite('model_data.xlsx',[IVsol(:),DVsol(:,1),DVsol(:,2),DVsol(:,3),...
    DVsol(:,4),DVsol(:,5)]);
```

Figure A.7. Solid distribution plot script file

```
%% Create a function
function Output = Torr(Input)
%% Assign the process varaibles to each element of the input matix
x1 = Input(1);
x2 = Input(2);
x3 = Input(3);
%% Store the predictive models of mass yield and HHV in f1 and f2
f1 = -(23.88 - 0.004992*x1 - 0.028083*x2 - 1.94667*x3 + ...
        0.000039*x1*x2- 0.002*x1*x3 + 0.001889*x2*x3 + 0.000092*x1^2 + ...
            0.000133*x2^2+ 0.241750*x3^2);

f2 = -(220.02450 - 1.30437*x1 + 0.490556*x2 + 13.20042*x3 - ...
        0.001477*x1*x2 - 0.0137*x1*x3 - 0.002389*x2*x3 + 0.002480*x1^2 -...
            0.001147*x2^2 - 1.071*x3^2);
%% Assign the predictive models as the elements to the output matrix
Output = [f1 f2];
end
```

Figure A.8. Genetic algorithm function file for torrefaction

```
%% Create a function
function Output = Solv(Input)
%% Assign the process varaibles to each element of the input matix
x1 = Input(1);
x2 = Input(2);
x3 = Input(3);
%% Store the predictive models of mass yield and HHV in f1 and f2
f1 = -(16.67034 + 0.0323*x1 + 0.010194*x2 - 0.353750*x3);

f2 = -(-95.35942 + 0.592475*x1 + 0.334250*x2 + 43.83250*x3 - ...
        0.001070*x1*x2 - 0.029400*x1*x3 + 0.00433*x2*x3 - ...
            0.001045*x1^2 - 0.001463*x2^2 - 3.92425*x3^2);
%% Assign the predictive models as the elements to the output matrix
Output = [f1 f2];
end
```

Figure A.9. Genetic algorithm function file for solvolysis

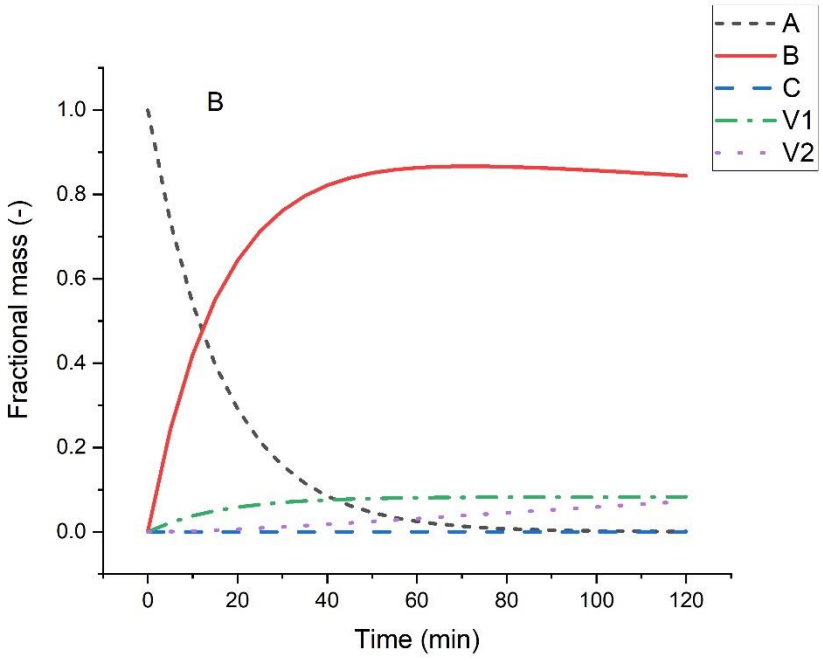


Figure A.10. Solid and gas distribution during torrefaction of PSD at 240 °C

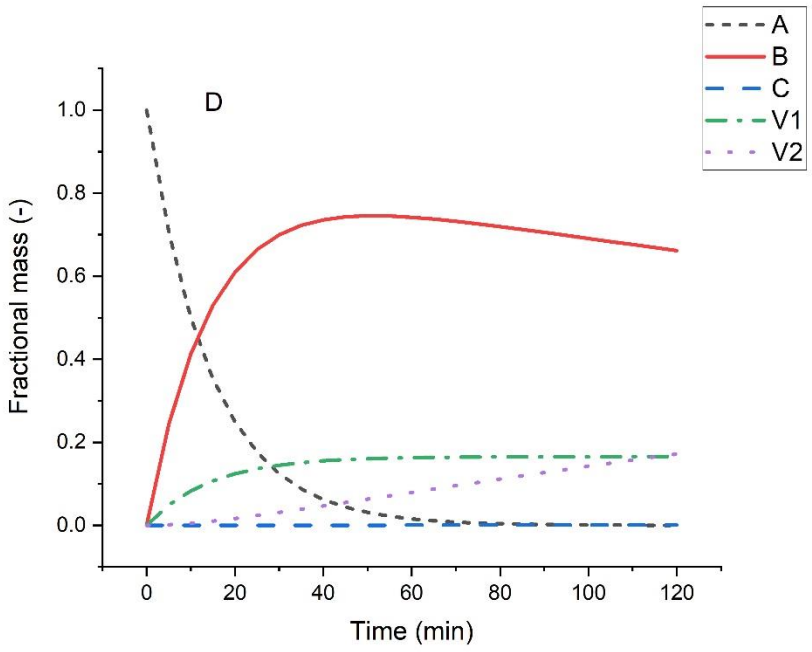


Figure A.11. Solid and gas distribution during torrefaction of PSD at 280 °C

B. Equations

From Equation (5.1),

$\frac{dM_A}{dt} = -K_1 M_A$

$\int_{M_0}^{M_A} \frac{dM_A}{M_A} = -K_1 \int_0^t dt$

$[\ln M_A - \ln M_0] = -K_1 t$

$M_A = M_0 e^{-K_1 t}$

From Equation (5.2)

$\frac{dM_B}{dt} = K_B M_A - K_2 M_B$

$\frac{dM_B}{dt} + K_2 M_B = K_B M_0 e^{-K_1 t}$

Comparing with ordinary differential equation form;

$\frac{dy}{dx} + Py = Q$

$P = K_2$

Integrating Factor (IF) $= e^{\int P(x)dx} = e^{\int K_2 dt} = e^{K_2 t}$

ODE formula: $ye^{\int P(x)dx} = \int e^{\int P(x)dx} . Qdx$

$M_B e^{K_2 t} = \int e^{K_2 t} . K_B M_0 e^{-K_1 t} dt$

$M_B e^{K_2 t} = K_B M_0 \int_0^t e^{K_2 t} . e^{-K_1 t} dt$

$M_B e^{K_2 t} = K_B M_0 \int_0^t e^{(K_2 - K_1)t} dt$

$M_B e^{K_2 t} = \frac{K_B M_0}{K_2 - K_1} \left[e^{(K_2 - K_1)t} - e^{(K_2 - K_1)(0)}\right]$

$M_B e^{K_2 t} = \frac{K_B M_0}{K_2 - K_1} \left[e^{(K_2 - K_1)t} - 1\right]$

$M_B = \frac{K_B M_0}{(K_2 - K_1)e^{K_2 t}} \left[e^{K_2 t} . e^{-K_1 t} - 1\right]$

$M_B = \frac{K_B M_0}{(K_2 - K_1)} e^{-K_1 t} - \frac{K_B M_0}{(K_2 - K_1)e^{K_2 t}}$

$$M_B = \frac{K_B M_0}{(K_2 - K_1)} e^{-K_1 t} - \frac{K_B M_0}{(K_2 - K_1)} e^{-K_2 t}$$

From Equation (5.3),

$$\frac{dM_C}{dt} = K_C M_B$$

$$\frac{dM_C}{dt} = \frac{K_c K_B M_0}{(K_2 - K_1)} e^{-K_1 t} - \frac{K_c K_B M_0}{(K_2 - K_1)} e^{-K_2 t}$$

$$\int_0^{M_c} dM_C = \frac{K_c K_B M_0}{(K_2 - K_1)} \int_0^t e^{-K_1 t} - \frac{K_c K_B M_0}{(K_2 - K_1)} \int_0^t e^{-K_2 t}$$

$$M_C = \frac{-K_c K_B M_0}{(K_2 - K_1) K_1} \left[e^{-K_1 t} - e^{-K_1(0)}\right] - \frac{-K_c K_B M_0}{(K_2 - K_1) K_2} \left[e^{-K_2 t} - e^{-K_2(0)}\right]$$

$$M_C = \frac{K_c K_B M_0}{(K_2 - K_1) K_1} \left[1 - e^{-K_1 t}\right] + \frac{K_c K_B M_0}{(K_2 - K_1) K_2} \left[e^{-K_2 t} - 1\right]$$

From Equation (5.4),

$$\frac{dM_{V1}}{dt} = K_{V1} M_A$$

$$\int_0^{M_{V1}} dM_{V1} = K_{V1} M_0 \int_0^t e^{-K_1 t} . dt$$

$$M_{V1} = \frac{-K_{V1} M_0}{K_1} \left[e^{-K_1 t} - e^{-K_1(0)}\right]$$

$$M_{V1} = \frac{K_{V1} M_0}{K_1} \left[1 - e^{-K_1 t}\right]$$

From Equation (5.5),

$$\frac{dM_{V2}}{dt} = K_{V2} M_B$$

$$\frac{dM_{V2}}{dt} = \frac{K_{V2} K_B M_0}{(K_2 - K_1)} e^{-K_1 t} - \frac{K_{V2} K_B M_0}{(K_2 - K_1)} e^{-K_2 t}$$

$$\int_0^{M_{V2}} dM_{V2} = \frac{K_{V2} K_B M_0}{(K_2 - K_1)} \int_0^t e^{-K_1 t} . dt - \frac{K_{V2} K_B M_0}{(K_2 - K_1)} \int_0^t e^{-K_2 t} . dt$$

$$M_{V2} = \frac{-K_{V2} K_B M_0}{(K_2 - K_1) K_1} \left[e^{-K_1 t} - e^{-K_1(0)}\right] - \frac{-K_{V2} K_B M_0}{(K_2 - K_1) K_2} \left[e^{-K_2 t} - e^{-K_2(0)}\right]$$

$$M_{V2} = \frac{K_{V2} K_B M_0}{(K_2 - K_1) K_1} \left[1 - e^{-K_1 t}\right] + \frac{K_{V2} K_B M_0}{(K_2 - K_1) K_2} \left[e^{-K_2 t} - 1\right]$$

Where W is the solid char remaining after the treatment, that is;

$$W = M_A + M_B + M_C$$

$$W = (M_0 e^{-K_1 t}) + \left(\frac{K_B M_0}{(K_2 - K_1)} e^{-K_1 t} - \frac{K_B M_0}{(K_2 - K_1)} e^{-K_2 t}\right) + \left(\frac{K_C K_B M_0}{(K_2 - K_1)K_1}\left[1 - e^{-K_1 t}\right] + \frac{K_C K_B M_0}{(K_2 - K_1)K_2}\left[e^{-K_2 t} - 1\right]\right)$$

$$\frac{W}{M_0} = e^{-K_1 t} + \frac{K_B}{(K_2 - K_1)} e^{-K_1 t} - \frac{K_C K_B}{(K_2 - K_1)K_1} e^{-K_1 t} - \frac{K_B}{(K_2 - K_1)} e^{-K_2 t} + \frac{K_C K_B}{(K_2 - K_1)K_2} e^{-K_2 t} + \frac{K_C K_B}{(K_2 - K_1)K_1} - \frac{K_C K_B}{(K_2 - K_1)K_2}$$

$$\frac{W}{M_0} = \left[1 + \frac{K_B}{(K_2 - K_1)} - \frac{K_C K_B}{(K_2 - K_1)K_1}\right] e^{-K_1 t} - \left[\frac{K_B}{(K_2 - K_1)} - \frac{K_C K_B}{(K_2 - K_1)K_2}\right] e^{-K_2 t} + \frac{(K_2 - K_1)K_C K_B}{(K_2 - K_1)K_1 K_2}$$

$$\frac{W}{M_0} = \left[\frac{(K_2 - K_1)K_1 + K_B K_1 - K_C K_B}{(K_2 - K_1)K_1}\right] e^{-K_1 t} - \left[\frac{K_B K_2 - K_C K_B}{(K_2 - K_1)K_2}\right] e^{-K_2 t} + \frac{K_C K_B}{K_1 K_2}$$